THE REACTIVITY OF ZIRCONIUM HYDRIDES WITH TRANSITION METAL CARBONYLS

Thesis by

Paul Theron Barger

In Partial Fulfillment of the Requirements

for the Degree of

Doctor of Philosophy

California Institute of Technology

Pasadena, California

1983

(Submitted April 27, 1983)

to Mom and Dad

Acknowledgments

I wish to thank all the members of the Bercaw group, past and present, for providing a stimulating environment in which to both do science and have fun. All have taught me something about chemistry. The groundwork in the chemistry of $Cp^*_2ZrH_2$ by Juan Manriquez, Bob Sanner, Don McAlister, Pete Wolczanski and Rich Threlkel made my entry into this field significantly easier. The crystallographic work described in Chapter II of Bernard Santarsiero and Justine Armantrout is gratefully acknowledged. Bernie was also very helpful in proofreading portions of this thesis. The expert typing of Henriette Wymar is greatly appreciated.

Some of the best times I have had during the last four years have been on the hiking or biking trail. I wish to thank all the people, fortunately too numerous to mention individually, who have shared these experiences with me.

The superb guidance, financial support and overall good sense of John Bercaw as my research advisor has made my graduate career at Caltech extremely valuable. It is nice to finish nearly five years of graduate school knowing I made some right decisions when I was young and ignorant; deciding to work for John was one of my best.

Finally, I am very grateful for the love and understanding of my parents and family.

Abstract

The reactivity of bis(pentamethylcyclopentadienyl) zirconium hydride complexes with a variety of Group VIII transition metal carbonyls has been investigated. These reactions are observed to follow two distinct pathways; one involving reductive loss of the zirconium hydrides as H_2, the other proceeding by hydride transfer to the carbon atom of a carbonyl to afford CO reduction. Treatment of $CpM(CO)_2$ (M = Co, Rh, RuH) with $Cp^*_2ZrH_2$ or $[Cp^*_2ZrN_2]_2N_2$ (Cp = C_5H_5, $Cp^* = C_5Me_5$) give the "early" and "late" metal dimers, $CpM(CO)_2ZrCp^*_2$ with elimination of H_2 or N_2. The X-ray crystal structure of $CpCo(CO)_2ZrCp^*_2$ is reported and shows that this molecule contains a Co-Zr single bond bridged by a conventionally bound μ-CO and a four-electron donating μ-η^1,η^2 CO. The reactions of Cp^*_2ZrHX (X = F, Cl) with these carbonyls proceed by the second pathway to give oxycarbene complexes, $Cp(CO)M = CHO\text{-}Zr(X)Cp^*_2$ (M = Co, Rh). These compounds demonstrate that the zirconium hydride reduction of a Group VIII metal carbonyl is reversible; an equilibrium is observed between the carbene complexes and the starting metal dicarbonyl and ziconium hydride. Treatment of $CpM(CO)(PMe_3)H$ or $CpM(CO)_2CH_3$ (M = Fe, Ru) with $Cp^*_2ZrH_2$, in the presence of PMe_3, affords $Cp(PMe_3)_2M\text{-}CH_2O\text{-}Zr(H)Cp^*_2$ or $Cp^*_2Zr(OCH{=}CH_2)H$. The mechanisms of the transformation are proposed to involve initial formation of an iron or ruthenium oxycarbene intermediate which undergoes migratory insertion into the metal hydride or alkyl bond followed by phosphine trapping or β-elimination to give the observed products.

Several zirconium oxycarbene complexes have been prepared by the reduction of the corresponding zirconium carbonyl by $Cp^*_2ZrH_2$. These molecules represent some of the first isolable examples of Group IV metal to carbon multiple bonding. The X-ray crystal structure of $Cp_2(PMe_3)Zr{=}CHO{-}Zr(I)Cp^*_2 \cdot C_6H_6$ is reported. Treatment of $Cp_2(CO)Zr{=}CHO{-}Zr(H)Cp^*_2$ with MeI or $Cp_2(PMe_3)Zr{=}CHO{-}Zr(I)Cp^*_2$ with CO gives a new product, the structure of which has been shown by X-ray diffraction to be $Cp^*_2\overline{ZrOCH{=}C(Zr(I)Cp_2)O}$. The mechanism for this transformation has been shown to involve an intramolecular coupling of carbene and carbonyl ligands on a zirconium center to give a zirconium ketene intermediate, which rearranges to the observed product. In the presence of pyridine the ketene intermediate can be trapped to give the isolable $Cp_2(pyr)Zr(O{=}C{=}CHO{-}Zr(H)Cp^*_2)$.

Table of Contents

INTRODUCTION

The recent demand for alternative chemical feedstocks other than petroleum has revived a major interest in the reduction of carbon monoxide by H_2 to make simple oxygenates, such as methanol and ethylene glycol.

While there has been a significant amount of work in this field using heterogeneous catalysts,[1] for example, the synthesis of methanol using Zn-Cu catalysts,[2] some of the best studied systems have been homogeneous in nature. Solutions of $HCo(CO)_4$[3] and $Ru(CO)_5$[4] have been observed to catalyze the hydrogenation of CO to alcohols and formates, as have mixtures of Cp_2ZrCl_2 and aluminum hydrides.[5] The synthesis of ethylene glycol from CO and H_2 using rhodium carbonyl clusters[6] demonstrates the selectivity possible by the use of homogenous catalysts.

While transition metal hydride intermediates are often invoked in speculative mechanism of these CO reductions,[7] $Cp^*_2ZrH_2$ remains the only isolable transition metal hydride complex clearly shown to act as a hydride transfer agent to the carbon atom of a metal carbonyl.[8,9] This reactivity is similar to that seen for borohydride reagents, such as $Li(C_2H_5)_3BH$, with rhenium carbonyls to cleanly afford formyl products.[10]

The first report that bis(pentamethylcyclopentadienyl) zirconium compounds were useful for CO reduction was that of the hydrogenation of $Cp^*_2Zr(CO)_2$ at 110° C to give $Cp^*_2Zr(OCH_3)H$.[11] It was also observed that under an atmosphere of CO at 25° C $Cp^*_2ZrH_2$ affords equal quantities of $Cp^*_2Zr(OCH_3)H$ and $Cp^*_2Zr(CO)_2$.[11] At temperatures below

-50° C a carbonyl adduct, $Cp^*_2ZrH_2(CO)$ can be observed; however, on warming to room temperature this intermediate gives trans-$[Cp^*_2ZrH]_2(\mu$-OCH=CHO-), $(Cp^*_2ZrH)_2(\mu$-OCH_2CH_2O-), $Cp^*_2Zr(OCH_3)H$ and $Cp^*_2Zr(CO)_2$ in ratios depending on the reaction conditions.[12] Two mechanisms have been proposed for these transformations that differ only in the way that hydrogen is transferred to the carbonyl carbon.[13] In Scheme I migratory insertion of CO into a zirconium hydride bond to give a formyl intermediate, followed by intermolecular reduction of the formyl carbonyl by a second equivalent of $Cp^*_2ZrH_2$ affords $Cp^*_2(H)Zr$-CH_2O-$Zr(H)Cp^*_2$, a common intermediate to the two mechanisms. The recent report of a thorium formyl complex, prepared by the low-temperature carbonylation of $Cp^*_2Th(H)(O^tBu)$,[14] provides good precedence of invoking the uncommon insertion of CO into a metal hydride bond in Scheme I. An alternative mechanism, Scheme II, proceeds by initial reduction of the zirconocene dihydride carbonyl adduct by $Cp^*_2ZrH_2$ to give an oxycarbene intermediate which would be expected to rapidly insert into one of the zirconium hydride bonds to give $Cp^*_2(H)Zr$-CH_2O-$Zr(H)Cp^*_2$. This mechanism is supported by the preparation of tungsten[8] and niobium[9] oxycarbene complexes by the treatment of the corresponding carbonyls with $Cp^*_2ZrH_2$ and by the ability of the niobium carbenes to insert into metal hydride and alkyl bonds.[9]

The carbonyls of $Cp^*_2Zr(CO)_2$ are also reduced by $Cp^*_2ZrH_2$ under H_2 at 25° C, to give cis-$(Cp^*_2ZrH)_2(\mu$-OCH=CHO-).[12a, 9] That the stereochemistry of this product is different from that of the previously described enediolate dimer indicates that an independent mechanism is

Scheme I

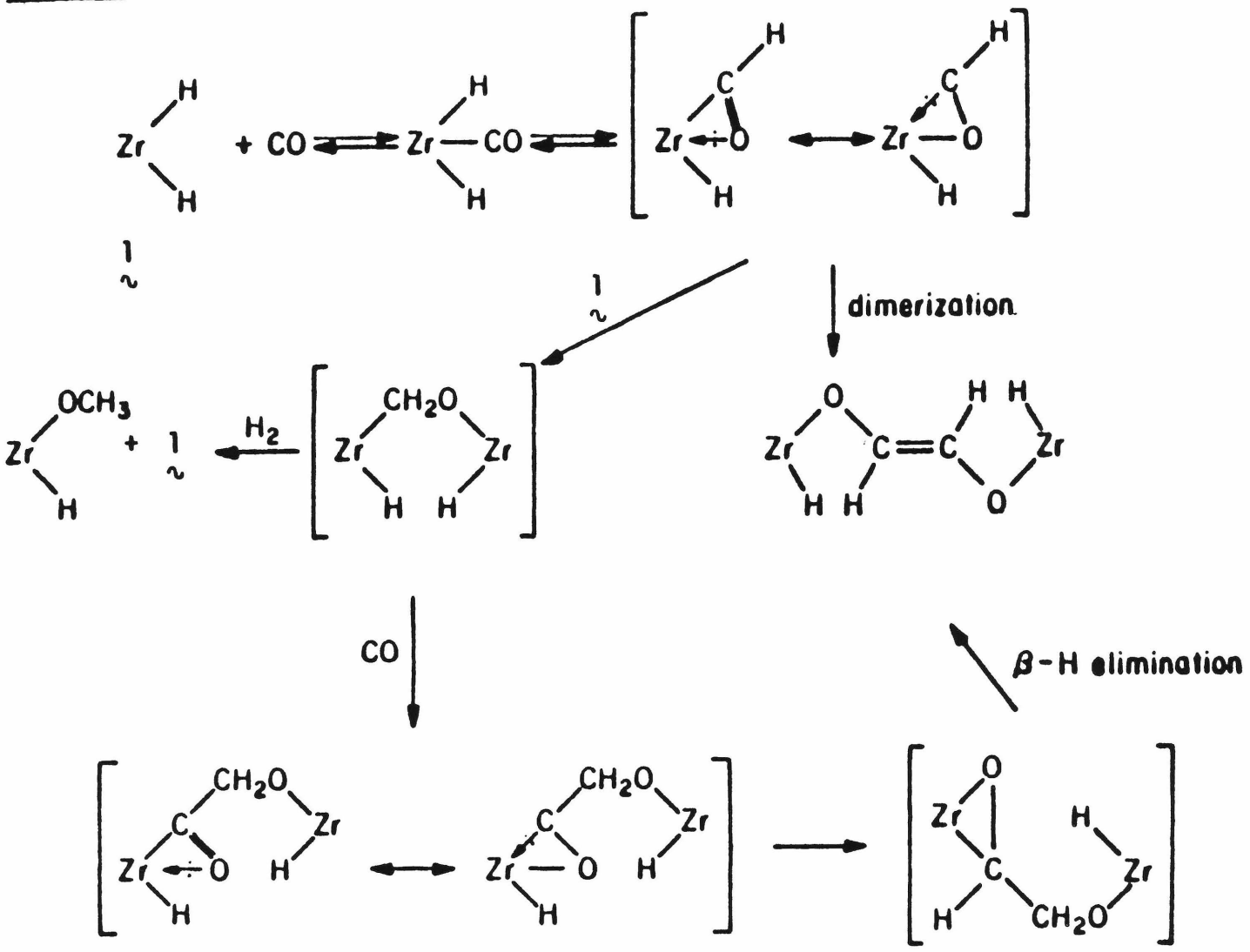

Scheme II

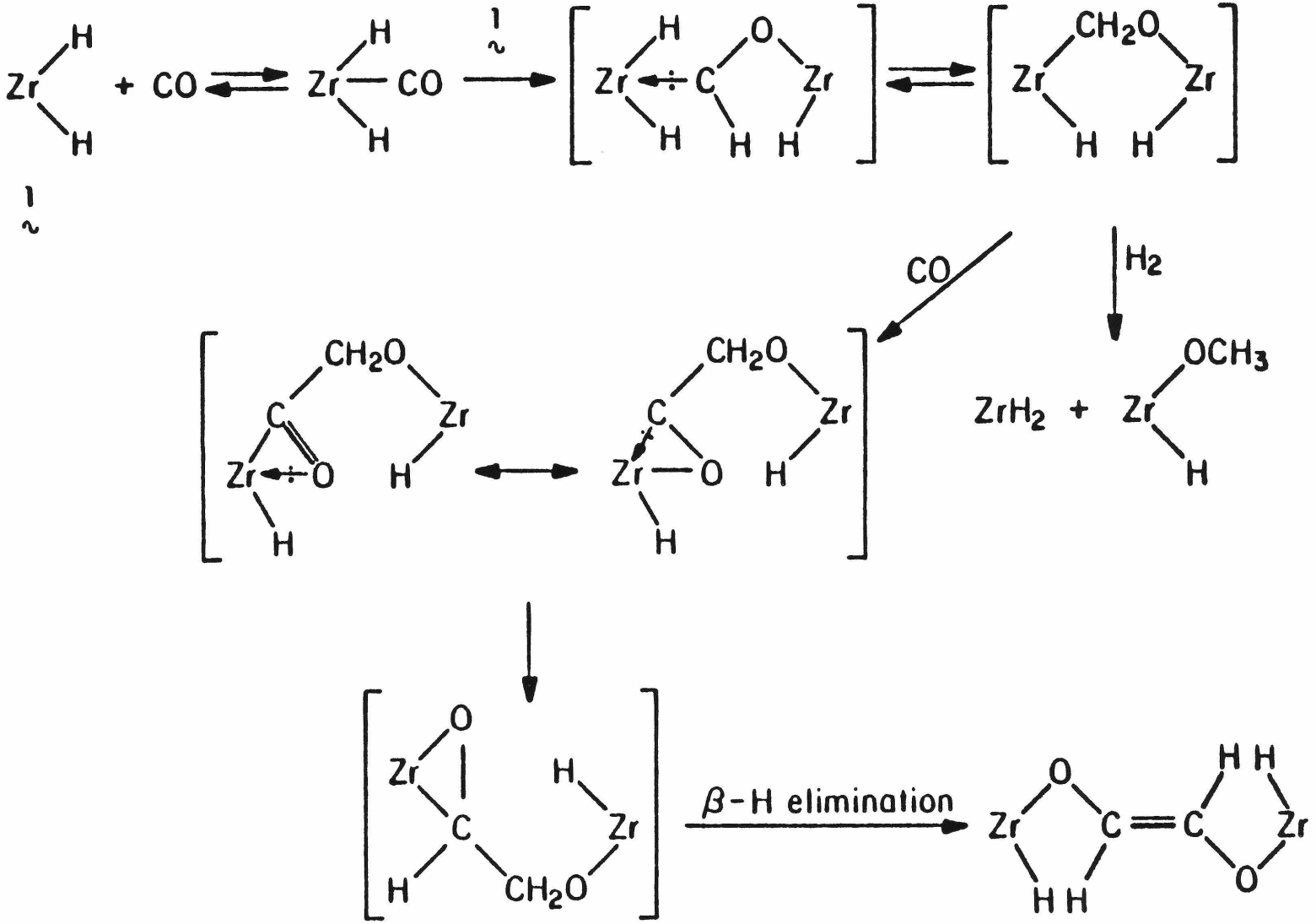

operating in this reaction. It was initially proposed that a bis-carbene intermediate was formed, followed by carbene coupling to give the observed product (Scheme III).[13] However, the reaction of $Cp^*_2Zr(CO)_2$ with $Cp^*_2HfH_2$ gives only the mixed metal enediolate complex,[14] discrediting this mechanism. The mechanism presently in favor (Scheme IV) involves initial formation of a zirconium carbene carbonyl complex that undergoes ligand coupling to coordinated ketene intermediate which is hydrogenated to give bis-(Cp^*_2ZrH)(μ-OCH=CHO-).[13]

This thesis reports on our further investigations of the reactivity of bis(pentmethylcyclopentadienyl) zirconium hydrides with Group VIII and Group IV transition metal carbonyls in an attempt to gain additional understanding of the mechanisms of CO reduction.

Scheme III

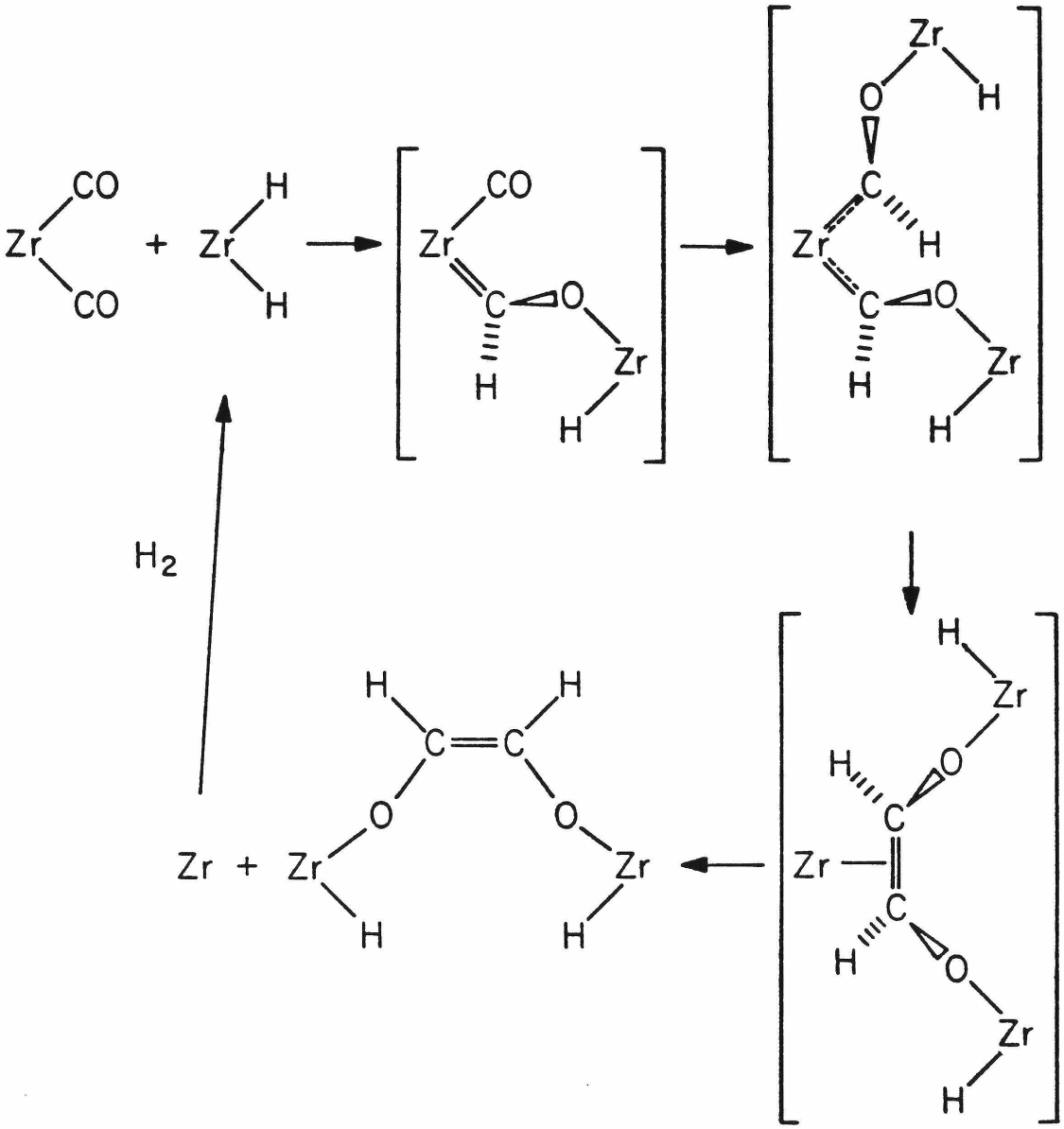
CO
Zr
CO
+
H
Zr
H
CO
Zr
C
O
Zr
H
H
Zr
O
H
C
Zr
H
C
O
Zr
H
H
H2
H
H
C
C
O
O
Zr + Zr
H
H
H
Zr
O
H
C
Zr
C
H
O
Zr
H

Scheme IV

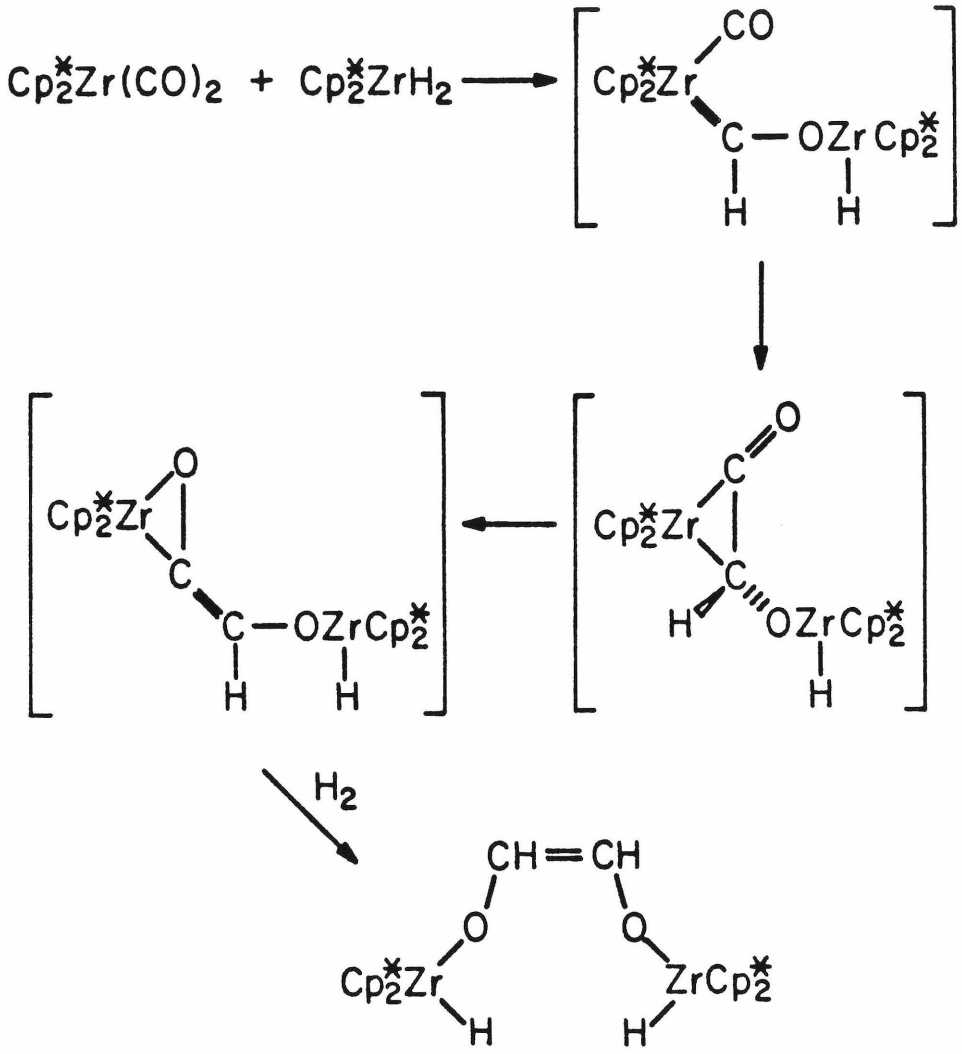
Cp*2Zr(CO)2 + Cp*2ZrH2
CO
Cp*2Zr
C — OZr Cp*2
H H
O
C
Cp*2Zr
H OZrCp*2
H
O
Cp*2Zr
C
C — OZrCp*2
H H
H2
CH = CH
O O
Cp*2Zr ZrCp*2
H H

References

1. Denny, P. J.; Whan, D. A. in "Catalysis", The Chemical Society: London, (1978), p. 46.

2. Herman, R. G.; Klier, K.; Simmons, G. W.; Finn, B. P.; Bulko, J. B.; Kobylinski, T. P. J. Catal. 56, 407 (1979).

3. (a) Rothke, J. W.; Feder, H. M. J. Amer. Chem. Soc. 100, 3623 (1978);

(b) Feder, H. F.; Rothke, J. W., Ann. N. Y. Acad. Sci. 333, 45 (1980).

4. (a) Bradly, J. S. J. Amer. Chem. Soc. 101, 7419 (1979);

(b) Dombek, B. D. J. Amer. Chem. Soc. 102, 6857 (1980).

5. Shoer, L. I.; Schwartz, J. J. Amer. Chem. Soc. 99, 5831 (1977).

6. Pruett, R. L.; Walker, W. E. (Union Carbide Corp.), West German Patent 2 262 318 (1972); U.S. Appl. 210 530 (1971).

7. Masters, C. Adv. Organomet. Chem. 17, 61 (1979) and references therein.

8. Wolczanski, P. T.; Threlkel, R. S.; Bercaw, J. E. J. Amer. Chem. Soc. 101, 218 (1978).

9. Threlkel, R. S.; Bercaw, J. E. J. Amer. Chem. Soc. 103, 2650 (1981).

10. (a) Casey, C. P.; Andrew, M. A.; Rinz, J. E. J. Amer. Chem. Soc. 101, 741 (1979);

(b) Tam, W.; Wong, W.-K.; Gladysz, J. A. J. Amer. Chem. Soc., 101, 1589 (1979);

(c) Sweet, J. R.; Graham, W. A. G. J. Organomet. Chem. 173, C9 (1979).

11. Manriquez, J. M.; Sanner, R. D.; Marsh, R. E.; Bercaw, J. E. J. Amer. Chem. Soc. 98, 6733 (1976).

12. (a) Manriquez, J. M.; McAlister, D. R.; Sanner, R. D.; Bercaw, J. E. J. Amer. Chem. Soc. 100, 2716 (1978); (b) Curtis, C. J.; Bercaw, J. E., unpublished results.

13. Wolczanski, P. T.; Bercaw, J. E. Acc. Chem. Res. 13, 121 (1980).

14. Fagan, P. J.; Moloy, K. G.; Marks, T. J. J. Amer. Chem. Soc. 103, 6959 (1981).

15. Roddick, D. M.; Bercaw, J. E., unpublished results.

CHAPTER I

The Reactivity of Bis(pentamethylcyclopentadienyl) Zirconium Hydrides with Group VIII Transition Metal Carbonyls

Introduction

In view of the ease with which $Cp^*_2ZrH_2$ (1) reduces Groups V and VI transition metal carbonyls to the corresponding oxycarbene complexes[1] we have investigated the reactions of 1 and related hydrides

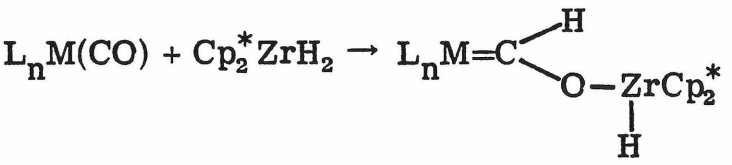

$$L_nM(CO) + Cp^*_2ZrH_2 \rightarrow L_nM{=}C(H)(O{-}ZrCp^*_2{-}H) \qquad (1)$$

(L_nM = Cp_2Cr, Cp_2Mo, Cp_2W, Cp_2NbR)

with other metal carbonyls. The major goals of this research have been to explore the generality of the zirconium hydride reduction of metal bound CO and to probe the reactivity of the oxycarbenes prepared by this technique.

Prior to this work $Cp^*_2Zr(CO)_2$ was the only transition metal dicarbonyl complex observed to give a clean product upon treatment with $Cp^*_2ZrH_2$, affording cis-$(Cp^*_2ZrH)_2(\mu$-OCH=CHO-$)$[1b, 2] in which

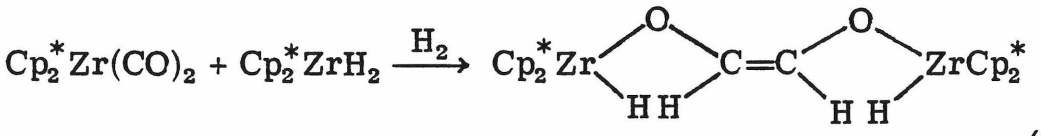

$$Cp^*_2Zr(CO)_2 + Cp^*_2ZrH_2 \xrightarrow{H_2} Cp^*_2Zr(O{-}CH{=}CH{-}O)ZrCp^*_2 \qquad (2)$$

both carbonyls have been reduced and a new carbon-carbon bond formed. Unfortunately, no intermediates could be identified during the course of this reaction to provide information as to the mechanism of this unique transformation. We were therefore interested in the reactivity of 1 with other transition metal dicarbonyl complexes to gain some understanding of reaction pathways available to compounds of this type.

A second area of interest centered on molecules containing zirconoxy carbene and a hydride or alkyl ligand on one metal center. Niobium complexes of this type have been previously observed to undergo migratory insertion of the carbene ligand into the metal hydride or alkyl bond.[1b] There are few reports of this type of insertion;[3] therefore we have attempted to prepare some carbene-hydride and carbene-alkyl complexes of iron and ruthenium to gain further insight about the mechanism of the migratory insertion.

This chapter reports our investigations of the reactions of Cp^*_2ZrHX (X = H, F, Cl) with a variety of Group VIII transition metal mono- and dicarbonyl complexes. These reactions have been observed to follow two different reaction pathways. The first proceeds by reductive elimination of the zirconium hydride ligands as H_2, followed by trapping of the zirconium(II) fragment by the metal carbonyl complex to afford an "early" and "late" mixed-metal dimer. The second class involves CO reduction by the zirconium hydride, giving Group VIII metal oxycarbene complexes or products arising from oxycarbene intermediates. A preliminary report of a portion of this work has appeared in print.[4]

Results

Reactivity of Zirconium Hydrides with Cobalt and Rhodium Carbonyls.

Opposed to the observed reactivity of $Cp^*_2ZrH_2$ (1) with several transition metal monocarbonyls to afford oxycarbene complexes,[1] the treatment of $CpM(CO)_2$ (M = Co (2a), Rh (2b)) with 1 in toluene yields $CpM(CO)_2ZrCp^*_2$ (M = Co (3a), Rh (3b)) where the zirconium hydrides are lost as H_2 and a new metal-metal bond is formed between the zirconium and cobalt or rhodium. The zirconium-cobalt dimer forms

$$\underset{2}{CpM(CO)_2} + \underset{1}{Cp^*_2ZrH_2} \rightarrow \underset{3}{CpM(CO)_2ZrCp^*_2} + H_2 \quad (M = Co,\ Rh) \qquad (3)$$

at ca. -20°, as indicated by a color change of the reaction solution from red to blue-green, and can be isolated as dark green crystals in 46% yield. In contrast, a mixture of $CpRh(CO)_2$ and 1 in a sealed NMR tube shows the initial formation of an intermediate with a down-field resonance in the ^1H NMR spectrum suggesting the presence of a zirconoxy carbene ligand. Over several minutes this transient species converts to 3b, the only product that can be isolated from the reaction mixture.

The ^1H NMR spectra (Table I) of 3a and 3b are very similar, showing only two resonances due to the Cp and Cp* ligands. The IR spectra have two intense bands, at 1737 and 1683 cm^{-1} for 3a and 1752 and 1696 cm^{-1} for 3b, assigned as the stretching frequencies of the remaining carbonyls. That neither band shows a shift to lower energy in the IR spectrum of 3a prepared from 2a and $Cp^*_2ZrD_2$ indicates that these bands are not due to any remaining metal hydrides.

The liberation of dihydrogen during the course of the reaction is confirmed by the recovery of 0.83 equivalents of H_2 per equivalent of $Cp^*_2ZrH_2$ by a Toepler pump after the formation of 3a. $CpM(CO)_2ZrCp^*_2$ can also be prepared from 2 and $[Cp^*_2ZrN_2]_2N_2$, with the loss of 1.5 equivalents of N_2, providing further evidence for the presence of zirconium in the +2 oxidation state in the product.

$$CpM(CO)_2 + \tfrac{1}{2}[Cp^*_2ZrN_2]_2N_2 \rightarrow CpM(CO)_2ZrCp^*_2 + \tfrac{3}{2}N_2 \qquad (4)$$

2 3 (M = Co, Rh)

Under an atmosphere of CO in a sealed NMR tube 3a cleanly converts to $CpCo(CO)_2$ and $Cp^*_2Zr(CO)_2$ after 5 hours at 80° C. The

$$CpCo(CO)_2ZrCp^*_2 + CO \xrightarrow{80^\circ C} CpCo(CO)_2 + Cp^*_2Zr(CO)_2 \qquad (5)$$

reaction of 3a with H_2 at 80° C affords $Cp^*_2Zr(OCH_3)(H)$ and $CpCo(CO)_2$ as the major products, but the ^1H NMR spectrum of the reaction solution indicates the presence of several other, unidentified products.

We were interested in the detailed structure of 3a for several reasons. $CpCo(CO)_2ZrCp^*_2$ is the first known heterometallic dimer containing zirconium and cobalt. Interestingly, there appear to be no reasonable symmetric structures which allow formal 18-electron, closed-shell electronic configurations for both metals. This fact, along with the low energy ν_{CO} stretching frequencies, suggested that the carbonyls of 3a might bridge the Co-Zr bond in a non-conventional fashion. Therefore, the structure was investigated using X-ray diffraction techniques.

Single crystals of 3a, suitable for X-ray diffraction, were grown by slow cooling of a saturated benzene solution. Unit cell parameters as well as data collection and refinement conditions are given in Table II. Atomic positions and Gaussian amplitudes for all atoms are listed in Table III. Tables IV and V give bond distances and angles.

The ORTEPs of 3a (Figures 1 and 2) confirm its formulation as CpCo(I) and $Cp^*_2Zr(II)$ moieties joined by a Co-Zr bond and two bridging carbonyls. The Cp and Cp* ligands are bound to the metals in a standard pentahapto manner. The Zr-C(rings) distances (2.501(6)-2.589(6) Å) and the Cp* ring centroid-zirconium-Cp* ring centroid angle of 139.2(5)° are similar to those of $[Cp^*_2ZrN_2]_2N_2$.[5] The Co-C(ring) distances (2.081(7)-2.106(7) Å) are typical for a η^5-C_5H_5 ring bound to Co(I).[6] The Cp ring centroid is skewed off the Co-Zr axis by 11.7° toward the μ_2 bridging carbonyl, presumably due to the different trans electronic effects of the two carbonyls.

$CpCo(CO)_2ZrCp^*_2$ is the first example of a molecule with a bond between zirconium and a Group VIII transition metal. The metal-metal distance of 2.926(1) Å can be compared to that observed for $Cp_2(CO)Nb(\mu\text{-}CO)Co(CO)_3$ of 2.992 Å,[7] another example of an "early" to "late" transition metal bond. This bond length indicates the presence of a Co-Zr single bond.

One of the most interesting features of the structure of 3a is that the two carbonyls have very different bonding interactions with the two metal centers. The metal-carbonyl substructure (Figure 2) is essentially planar as is demonstrated by the small deviations from the least-squares plane of the metal and carbonyl atoms (Table VI).

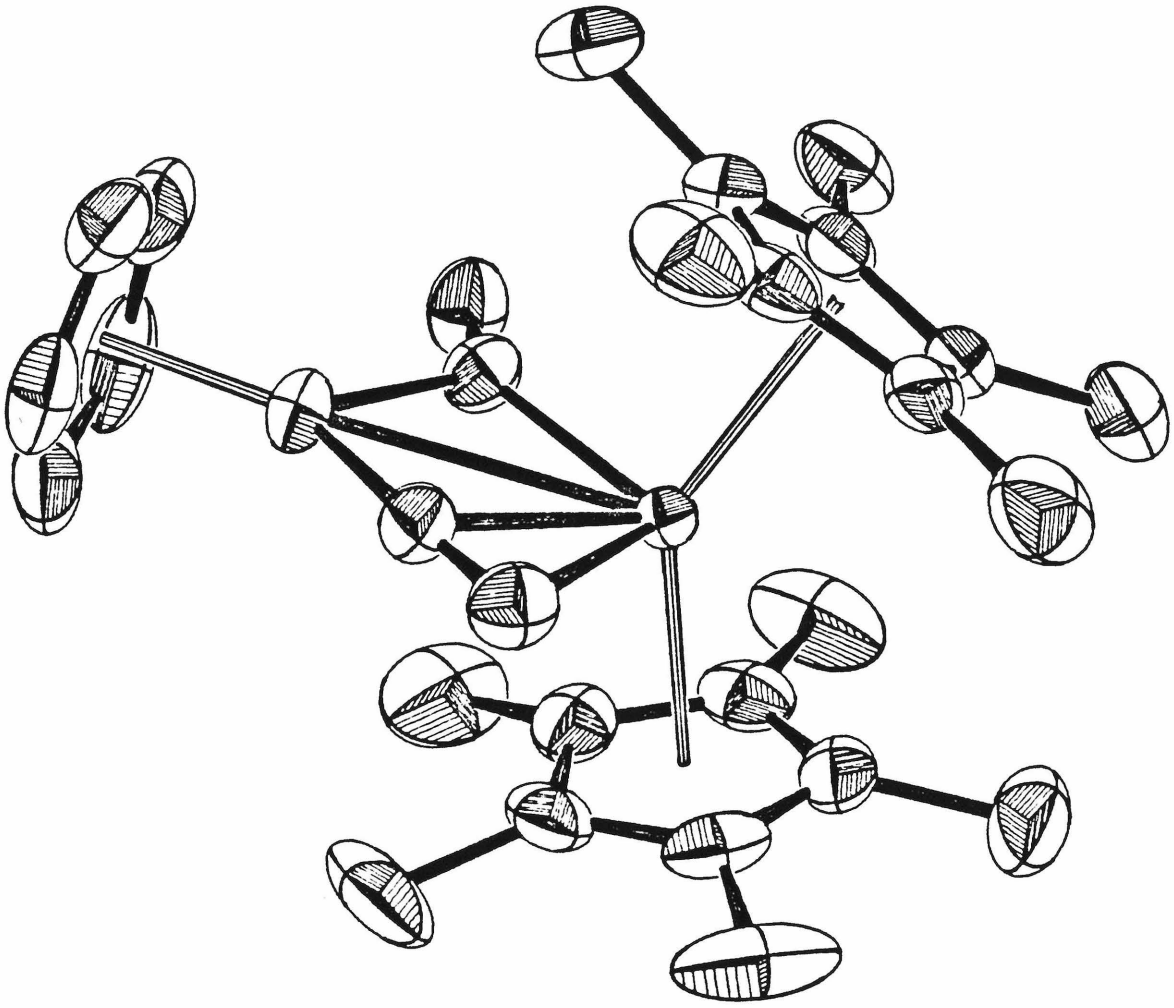

Figure 1. ORTEP drawing of $CpCo(CO)_2ZrCp^*_2$ showing 50% probability ellipsoids for non-hydrogen atoms.

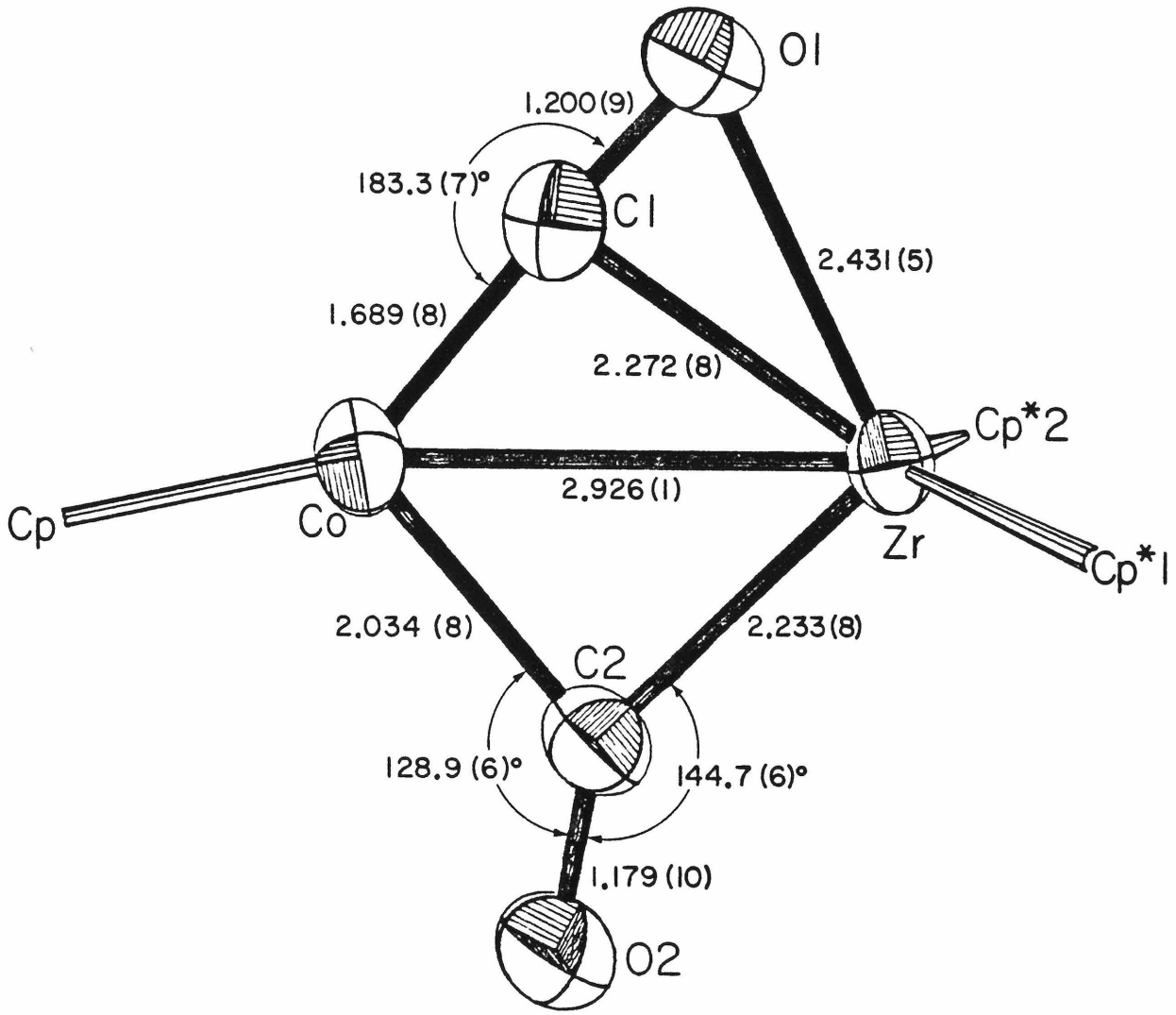

Figure 2. ORTEP drawing of the planar metal-carbonyl substructure, including important bond lengths (Å) and angles.

One carbonyl, C(2)-O(2), bridges the metal centers in a conventional μ_2 fashion, although there is some inherent asymmetry due to the large difference in size of the two metals.

The other carbonyl, C(1)-O(1), interacts with the two metals in an unique μ_2-η^1,η^2 manner. The nearly linear Co-C(1)-O(1) angle (176.7(7)°) and short Co-C(1) distance (1.689(8) Å) indicate that the cobalt-carbonyl bonding is essentially terminal. Both C(1) and O(1) are well within bonding distance to the Zr, indicative of interaction of a C(1)O(1) π bond with zirconium similar to that observed for ethylene in $Cp_2Nb(C_2H_4)(C_2H_5)$.[8] The lengthening of the C(1)-O(1) distance from that normally observed for terminal cobalt carbonyls[9] also supports a zirconium-carbonyl π-interaction, as donation of electron density to the metal center lowers the C-O bond order. This is also consistent with the very low IR stretching frequency assigned to this carbonyl. Since there is only one orbital in the equatorial wedge of the zirconocene center for bonding to C(1)O(1) in 3a this interaction cannot be regarded as similar to that of the η^2-acyl in $Cp_2Zr(\eta^2\text{-}COCH_3)(CH_3)$[10] where the carbon and oxygen atoms interact with different metal orbitals. Thus in the μ-n^1,n^2 bridging mode the carbonyl acts as a two-electron donor to both the cobalt and zirconium, bringing both metal centers to closed-shell, 18-electron configurations.

The ^{13}C NMR spectrum of $CpRh(CO)_2ZrCp^*_2$ enriched with ^{13}CO has only one resonance for the carbonyls at room temperature (254 δ, $^1J_{C\text{-}Rh}$ = 59 Hz) indicating that the two carbonyls are rapidly interchanging bonding modes. Variable temperature 22.5 MHz NMR spectra show coalescence of this resonance at ca. -60° C, but attempts

to observe the low temperature limit, where the carbonyls are inequivalent, were unsuccessful at this field strength. However, the 125.8 MHz spectrum at -70° C shows to broad resonances at 298 and 215 δ, assigned as the resonances of the carbonyls in the two different bonding modes. The chemical shift difference and the coalescence temperature give an upper limit of 8 kcal/mole for the activation barrier of the fluxional process.

The reductive elimination of H_2 from 1 that leads to the formation of the mixed-metal dimers can be prevented by replacement of one of the zirconium hydrides by a halide. Thus, treatment of an excess of 2 with Cp_2^*ZrHCl (4) in toluene affords the cobalt or rhodium zirconoxy carbene complexes, $Cp(CO)M{=}CHO{-}Zr(Cl)Cp_2^*$ (M = Co (5a), Rh (5b)) in good yield after 2 hours at room temperature. The carbene complexes

$$\underset{2}{CpM(CO)_2} + \underset{4}{Cp_2^*ZrHCl} \rightleftharpoons \underset{5}{\begin{matrix} CpM{=}CHO{-}ZrCp_2^* \\ | \qquad\quad | \\ CO \qquad Cl \end{matrix}} \quad (M = Co,\ Rh) \tag{6}$$

can be isolated free of dicarbonyl by precipitation with pet ether at -78° C. The corresponding fluoride carbene complexes (7) can be prepared in an analogous manner using Cp_2^*ZrHF (6) in place of Cp_2^*ZrHCl.

$$\underset{2}{CpM(CO)_2} + \underset{6}{Cp_2^*ZrHF} \rightarrow \underset{7}{\begin{matrix} CpM{=}CHO{-}ZrCp_2^* \\ | \qquad\quad | \\ CO \qquad F \end{matrix}} \quad (M = Co,\ Rh) \tag{7}$$

The ^1H NMR spectra of 5 (Table I) show resonances attributable to the Cp and Cp^* ligands as well as a down-field peak (5a, 12.6 δ;

5b, 13.1 δ), integrating to one proton, for the carbene hydrogen. The IR spectra of nujol mulls of 5 show one strong band in the CO stretching region at 1947 cm^{-1} for 5a and 1952 cm^{-1} for 5b. The ^1H NMR and IR spectra for 7 (Table I) are similar.

The equilibrium depicted in equation 6, between the zirconoxy carbene complex and the Group VIII dicarbonyl and Cp_2^*ZrHCl can be attained from either direction. Thus at the completion of the reaction of 2 and 4 both starting materials can be observed in the reaction mixture. Likewise, resonances due to 2 and 4 slowly grow into the ^1H NMR spectra of isolated 5 over several days. In the case of 5a the equilibrium consists of approximately 70% $Cp(CO)Co{=}CHO{-}Zr(Cl)Cp_2^*$ to 30% $CpCo(CO)_2$ and Cp_2^*ZrHCl; for 5b the observed ratio is about 90:10, 5b to 2b and 4.

In the presence of protic acids, HX ($X = Cl^-$, $PhCOO^-$), 5b is rapidly converted to $CpRh(CO)_2$ and $Cp_2^*Zr(Cl)(X)$ at 25° C with the evolution H_2. Attempts to prepare amine-substituted rhodium carbene

$$\underset{\text{5b}}{CpRh(CO){=}CHO{-}ZrCl(Cp_2^*)} + HX \rightarrow \underset{\text{2b}}{CpRh(CO)_2} + Cp_2^*Zr(Cl)(X) + H_2 \qquad (8)$$

complexes by aminolysis of 5b with $HNMe_2$, a reaction pathway that is common for Fischer-type carbenes,[11] have been unsuccessful.

$$L_nM{=}C\begin{matrix}\diagup OR \\ \diagdown R'\end{matrix} + HNMe_2 \rightarrow L_nM{=}C\begin{matrix}\diagup NMe_2 \\ \diagdown R'\end{matrix} + ROH \qquad (9)$$

$Cp(CO)Rh{=}CHO{=}Zr(Cl)Cp_2^*$ is unaffected by an excess of Cp_2^*ZrHCl indicating that the remaining carbonyl is inert toward reduction to give

a bis-carbene complex.

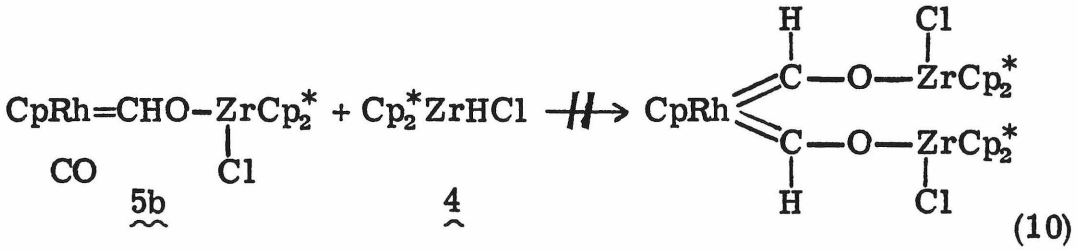

(10)

Reactivity of Zirconium Hydrides with Iron and Ruthenium Carbonyls.

Addition of $Cp^*_2ZrH_2$ to a heptane solution of $CpRu(CO)_2H$ (8) affords the dark red $Cp(H)Ru(CO)_2ZrCp^*_2$ (9) in 59% isolated yield after one hour at room temperatures. Like $CpM(CO)_2ZrCp^*_2$ (M = Co, Rh),

$$CpRu(CO)_2H + Cp^*_2ZrH_2 \rightarrow Cp(H)Ru(CO)_2ZrCp_2^* \qquad (11)$$

9 can also be prepared from 8 and $[Cp^*_2ZrN_2]_2N_2$ with the liberation of 2.56 equivalents of N_2 per equivalent of $[Cp^*_2ZrN_2]_2N_2$ as measured by Toepler pump. The IR spectrum of a nujol mull of 9 is similar to

$$CpRu(CO)_2H + [Cp^*_2ZrN_2]_2N_2 \rightarrow Cp(H)Ru(CO)_2ZrCp^*_2 + \tfrac{3}{2}N_2 \qquad (12)$$

those of 5a and 5b and shows two intense bands in the carbonyl stretching region at 1706 and 1671 cm^{-1}. The ^1H NMR spectrum of 9 (Table I) shows a peak at 5.17 δ for the Cp ring on Ru and two resonances for the Cp* rings at 1.67 and 1.74 δ. A small peak, integrating to one proton, appears at -15.7 δ and is assigned as the signal of a remaining ruthenium hydride. These results suggest the structure of 9 is similar to those of 3 with Cp and hydride ligands on opposite sides of the metal-carbonyl plane, making the Cp* rings inequivalent.

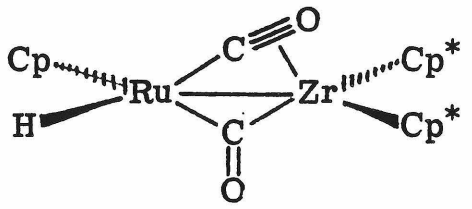

9

Treatment of 9 with an excess of CO gives a mixture of $CpRu(CO)_2H$ and $Cp^*_2Zr(CO)_2$ after 24 hours at room temperature.

Replacement of one of the carbonyls of 8 by PMe_3, giving $CpM(CO)(PMe_3)H$ (M = Fe (10a), Ru (10b)), prevents formation of a mixed-metal dimer upon treatment with $Cp^*_2ZrH_2$. Instead, a solution of 10 and 1 shows no change by NMR spectroscopy after 7 weeks at room temperature. However, addition of 4 equivalents of PMe_3 to a solution of 10a and 1 affords $Cp(PMe_3)_2Fe\text{-}CH_2O\text{-}Zr(H)Cp^*_2$ (11a) in 51% isolated yield after 10 minutes at room temperature. In the case of 10b the formation of $Cp(PMe_3)_2Ru\text{-}CH_2O\text{-}Zr(H)Cp^*_2$ (11b) is significantly slower; after 3 weeks at 25° C a mixture of 10b, 1, and 2 equivalents of PMe in a sealed NMR tube is at 75% completion; increasing the PMe_3 concentration to 10 equivalents does not significantly affect the rate of formation of 11b.

$$CpM(CO)(PMe_3)H + Cp^*_2ZrH_2 \xrightarrow{PMe_3} Cp(PMe_3)_2M\text{-}CH_2O\text{-}Zr(H)Cp^*_2$$
$$\underset{\sim}{10} \qquad\qquad \underset{\sim}{1} \qquad\qquad \underset{\sim}{11} \quad (M = Fe,\ Ru) \quad (13)$$

The ^1H NMR spectrum of 11a (Table I) is consistent with its formulation as a methylene oxo bridged dimer. The presence of two

phosphine ligands on the iron center is clearly indicated by the pseudo triplet pattern of the resonance due to the methyl groups on phosphorus and the triplet splitting ($^2J_{PH}$ = 2 Hz) of the Cp resonance at 3.87 δ. A broad peak at 5.26 δ, integrating to one proton, is assigned as the resonance of the remaining zirconium hydride. The signal for the methylene group appears as a triplet due to phosphorus coupling at 5.07 δ. The ^1H NMR spectrum of 11b (Table I) is more complicated than that of 11a. The phosphine methyl resonance appears as a complex multiplet centered at 1.11 δ. Unlike the spectrum of 11a, the resonance for the ruthenium Cp of 11b is a singlet similar to that observed in the spectrum of 10b. The methylene protons give rise to an apparent doublet of doublets centered at 5.32 δ in both the 90 MHz and 500 MHz spectra; the splitting patterns are similar at the two different fields suggesting that the two protons are magnetically equivalent and being split by two inequivalent phosphorus atoms. At the present time no satisfactory explanation for the differences in the spectra of 11a and 11b has been developed.

In the absence of PMe_3 the hydride ligands of 10a and 1 readily exchange between the two metal centers. Treatment of a mixture of 10a and 1 with a large excess of D_2 at 0° C for 1 hour places deuterium into both iron and zirconium hydride sites. The hydrides of $Cp^*_2ZrH_2$

$$\underset{\underset{\sim}{10}}{CpFe(CO)(PMe_3)H} + \underset{\underset{\wedge}{1}}{Cp^*_2ZrH_2} \xrightarrow{\text{xs } D_2} \underset{\underset{\sim}{10\text{-}d_1}}{CpFe(CO)(PMe_3)D} + Cp^*_2ZrD_2 \qquad (14)$$

are known to rapidly exchange with D_2,[12] however, $CpFe(CO)(PMe_3)H$ alone is inert to D_2 under these conditions indicating that the exchange

between D_2 and the iron hydride is catalyzed by 1 (Scheme I).

The reactions of $Cp^*_2ZrH_2$ and the dicarbonyl, alkyl complexes $CpM(CO)_2CH_3$ (M = Fe (12a), Ru (12b)) also proceed by a pathway involving CO reduction, rather than yielding a mixed-metal dimer analogous to 9. Thus, a mixture of 12b and 1 with 2 equivalents of PMe_3 in a sealed NMR tube affords the previously reported $Cp^*_2Zr(OCH{=}CH_2)(H)$[1b] (13) and $CpRu(CO)(PMe_3)H$ quantitatively after 2 hours at 25° C. In the case of 12a the major zirconium containing

$$\underset{\text{12b}}{CpRu(CO)_2CH_3} + \underset{\text{1}}{Cp^*_2ZrH_2} \xrightarrow{PMe_3} Cp^*_2\underset{H}{Zr}(OCH{=}CH_2) + \underset{\text{10b}}{CpRu(CO)(PMe_3)H} \qquad (15)$$

product is again 13, but $CpFe(CO)(PMe_3)H$ is only a minor component of the resulting myriad of iron complexes. A plausible mechanism for this transformation will be discussed in the following section.

Treatment of $CpM(CO)(PMe_3)CH_3$ (M = Fe, Ru) with $Cp^*_2ZrH_2$ appears to give products in which the metal carbonyl has been reduced, but these complexes have proven to be too unstable for proper characterization.

Scheme I

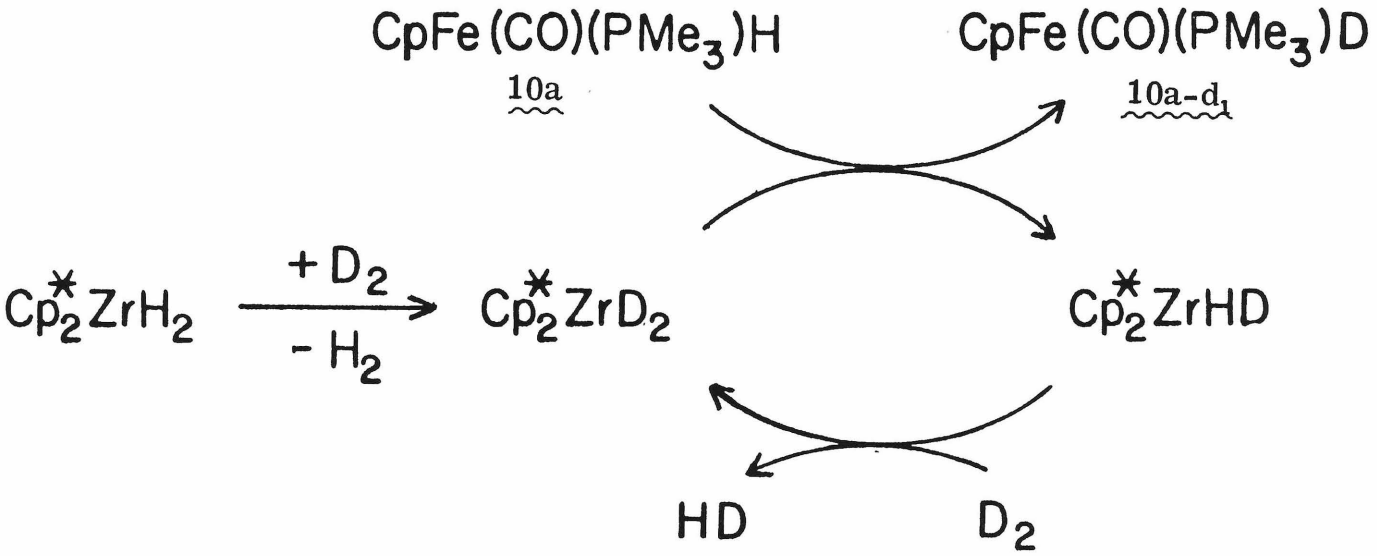
CpFe(CO)(PMe3)H
10a
CpFe(CO)(PMe3)D
10a-d1
Cp*2ZrH2
+ D2
- H2
Cp*2ZrD2
Cp*2ZrHD
HD
D2

Discussion

The reactions of bis(pentamethylcyclopentadienyl)zirconium hydrides with Group VIII transition metal carbonyls have been observed to follow two distinct pathways depending upon the natures of the reactants. Mixed-metal dimers are prepared by treating the dicarbonyls, $CpM(CO)_2$ (M = Co, Rh, RuH), with $Cp^*_2ZrH_2$. These molecules are the first examples of metal-metal bonding between Zr and a Group VIII metal. When the metal dimer formation is prohibited by the use of zirconium monohydrides, such as Cp^*_2ZrHCl, or Group VIII metal monocarbonyl or dicarbonyl alkyl complexes carbonyl reduction is observed, affording either oxycarbene complexes or products can be viewed as coming from the rearrangement of oxycarbene intermediates.

The zirconium-Group VIII metal dimers, $CpM(CO)_2ZrCp^*_2$ (M = Co, Rh, RuH), have similar structures consisting of a metal-metal single bond bridged by one conventionally bonded carbonyl and a CO that is bound in a linear, terminal fashion to the Group VIII metal but is also bent over in an unusual π-interaction with the zirconium (a μ-η^1, η^2 bonding mode). This formulation has been confirmed by the

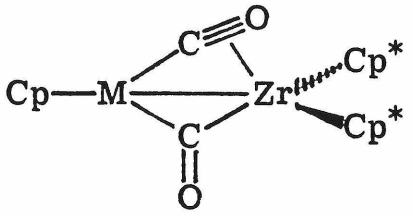

single crystal X-ray diffraction structure determination of $CpCo(CO)_2ZrCp^*_2$ (see above). The μ-η^1, η^2 mode of bonding for a carbonyl bridging two or more metals has been previously seen in

six molecules. The first such bridge was reported by Colton et al. in 1975 in the structure of $Mn_2(CO)_5(Ph_2P(CH_2)_3PPh_2)_2$.[13] Since that time η^1,η^2 carbonyls have been observed in $Fe_4(CO)_{13}H^-$,[14] $Cp_2Nb(CO)_3MoCp$,[15] $Cp_2(CH_3)Zr(CO)Mo(CO)_2Cp$,[16] $Cp_2Zr(CO)(COCH_3)Mo(CO)Cp$[16] and $Cp_3Nb_3(CO)_7$,[17] the last being unique in that the CO has a π-interaction with two niobiums of the triangular cluster. In each of these compounds, as well as in 3 and 9, the additional electron donation from the CO π-bond is needed to fill the valence electron shells of the metals. All of these molecules are also characterized by a low carbonyl stretching frequency in the IR spectrum due to the η^1,η^2 CO. 3 and 9 join this class of compounds as the first examples of an η^1,η^2 carbonyl bridging two significantly different metal centers.

That 3 and 9 can also be made from the metal dicarbonyls and $[Cp_2^*ZrN_2]_2N_2$, a ready source of coordinatively unsaturated Cp_2^*Zr(II) due to the lability of the N_2 ligands, suggests that pentamethylzirconocene, formed by reductive elimination of H_2 from 1, could be a feasible intermediate in the reaction of 1 with 2 or 8. However, the fact that $Cp_2^*ZrH_2$ and $[Cp_2^*ZrN_2]_2N_2$ are stable toward ligand loss in the absence of 2 or 8 under the reaction conditions at which 3 and 9 form indicates that the dicarbonyl induces the H_2 or N_2 elimination, possibly by an interaction between the empty zirconium $1a_1$ orbital and the oxygen lone pair of a carbonyl (Scheme II). That 1 does not lose H_2 in the presence of the monocarbonyl complexes, 10, suggests that the second carbonyl of 2 and 9 may also play a role in this elimination.

An alternative mechanism for the formation of H_2 in the reaction of $Cp_2^*ZrH_2$ and $CpRu(CO)_2H$ is by an intermolecular reductive

Scheme II

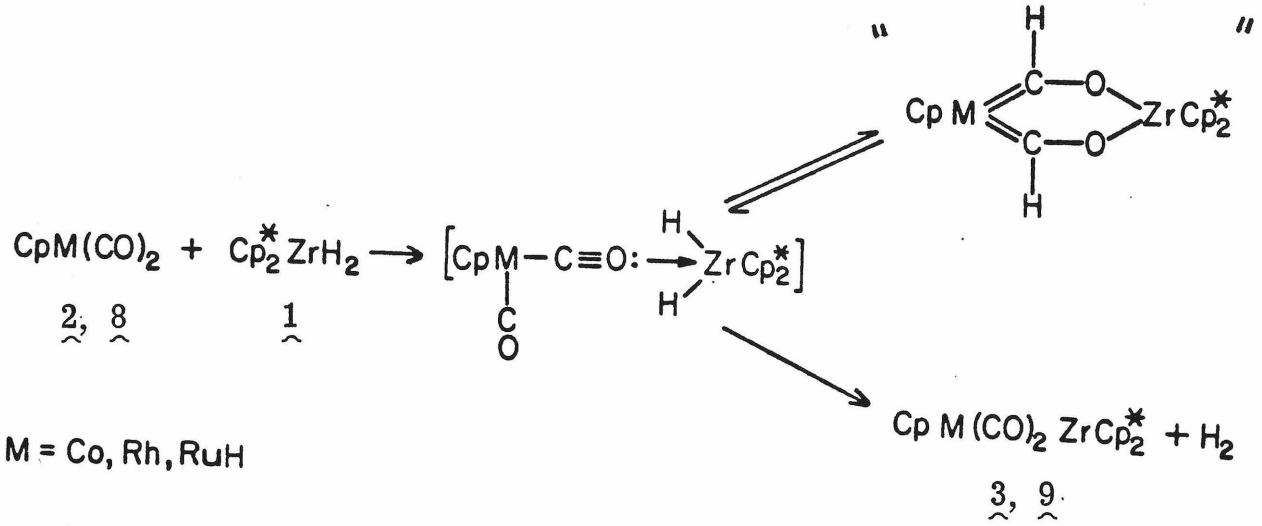

Scheme III

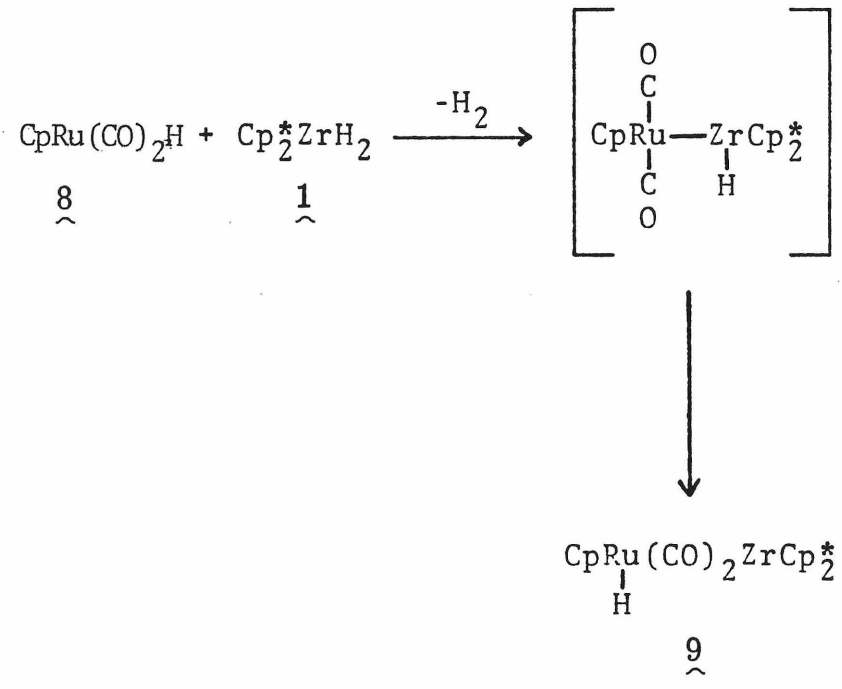

elimination of the ruthenium hydride and one of the zirconium hydrides, followed by transfer of the remaining hydride to the ruthenium (Scheme III). The H_2 elimination can be viewed as an acid-base reaction between the hydridic ZrH and protic RuH and has precedence in the reaction of $Cp_2^*ZrH_2$ and $CpMo(CO)_3H$ to give $Cp_2^*Zr(OC\text{-}Mn(CO)_2Cp)_2$ and H_2.[18]

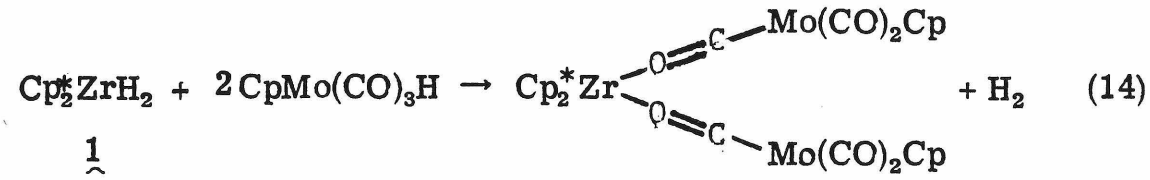

$$Cp_2^*ZrH_2 \ (\underset{\sim}{1}) + 2\,CpMo(CO)_3H \rightarrow Cp_2^*Zr(OC\text{-}Mo(CO)_2Cp)_2 + H_2 \qquad (14)$$

The low activation barrier (less than 8 kcal/mole) for interchange of the carbonyls of $\underset{\sim}{5b}$ between the two bonding modes is smaller than the barriers observed for the $\eta^1:\eta^2$ carbonyl fluxionality in $Cp_3Nb_3(CO)_7$[19] and $Mn_2(CO)_5(Ph_2P(CH_2)_3PPh_2)$[20] and suggests that the zirconium-carbonyl π-interaction is fairly weak. This is supported by the reactions of $\underset{\sim}{5a}$ and $\underset{\sim}{9}$ with CO to give $Cp_2^*Zr(CO)_2$ and $CpM(CO)_2$ (M = Co, RuH), which are presumably initiated by the opening of a coordination site on zirconium by the breaking of the zirconium-carbonyl π bond. (Scheme IV).

Scheme IV

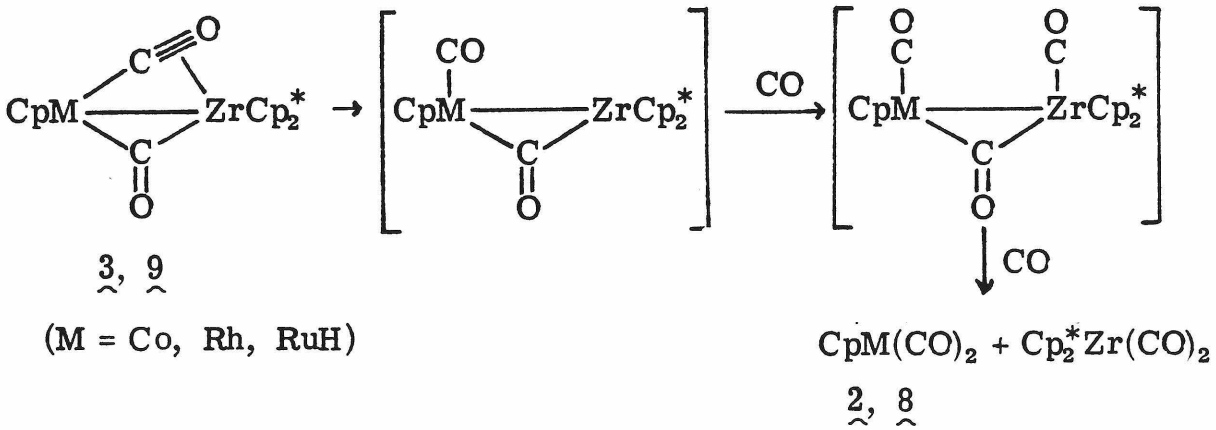

$\underset{\sim}{3}$, $\underset{\sim}{9}$ (M = Co, Rh, RuH) $\rightarrow$ $CpM(CO)_2 + Cp_2^*Zr(CO)_2$ ($\underset{\sim}{2}$, $\underset{\sim}{8}$)

The spectroscopic observation of a transient species, immediately upon mixing of $CpRh(CO)_2$ and $Cp^*_2ZrH_2$, with the spectral characteristics of a rhodium oxycarbene complex suggests that addition of a zirconium hydride of 1 across the C-O bond of a carbonyl of 2 is facile, but reversible (Scheme II). The final preference for 3 or 9 over an oxycarbene complex is probably due to the irreversibility of H_2 loss.

Treatment of 2 with Cp^*_2ZrHX (X = Cl, F), which are much more stable to reductive loss of the hydride ligand than $Cp^*_2ZrH_2$, does not give metal-metal dimers;instead, oxycarbene complexes are isolated (eqs. 6 and 7). However, the reversible nature of the zirconium hydride addition to cobalt and rhodium carbonyls is clearly demonstrated by the equilibrium observed between $CpM(CO)_2$, Cp^*_2ZrHCl and $Cp(CO)M{=}CHO{-}Zr(Cl)Cp^*_2$ (M = Co, Rh) (eq. 6). The equilibrium ratios indicate that the cobalt or rhodium oxycarbene complexes are only slightly more stable than 2 and 4, even with the presence of a new Zr-O bond worth about 120 kcal/mol.[21]

The poor π-accepting ability of the oxycarbene ligand relative to CO is similar to that observed for other Fischer-type carbenes.[22] Because of this, the remaining carbonyl of 5 is more electron-rich than those of 2 as shown by the lowering of the CO stretching frequencies of 5 (ν_{CO} = 1947 (5a), 1952 cm^{-1} (5b)) compared to those of 2 (ν_{CO} = 2028, 1967 (2a),[23] 2051, 1987 cm^{-1} (2b)).[24] The increased electron density at the carbonyl of 5 and the steric bulk of the decamethylzirconocene substituent on the oxycarbene should make this CO

less susceptible to hydridic attack. Therefore, it is not surprising that 5b does not react with an excess of 4 to give a bis-carbene complex.

Attempts to isolate or spectroscopically observe iron or ruthenium oxycarbene hydride or alkyl complexes have been thwarted by the apparent ease with which the carbene ligand reverts to the metal carbonyl and zirconium hydride or inserts into the Group VIII metal hydride or alkyl bond.

The mechanism for the formation of $Cp(PMe_3)_2M\text{-}CH_2O\text{-}Zr(H)Cp^*_2$ (M = Fe, Ru) (Scheme V) is believed to proceed through the initial formation of a transient oxycarbene complex, 14, which is in equilibrium with 15, where the carbene ligand has inserted into the M-H bond. Trapping of the coordinatively unsaturated 15 by free PMe_3 to give 11 is rapid, since the rate of formation of 11 is independent of phosphine concentration. That only 10 and 1 are observed in solution in the absence of PMe_3 indicates that the equilibria between the starting complexes, 14 and 15, lie far toward the metal carbonyl and zirconium hydride. These equilibria also provide a mechanism for hydride exchange between iron and zirconium that is required to explain deuterium incorporation into the hydride site of 10a from D_2 in the presence of 1.

In the case of the reaction of 1 with the iron and ruthenium methyl complexes 12 an intramolecular rearrangement pathway, via β-elimination, is available to the coordinatively unsatured intermediate, 16, formed upon carbene insertion into the $M\text{-}CH_3$ bond

Scheme V

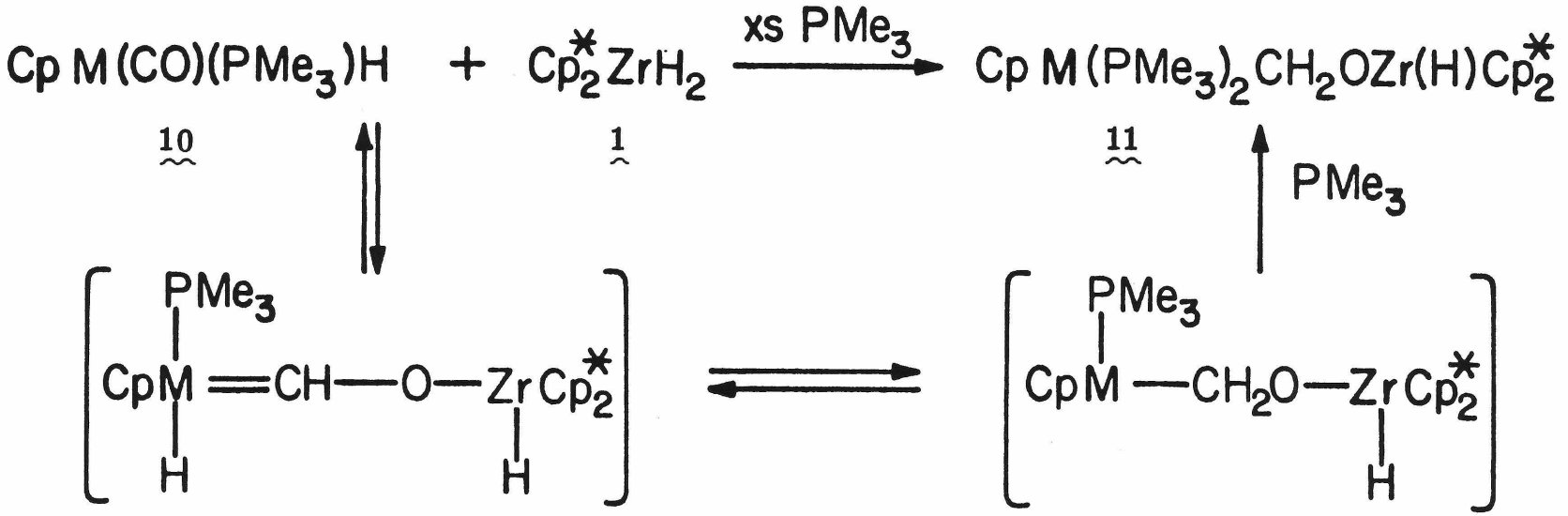

M = Fe, Ru

(Scheme VI). This step affords the zirconium-containing product, $Cp^*_2Zr(OCH{=}CH_2)H$, and CpM(CO)H which can be trapped by free PMe_3 to give the observed ruthenium product, 10b, or react further to give the myriad of iron products seen. As in the reaction of 10 with 1 neither the oxycarbene nor inserted intermediates have been observed by spectroscopic methods.

The results discussed above have shown that bis(pentamethylcyclopentadienyl)zirconium hydrides readily add to the C-O bond of Group VIII transition metal carbonyls. However, the oxycarbene species formed are often unobservable due to the reversibility of the hydride addition or the rapid migratory insertion of the carbene ligand into a metal hydride or alkyl bond. The spectroscopic properties of the cobalt and rhodium oxycarbene compounds that can be isolated suggest that the oxycarbene ligand is similar to those of Fischer-Type carbene complexes.

Scheme VI

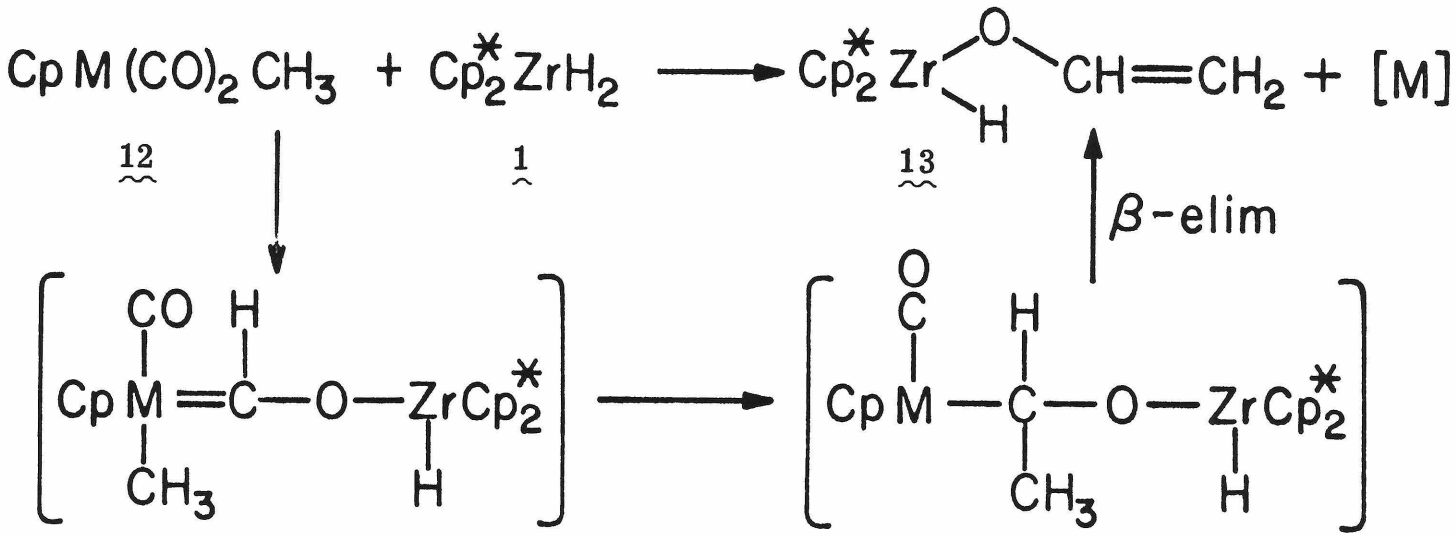

M = Fe, Ru

Table I. NMR[a] and IR[b] data.

Compound	IR	^{1}H NMR	
$CpCo(CO)_2ZrCp^*_2$ (3a)	ν(CO) 1737, 1683	$C_5\underline{H}_5$	4.91 s
		$C_5(C\underline{H}_3)_5$	1.71 s
$CpRh(CO)_2ZrCp^*_2$ (3b)	ν(CO) 1752, 1696	$C_5\underline{H}_5$	5.40 s
		$C_5(C\underline{H}_3)_5$	1.76 s
$Cp(CO)Co{=}CHO{-}Zr(Cl)Cp^*_2$ (5a)	ν(CO) 1947	$Co{=}C\underline{H}O{-}Zr$	12.6 s
		$C_5\underline{H}_5$	5.48 s
		$C_5(C\underline{H}_3)_5$	1.82 s
$Cp(CO)Rh{=}CHO{-}Zr(Cl)Cp^*_2$ (5b)	ν(CO) 1952	$Rh{=}C\underline{H}O{-}Zr$	13.1 s
		$C_5\underline{H}_5$	4.94 s
		$C_5(C\underline{H}_3)_5$	1.87 s
$Cp(CO)Co{=}CHO{-}Zr(F)Cp^*_2$ (7a)	ν(CO) 1948	$Co{=}C\underline{H}O{-}Zr$	12.6 s
		$C_5\underline{H}_5$	4.87 s
		$C_5(CH_3)_5$	1.80 s
$Cp(CO)Rh{=}CHO{-}Zr(F)Cp^*_2$ (7b)[c]	ν(CO) 1956	$Rh{=}C\underline{H}O{-}Zr$	13.1 s
		$C_5\underline{H}_5$	5.41 s
		$C_5(C\underline{H}_3)_5$	1.80 s
$Cp(H)Ru(CO)_2ZrCp^*_2$ (9)	ν(CO) 1706, 1671	$C_5\underline{H}_5$	5.17 s
		$C_5(C\underline{H}_3)_5$	1.67 s
		$C_5(C\underline{H}_3)_5$	1.74 s
		$Ru\underline{H}$	-15.7 s

Table I (continued)

Compound	IR	^{1}H NMR		
$Cp(PMe_3)_2Fe\text{-}CH_2O\text{-}Zr(H)Cp^*_2$ (11a)		Fe-C<u>H</u>$_2$O-Zr	5.07 t	$^3J_{PH}$ = 7
		$C_5\underline{H}_5$	3.87 t	$^3J_{PH}$ = 2
		$C_5(C\underline{H}_3)_5$	2.07 s	
		$P(C\underline{H}_3)_3$	1.04 t	$^2J_{PH}$ = 3
		Zr<u>H</u>	5.25 s	
$Cp(PMe_3)_2Ru\text{-}CH_2O\text{-}Zr(H)Cp^*_2$ (11b)		Ru-C<u>H</u>$_2$O-Zr	5.32 dd	$^3J_{PH}$ = 7, 9
		$C_5\underline{H}_5$	4.99 s	
		$C_5(C\underline{H}_3)$	2.09 s	
		$P(C\underline{H}_3)_3$	1.11 m	
		Zr<u>H</u>	5.22 s	

a) NMR spectra in benzene-$\underline{d}_6$ or toluene-$\underline{d}_8$ at 34° C at 90 MHz. Chemical shifts in δ measured from internal TMS, coupling constants in Hz.

b) IR spectra recorded as nujol mulls. Values given in cm^{-1}. Detailed spectra are listed in the experimental section.

c) IR spectrum in C_6H_6.

Table II. Data Collection and Refinement Conditions for $CpCo(CO)_2ZrCp^*_2$.

Formula	$C_{27}H_{35}CoO_2Zr$
Formula weight	541.73 g/mol
Space group	$P2_1/c$
a	15.624(6) Å
b	13.885(13) Å
c	11.221(4) Å
β	94.01(3)°
V	2424.7(1.0) Å
Z	4
ρ_{calc}	1.49 g/cm^{-3}
Crystal size	0.5 × 0.4 × 0.2 mm
λ	0.71069 Å (MoK_α, graphite monochromator)
μ	1.95 cm^{-1}
Scan range	0.75° in 2θ below K_{α_1}
	0.75° in 2θ above K_{α_2}
2θ limits	2.5-65°
Scan rate	1.2°/min
Bkgrd time/scan time	0.7
Total number of averaged data	8824
Refinement on	F_o^2

Table III, Part A. Atomic Positions and Gaussian Amplitudes of Non-Hydrogen Atoms.

Atom	X*	Y	Z	U^*_{11}	U_{22}	U_{33}	U_{12}	U_{13}	U_{23}
Zr	74565(3)	48394(4)	32578(2)	240(2)	334(2)	246(2)	-7(3)	19(2)	12(2)
Co	76280(5)	46318(6)	6909(6)	458(5)	429(5)	263(3)	20(4)	57(2)	18(3)
O1	74422(35)	31946(35)	25153(45)	470(33)	382(31)	464(31)	-6(27)	41(26)	70(26)
O2	76807(41)	66470(40)	14429(46)	777(45)	394(34)	435(33)	-36(32)	46(31)	42(26)
C1	75203(56)	37708(53)	17328(68)	375(40)	439(46)	353(42)	6(43)	46(35)	-20(39)
C2	76224(54)	58335(54)	17272(67)	438(48)	389(46)	388(42)	16(42)	66(42)	69(39)
C3	76628(52)	39250(51)	90596(52)	939(61)	687(50)	329(43)	51(45)	140(37)	-110(33)
C4	69831(50)	45938(54)	89792(51)	864(57)	790(56)	317(32)	-80(46)	-37(34)	-54(34)
C5	73462(59)	54964(52)	91936(52)	1207(69)	691(50)	285(31)	385(51)	60(39)	135(32)
C6	82310(54)	53790(56)	93762(55)	976(61)	820(60)	365(35)	-217(50)	190(38)	8(37)
C7	84215(45)	44252(54)	92874(54)	590(43)	824(53)	425(37)	16(42)	192(33)	-16(36)
C8	58605(34)	45301(46)	27634(53)	252(29)	587(42)	549(38)	-59(29)	22(27)	-130(31)
C9	59727(37)	55451(46)	27289(53)	319(33)	599(41)	471(37)	101(31)	56(29)	72(31)
C10	62245(36)	58594(44)	38825(57)	260(32)	482(39)	671(43)	37(29)	99(31)	-126(33)
C11	62501(33)	50422(50)	46476(46)	270(27)	776(48)	383(48)	58(32)	76(23)	-41(32)
C12	60550(37)	42340(46)	39490(58)	314(32)	518(42)	679(44)	-7(30)	183(31)	119(34)
C13	54864(45)	39327(62)	17468(71)	379(40)	1196(73)	950(59)	-56(45)	-168(40)	-501(53)
C14	56929(48)	61788(67)	16804(75)	488(48)	1260(79)	1026(66)	249(50)	-4(48)	437(59)
C15	63294(50)	69025(54)	42291(83)	529(50)	624(52)	1426(79)	95(42)	17(52)	-329(51)
C16	62584(45)	50211(70)	59860(55)	512(41)	1764(90)	405(35)	92(57)	97(30)	-23(51)
C17	59440(50)	32212(59)	43982(86)	522(49)	787(59)	1546(84)	-109(44)	355(44)	396(57)
C18	90891(34)	51732(47)	33217(48)	272(27)	688(42)	420(30)	-82(32)	27(23)	9(33)
C19	87244(37)	58489(43)	40675(50)	343(34)	489(39)	434(34)	-106(30)	-95(28)	11(29)
C20	84232(34)	53510(41)	50478(44)	309(28)	525(41)	326(28)	-53(28)	-16(23)	-63(27)
C21	85483(35)	43575(43)	48852(47)	304(31)	507(37)	372(31)	-20(29)	-75(26)	116(27)
C22	89703(36)	42356(43)	38149(53)	265(31)	433(38)	597(39)	46(28)	-63(29)	-72(31)
C23	96005(41)	53777(55)	22657(61)	395(35)	982(61)	672(43)	-113(40)	171(33)	70(42)
C24	88007(46)	69314(49)	39677(62)	605(46)	554(45)	708(47)	-193(37)	-195(38)	94(36)
C25	82076(45)	58410(53)	61944(56)	555(44)	823(54)	494(39)	-79(41)	-89(34)	-126(37)
C26	83890(47)	35624(51)	57716(61)	633(49)	671(50)	631(45)	-68(41)	-150(39)	175(38)
C27	93148(42)	33060(53)	33646(67)	414(41)	708(51)	899(56)	131(38)	-59(40)	-85(42)

Final Scale Factor = 0.9158(20)

Final Secondary Extinction Factor = $0.0692(181) \times 10^{-6}$

*Positional parameters x 10^5, thermal parameters x 10^4; the form of the thermal ellipsoid is $\exp[-2\pi^2(h^2a^{*2}U_{11} + \ldots + 2klb^*c^*U_{23})]$.

Table III, Part B. Atomic Positions ($\times 10^4$) for Hydrogen Atoms.

Atom	X	Y	Z	Atom	X	Y	Z
H3	7623	3265	8961	H171	5457	2930	4010
H4	6405	4468	8830	H172	6512	2886	4325
H5	7078	6097	9203	H173	5862	3299	5331
H6	8672	5870	9573	H231	9431	4789	1650
H7	8992	4152	9353	H232	9530	6029	2032
H131	4912	3675	1977	H233	245	5184	2560
H132	5396	4331	1064	H241	8255	7202	3728
H133	5890	3387	1636	H242	9106	7164	4850
H141	5080	6135	1541	H243	9245	7051	3280
H142	5915	6798	1827	H251	7747	6350	5961
H143	5967	5879	968	H252	8029	5365	6736
H151	5814	7264	3950	H253	8751	6211	6487
H152	6547	6992	4996	H261	8153	3857	6502
H153	6812	7331	3638	H262	8068	3062	5370
H161	5678	5092	6237	H263	9023	3297	6038
H162	6597	4479	6355	H271	8883	2828	3332
H163	6587	5687	6271	H272	9598	3438	2603
				H273	9837	3100	3990

B^* = 7.00 for all hydrogens.

* Thermal parameters are of the form $\exp[-B((\sin^2\theta)/\lambda^2)]$.

Table IV. Bond Distances (Å) in $CpCo(CO)_2ZrCp^*_2$.

Zr-Co	2.926(1)	C10-C11	1.422(8)
Zr-C1	2.272(8)	C11-C12	1.390(8)
Zr-O1	2.431(5)	C12-C8	1.405(8)
Co-C1	1.687(8)	C8-C13	1.496(10)
Co-O1	2.888(5)	C9-C14	1.509(10)
C1-O1	1.200(9)	C10-C15	1.506(10)
Zr-C2	2.233(8)	C11-C16	1.501(9)
Zr-O2	3.266(6)	C12-C17	1.508(11)
Co-C2	2.034(8)	Zr-Cp*1*	2.238(6)
Co-O2	2.922(6)	Zr-C18	2.589(6)
C2-O2	1.179(10)	Zr-C19	2.542(6)
Co-C3	2.081(7)	Zr-C20	2.529(5)
Co-C4	2.106(7)	Zr-C21	2.501(6)
Co-C5	2.087(7)	Zr-C22	2.546(6)
Co-C6	2.082(7)	C18-C19	1.404(8)
Co-C7	2.091(7)	C19-C20	1.408(8)
C3-C4	1.409(10)	C20-C21	1.407(8)
C4-C5	1.390(10)	C21-C22	1.420(8)
C5-C6	1.393(10)	C22-C18	1.432(8)
C6-C7	1.363(10)	C18-C23	1.502(9)
C7-C3	1.382(10)	C19-C24	1.513(9)
Co-Cp*	1.725(7)	C20-C25	1.514(9)
Zr-C8	2.553(6)	C21-C26	1.518(9)
Zr-C9	2.548(6)	C22-C27	1.500(9)
Zr-C10	2.528(6)	Zr-Cp*2*	2.239(6)
Zr-C11	2.545(6)		
Zr-C12	2.518(6)		
C8-C9	1.421(8)		
C9-C10	1.396(8)		

*Cp = C3-C7 ring centroid, Cp*1 = C8-C12 ring centroid, Cp*2 = C18-C22 ring centroid.

Table V. Bond angles (deg) in $CpCo(CO)_2ZrCp^*_2$.

Zr-C1-O1	82.7(5)	C9-C8-C13	124.8(6)
Co-C1-O1	176.7(7)	C12-C8-C13	127.4(6)
Zr-C1-Co	94.1(3)	C8-C9-C14	124.7(6)
Zr-Co-C1	50.8(3)	C10-C9-C14	126.0(6)
Co-Zr-C1	35.2(2)	C9-C10-C15	124.0(6)
Co-Zr-O1	64.5(1)	C11-C10-C15	127.9(6)
Zr-C2-O2	144.7(6)	C10-C11-C16	128.1(6)
Co-C2-O2	128.9(6)	C12-C11-C16	122.3(6)
Zr-C2-Co	86.4(3)	C11-C12-C17	126.2(6)
Zr-Co-C2	49.6(2)	C8-C12-C17	124.5(6)
Co-Zr-C2	44.0(2)	C18-C19-C20	108.0(5)
Zr-Co-Cp	168.2(5)	C19-C20-C21	108.9(5)
Co-Zr-Cp*1	109.5(5)	C20-C21-C22	107.7(5)
Co-Zr-Cp*2	110.2(5)	C21-C22-C18	107.4(5)
Cp*1-Zr-Cp*2	139.2(5)	C22-C18-C19	108.0(5)
C3-C4-C5	106.7(6)	C19-C18-C23	127.2(5)
C4-C5-C6	108.0(6)	C22-C18-C23	124.6(5)
C5-C6-C7	108.8(7)	C18-C19-C24	125.6(5)
C6-C7-C3	108.2(6)	C20-C19-C24	125.3(5)
C7-C3-C4	108.3(6)	C19-C20-C25	123.3(5)
C8-C9-C10	108.2(5)	C21-C20-C25	126.3(5)
C9-C10-C11	107.7(5)	C20-C21-C26	126.7(5)
C10-C11-C12	107.9(5)	C22-C21-C26	125.1(5)
C11-C12-C8	108.8(5)	C21-C22-C27	125.9(5)
C12-C8-C9	107.3(5)	C18-C22-C27	126.4(5)

Table VI. Least-Squares Planes.

Metal-Carbonyl Substructure

Atom	Deviation from Plane (A)
Zr	0.0101(5)
Co	0.0097(7)
C1	-0.0013(78)
C2	-0.0055(78)
O1	-0.0086(51)
O2	-0.0044(56)
Cp	0.0283
Cp*1	2.1170
Cp*2	-2.0754

Cp Ring

Atom	Deviation from Plane (A)
C3	0.0081(69)
C4	-0.0078(70)
C5	0.0046(74)
C6	0.0004(74)
C7	-0.0054(68)

Cp*1 Ring

Atom	Deviation from Plane (A)
C8	0.0080(58)
C9	0.0026(60)
C10	-0.0120(60)
C11	0.0171(57)
C12	-0.0157(62)

Cp*2 Ring

Atom	Deviation from Plane (A)
C18	0.0132(56)
C19	-0.0195(57)
C20	0.0182(53)
C21	-0.0098(55)
C22	-0.0021(58)

Experimental

General Considerations. All manipulations were performed under an inert atmosphere by employing a nitrogen-filled glove box and vacuum-line techniques. Hydrogen, deuterium, nitrogen and argon were purified by passing through MnO on vermiculate[25] and activated 4 Å molecular sieves. Benzene, toluene and pet ether (30°-60°), including NMR solvents, were vacuum transferred from $LiAlH_4$ or molecular sieves, then from "titanocene"[26] prior to use Carbon monoxide (MCB), ^{13}C carbon monoxide (Monsanto-Mound) and PMe_3 (Strem) were used as received; $NHMe_2$ was vacuum transferred from 4 Å molecular sieves.

$CpCo(CO)_2$,[23] $CpRh(CO)_2$,[24] $CpFe(CO)_2CH_3$,[27] $CpRu(CO)_2CH_3$,[28] $CpRu(CO)_2H$,[29] $CpFe(CO)(PMe_3)H$,[30] were prepared by literature methods. $CpFe(CO)(PMe_3)CH_3$ was made by treatment of $CpFe(CO)(PMe_3)H$ with CCl_4 followed by CH_3MgBr and isolated by sublimation. $CpRu(CO)(PMe_3)H$ was made by a variation of the reported synthesis of $CpRu(CO)(PPh_3)H$.[29] ^{13}CO enrichment of the carbonyls of $CpRh(CO)_2$ was done by photolysis under a ^{13}CO atmosphere. $Cp^*_2ZrH_2$[2] and $[Cp^*_2ZrN_2]_2N_2$[31] were prepared by literature methods. Conproportionation of $Cp^*_2ZrH_2$ and $Cp^*_2ZrX_2$ (X = F, Cl) at 150° C for 2 weeks under an H_2 atmosphere affords Cp^*_2ZrHX in excellent yield.

^1H NMR spectra were recorded in C_6D_6 or C_7D_8 with TMS as an internal reference using Varian EM-390, JOEL FX90Q and Bruker WM-500 spectrometers. ^{13}C NMR spectra were recorded on the JOEL and Bruker instruments. IR spectra were recorded as IR mulls or

benzene solutions on a Beckmann IR H240 spectrophotomer. Elemental analyses were performed by Alfred Bernhardt Analytical Laboratory and Dornis and Kolbe Microanalytical Laboratory.

Procedures: $CpCo(CO)_2ZrCp^*_2$ (3a). A 0.75 M toluene solution of $CpCo(CO)_2$ (950 μl, 0.714 mmol) was added via syringe to $Cp^*_2ZrH_2$ (250 mg, 0.689 mmol) dissolved in 30 ml pet ether at -78° C. On warming to room temperature and stirring for 3 hours the reaction solution turned dark green. The solution was concentrated to ca. 3 ml and filtered to afford dark green, crystalline $CpCo(CO)_2ZrCp^*_2$ (170 mg, 46%) which was washed with cold pet ether and dried in vacuo to remove excess $CpCo(CO)_2$. 0.83 equivalents of H_2 per equivalent of $Cp^*_2ZrH_2$ were recovered through a Toepler pump at the completion of the reaction.

In an alternative synthesis, neat $CpCo(CO)_2$ (175 μl, 1.36 mmol) was added to a pet ether solution of $[Cp^*_2ZrN_2]_2N_2$ (500 mg, 0.62 mmol) via syringe at -78° C. Similar work-up as before afforded 3a (500 mg, 74%) as dark green-black crystals. Anal. Calcd. for $C_{27}H_{35}CoO_2Zr$: C, 59.86; H, 6.51; Co, 10.88; O, 5.91; Zr, 16.84. Found: C, 59.98; H, 6.62; Co, 10.91; O, 5.74; Zr, 17.01. IR (nujol mull): 1737 vs, 1683 cs, 1125 w, 1020 w, 800 m, 660 m.

$CpCo(CO)_2ZrCp^*_2 + CO$. A C_6D_6 solution of 3a (40 mg) in a NMR tube was placed under 650 Torr CO at -78°, sealed, warmed to room temperature and then to 80° C to effect reaction.

Structure Determination for $CpCo(CO)_2ZrCp^*_2$. A single crystal of 3a was mounted in a glass capillary under N_2. Rotation and Weisenberg photographs (using CuKα radiation) indicated a monoclinic

lattice with systematic absences in the a* and c* axes (h01, $1 = 2n+1$) consistent with the space group P_{2_1}/c. Observation of systematic absences along the b* axis (0k0, $k = 2n+1$) on the diffractometer confirmed this assignment. The crystal was mounted with its long axis (b) slightly skew to the φ axis of a locally modified Syntex $P2_1$ diffractometer; details on unit cell parameters and data collection are given in Table II.

The intensities of four check reflections were monitored every 100 reflections and showed a small (2%) decrease over the course of the data collection. A fifth check reflection, the 415, had a significant (25%) decrease in intensity during the last fourth of the data set, when reflections were being measured at high 2θ angles in the $hk\bar{l}$ octant. Examination of peak profiles indicated that this intensity loss was due to improper centering of the diffractometer on the check reflection, rather than crystal movement or decomposition. Measurement of the intensity of this reflection outside the scan sequence remained consistent with the other four reflections.

An averaged data set of 8824 reflection intensities was assembled from the collected data after deletion of duplications and systematic absences. The data set was placed on an absolute scale by means of a Wilson plot using scattering factors for Zr and Co calculated from Cromer and Mann[32] and for C, H and O from Cromer and Waber.[33] No absorption correction was applied.

The locations of the two metal atoms were determined from a three-dimensional Patterson map. A structure factors computation using these positions gave an R index ($\Sigma \| F_o | - | F_c \| / \Sigma | F_o |$) of 0.367.

Generation of a Fourier map led to the locating of all non-hydrogen atoms which were then placed into the structure factors program in two stages, yielding an R index of 0.314. Several cycles of least-squares refinement, minimizing $\Sigma w[F_o^2-(F_c/k)^2]^2$, interspaced by Fourier and difference Fourier syntheses, led to an R factor of 0.159, using isotopic thermal parameters for all atoms. At this point anisotropic thermal parameters were introduced in two least-squares cycles, initially for the two metals and then for all other non-hydrogens, yielding an 0.130 R index. A least-squares cycle refining the temperature parameters of all atoms, followed by two cycles refining metal parameters and the scale factor gave a R factor of 0.125. Examination of the structure factors showed that significant noise was being introduced into the calculation by the low intensity data. It was determined that the R index for the 3843 data with $F_o^2 \geq 3\sigma(F_o^2)$ was approximately 0.065 compared to 0.125 for all data. The calculation was therefore continued using only the higher intensity data. A secondary extinction coefficient of 0.05 was also introduced.[34] At this point a difference Fourier map was generated in the plane of the Cp ring and the five hydrogens were tentatively located. Planes were also generated perpendicular to the ring carbon-methyl carbon axes of the Cp* rings at a distance of 0.30A from each methyl carbon and these hydrogens were placed at 0.92A from each carbon. All hydrogens were given an arbitrary isotopic temperature factor of 7.00, about 1.00 greater than that of the carbon to which they were attached. Addition of the hydrogen atoms and several least-squares cycles refining the non-hydrogen atoms, scale factor and secondary extinction

coefficient in varyingly blocked matrices, gave an R factor of 0.063. Re-positioning the hydrogens as above and three additional cycles gave a final R factor of 0.056 with a goodness of fit ($[\Sigma w(F_o^2-s^2F_c^2)/(n-p)]^{\frac{1}{2}}$, $w = 1/\sigma^2(F_o^2)$, $1/s$ = scale factor for F_o, n = total number of reflections, p = total number of parameters) of 1.94 for 3842 reflections with $F_o \geq 3\sigma(F_o)$ giving a data-to-parameter ratio of 13.7. A structure factors calculation using all data gave an R index of 0.120.

CpRh(CO)$_2$ZrCp$^*_2$ (3b). Pet ether solutions of Cp$^*_2$ZrH$_2$ (500 mg, 1.38 mmol) and CpRh(CO)$_2$ (200 μl, 375 mg, 1.67 mmol) were combined at -78° C, warmed, and stirred at room temperature for 20 minutes. After this time all solvent and excess CpRh(CO)$_2$ were removed in vacuo. CpRh(CO)$_2$Zr Cp$^*_2$ (510 mg, 44%) was recrystallized from toluene. IR (nujol mull): 1752 vs, 1696 vs, 1027 w, 780 s, 650 m.

Addition of CpRh(CO)$_2$ (ca. 10 μL, ca. 0.08 mmol)) to a C_6D_6 solution of [Cp$^*_2$ZrN$_2$]$_2$N$_2$ (30 mg, 0.04 mmol) in an NMR tube gave an ^{1}H NMR spectrum identical to that of 3b prepared from Cp$^*_2$ZrH$_2$. The IR spectrum of the C_6D_6 solution was also the same as that of 3b prepared by the above procedure.

Variable Temperature ^{13}C NMR of CpRu(CO)$_2$ZrCp$^*_2$. Substitution of CpRh(^{13}CO)$_2$ for CpRh(CO)$_2$ in the above procedure allowed the preparation of 3b enriched with ^{13}C at the carbonyl carbons. Variable temperature ^{13}C NMR spectra at 22.5 MHz yielded the coalescence temperature and a spectrum at -70° C at 125.8 MHz provided an approximate chemical shift difference of the resonances of the inequivalent carbonyl carbons in the low temperature limit. Use of the Gutowsky-Holm approximation[35] allowed the calculation of an upper

limit for the barrier to carbonyl interchange.

Cp(CO)Co=CHO-Zr(Cl)Cp_2^* (5a). Toluene solutions of Cp_2^*ZrHCl (400 mg, 1.01 mmol) and $CpCo(CO)_2$ (150 μl, 220 mg, 1.20 mmol) were mixed at -78°C, then warmed to 25° C with stirring for 2 hours to effect reaction. Concentration to ca. 2 ml and addition of 10 ml pet ether afforded red crystals which were isolated by filtration, washed with cold pet ether and dried to give Cp(CO)Co=CHO-Zr(Cl)Cp_2^* (260 mg, 45%). Anal. Calcd. for $C_{27}H_{36}ClCoO_2Zr$: C, 56.09; H, 6.28; Cl, 6.13. Found: C, 51.87; H, 5.96; Cl, 5.74. IR (nujol mull): 1947 vs, 1350 m, 1308 m, 1295 vs, 1165 w, 1110 w, 1020 w, 802 m, 670 w, 532 w, 495 m.

Cp(CO)Rh=CHO-Zr(Cl)Cp_2^* (5b). Treatment of $CpRh(CO)_2$ (200 μl, 1.67 mmol) instead of $CpCo(CO)_2$ with Cp_2^*ZrHCl (600 mg, 1.51 mmol) by the above procedure afforded 5b (720 mg, 78%) as golden crystals. Anal. Calcd. for $C_{27}H_{36}ClO_2RhZr$: C, 52.12; H, 5.83; Cl, 5.70. Found: C, 51.95; H, 6.04; Cl, 5.78. IR (nujol mull): 1952 vs, 1353 s, 1308 m, 1015 w, 783 m, 712 w, 650 w.

Cp(CO)Co=CHO-Zr(F)Cp_2^* (7a). Treatment of $CpCo(CO)_2$ (165 mg, 150 μl, 0.94 mmol) with Cp_2^*ZrHF (300 mg, 0.83 mmol) by the method used for 5a afforded 7a (260 mg, 57%) as orange crystals. IR (nujol mull): 1948 vs, 1350 m, 1300 vs, 1167 w, 1111 w, 1021 w, 801 m, 670 w, 614 w, 538 m, 498 m.

Cp(CO)Rh=CHO-Zr(F)Cp_2^* (7b). $CpRh(CO)_2$ (15 μl, 0.12 mmol) was added to a C_6D_6 solution of Cp_2^*ZrHF (30 mg, 0.08 mmol) in a NMR tube at 25° C. Cp(CO)Rh=CHO-Zr(F)Cp_2^* was identified by its ^1H NMR and IR spectra. IR (C_6H_6 solution): 1953 vs, 1382 m, 1304 s, 1166 w, 1008 w, 792 w.

Cp(CO)Rh=CHO-Zr(Cl)Cp^*_2 + HCl. HCl (0.05 mmol) was condensed onto a C_7D_8 solution of 5b (25 mg, 0.05 mmol) at -196° C in an NMR tube, which was then sealed and warmed to room temperature. The reaction was followed by ^{1}H NMR spectroscopy.

Cp(H)$Ru(CO)_2ZrCp^*_2$ (9). $CpRu(CO)_2H$ was prepared using the procedure of Humphries and Knox[29] by reflux of $Ru_3(CO)_{12}$ (250 mg, 0.39 mmol) and cyclopentadiene (ca. 3 ml, ca. 36 mmol) in 60 ml heptane for 1½ hour. $Cp^*_2ZrH_2$ (405 mg, 1.12 mmol) was added to this reaction mixture at 25° C causing the solution to turn red over 10 minutes. Concentration to ca. 5 ml and cooling to -78° C precipitated the product which was isolated by filtration and washed with cold pet ether giving Cp(H)$Ru(CO)_2ZrCp^*_2$ (380 mg, 59%) as brick red crystals.

Alternatively, 9 was prepared from $Ru_3(CO)_{12}$ (170 mg, 0.27 mmol), CpH (ca. 3 ml, aa. 36 mmol) and $[Cp^*_2ZrN_2]_2N_2$ (290 mg, 0.36 mmol) using a similar procedure. In this case all gas liberated during the course of the reaction was collected through a Toepler pump. The ^{1}H NMR and IR spectra of 9 prepared from $[Cp^*_2ZrN_2]_2N_2$ were identical to those of 9 made from $Cp^*_2ZrH_2$. Anal. Calcd. for $C_{27}H_{36}O_2RuZr$: C, 55.45; H, 6.20; Ru, 17.28. Found: C, 55.09; H, 6.03; Ru, 17.50. IR (nujol mull): 1706 vs, 1671 vs, 1021 m, 831 w, 794 m, 718 m, 668 m.

Cp(H)$Ru(CO)_2ZrCp^*_2$ + CO. A C_6D_6 solution of 9 (27 mg, 0.05 mmol) was placed under 700 Torr CO at -78° C in an NMR tube, sealed, and warmed to room temperature.

$Cp(PMe_3)_2Fe\text{-}CH_2O\text{-}Zr(H)Cp^*_2$ (11a). Toluene (15 ml) and PMe_3 (0.49 mmol) were added to a mixture of $CpFe(CO)(PMe_3)H$ (90 mg, 0.40 mmol) and $Cp^*_2ZrH_2$ (135 mg, 0.37 mmol) at -196° C. On warming to room temperature for 2 hours red crystals formed. Concentration to ca. 2 ml, filtration and washing with cold pet ether afforded $Cp(PMe_3)_2Fe\text{-}CH_2O\text{-}Zr(H)Cp^*_2$ (125 mg, 51%). Anal. Calcd. for $C_{32}H_{56}FeOP_2Zr$: C, 57.73; H, 8.48; P, 9.30. Found: C, 57.88; H, 8.10; P, 9.30.

$Cp(PMe_3)_2Ru\text{-}CH_2O\text{-}Zr(H)Cp^*_2$ (11b). C_6D_6 and PMe_3 (0.08 or 0.68 mmol) were added to a mixture of $CpRu(CO)(PMe_3)H$ (20 mg, 0.07 mmol) and $Cp^*_2ZrH_2$ (25 mg, 0.07 mmol) at -196° C in an NMR tube. The tube was sealed, warmed to room temperature and the reaction monitored by NMR spectroscopy. $Cp(PMe_3)_2Ru\text{-}CH_2O\text{-}Zr(H)Cp^*_2$ was identified by the similarity of its ^1H NMR spectrum to that of 11a.

$CpFe(CO)_2CH_3 + Cp^*_2ZrH_2$. NMR samples of 1 (50 mg, 0.14 mmol) and 12a (30 mg, 0.15 mmol) were prepared in C_7D_8 with and without PMe_3 (0.25 mmol) at -196° C. After sealing the samples were warmed to -78° C to liquify the solvent, then to 25° C. The reactions were monitored by ^1H NMR spectroscopy the products being identified by comparison to previously reported spectra.

$CpRu(CO)_2CH_3 + Cp^*_2ZrH_2$. A similar procedure to that above was employed using 1 (30 mg, 0.08 mmol), 12b (20 mg, 0.08 mmol) and PMe_3 (0.10 mmol).

References

1. (a) Wolczanski, P. T.; Threlkel, R. S.; Bercaw, J. E. J. Amer. Chem. Soc. 101, 218 (1979);
(b) Threlkel, R. S.; Bercaw, J. E. J. Amer. Chem. Soc. 103, 2650 (1981).
2. Manriquez, J. M.; McAlister, D. R.; Sanner, R.D.; Bercaw, J. E. J. Amer. Chem. Soc. 100, 2716 (1978).
3. (a) Mango, F. D.; Dvoretzky, I. J. Amer. Chem. Soc. 88, 2654 (1966);
(b) Empsall, H. D.; Hyde, E. M.; Markham, M.; McDonald, W. S.; Norton, M. C.; Shaw, B. L.; Weeks, B. J. Chem. Soc., Chem. Commum., 589 (1977).
4. Barger, P. T.; Bercaw, J. E. J. Organomet. Chem. 201, C39 (1980).
5. Sanner, R. D.; Manriquez, J. M.; Marsh, R. E.; Bercaw, J. E. J. Amer. Chem. Soc. 98, 8351 (1976).
6. Rattinger, E.; Muller, R.; Vahrenkamp, H. Angew. Chem. Int. Ed. Engl. 16, 332 (1977).
7. Wong, K. S.; Scheidt, W. R.; Labinger, J. A. Inorg. Chem. 18, 1709 (1979).
8. Guggenberger, L. J.; Meakin, P.; Tebbe, F. N. J. Amer. Chem. Soc. 96, 5420 (1976).
9. Dahan, F.; Jeannin, Y. J. Organomet. Chem. 136, 25 (1977).
10. Fachinetti, G.; Fochi, G.; Floriani, C. J. Chem. Soc., Dalton Trans., 1946 (1977).

11. (a) Connor, J. A.; Fischer, E. O. J. Chem. Soc. A, 578 (1969).
(b) Fischer, E. O.; Kollmeier, H.-J., Chem. Ber. 104, 1339 (1971).
(c) Klabunde, U.; Fischer, E. O. J. Amer. Chem. Soc. 89, 7141 (1967).

12. (a) Erwin, D. K.; Ph.D. Thesis, California Institute of Technology, 1979.
(b) Bercaw, J. E. Adv. Chem. Ser. N . 167, 136 (1978).

13. Colton, R.; Commons, C. J.; Haskins, B. F. J. Chem. Soc., Chem. Commun., 363 (1975).

14. Manassero, M.; Sansoni, M.; Longoni, G. J. Chem. Soc., Chem. Commun., 919 (1976).

15. Pasynskii, A.; Skripkin, Y.; Eremenkov, I. L.; Kalinnikov, V.; Aleksandrov, G.; Andrianov, V. G.; Struchkov, Y. J. Organomet. Chem. 165, 49 (1979).

16. (a) Longato, B.; Norton, J. R.; Huffman, J. C.; Marsella, J. A.; Caulton, K. G. J. Amer. Chem. Soc. 103, 209 (1981).
(b) Marsella, J. A.; Huffman, J. C.; Caulton, K. G.; Longato, B.; Norton, J. R. J. Amer. Chem. Soc. 104, 6360 (1982).

17. Herrmann, W. A.; Ziegler, M. L.; Weidenhammer, K.; Biersack, H. Angew. Chem. Int. Ed. Engl. 18, 960 (1979).

18. Berry, D. H.; Bercaw, J. E., manuscript in preparation.

19. Lewis, L. N.; Caulton, K. G. Inorg. Chem. 19, 3201 (1980).

20. Marsella, J. A.; Caulton, K. G. Organometallics 1, 274 (1982).

21. Connor, J. A. Topics in Current Chemistry 71, 72 (1977).

22. Brown, F. J. Prog. Inorg. Chem. 27, 1 (1980).

23. Piper, T. S.; Cotton, F. A.; Wilkinson, G. J. Inorg. Nucl. Chem. 1, 165 (1955).

24. Fischer, E. O.; Bittler, K. Z. Naturforsch. 16b, 225 (1961).

25. Brown, T. L.; Dickerhoof, D. W.; Bafus, D. A.; Morgan, G. L. Rev. Sci. Instrum. 33, 491 (1962).

26. Marvich, R. H.; Brintzinger, H. H. J. Amer. Chem. Soc. 93, 2046 (1971).

27. Piper, T. S.; Wilkinson, G. J. Inorg. Nucl. Chem. 3, 104 (1956).

28. Davison, A.; McCleverty, J. A.; Wilkison, G. J. Chem. Soc., 1133 (1963).

29. Humphries, A. P.; Knox, S. A. R. J. Chem. Soc., Dalton Trans. 1710 (1975).

30. Kalck, P.; Poilblanc, R. C. R. Acad. Sc. Paris C 274, 66 (1972).

31. Manriquez, J. M.; Bercaw, J. E. J. Amer. Chem. Soc. 96, 6229 (1974).

32. Cromer, D. T.; Mann, B. Acta Cryst. 24A, 321 (1968).

33. Cromer, D. T.; Waber, J. T. Acta Cryst. 18, 104 (1965).

34. Larson, A. C. Acta Cryst. 23, 664 (1967).

35. Gutowsky, H. S.; Holm, C. H. J. Chem. Phys. 25, 1228 (1956).

CHAPTER II

Synthesis and Reactivity of Some Zirconium Oxycarbene Complexes

Introduction

Bis(pentamethylcyclopentadienyl) zirconium hydrides have proven to be useful reagents for the reduction of transition metal bound carbon monoxide.[1,2,3] Previous work has demonstrated that these hydrides, in particular $Cp^*_2ZrH_2$, can add across the carbon-oxygen bond of a carbonyl on a variety of metals to afford a zirconoxy carbene product.

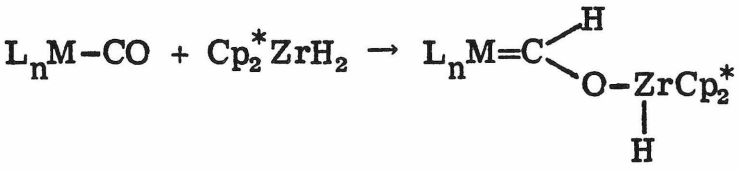

(1)

By this method oxycarbene complexes of niobium,[2] chromium,[3] molybdenum,[3] tungsten,[3] cobalt[4] and rhodium[4] have been prepared; $Cp^*_2ZrH_2$ also appears to add readily to iron and ruthenium carbonyls,[4] but the carbenes prepared have proven unstable toward further rearrangement.

The first evidence that $Cp^*_2ZrH_2$ could reduce carbon monoxide bound to zirconium was the preparation of cis-$(Cp^*_2ZrH)_2(\mu$-OCH=CHO-) by the treatment of $Cp^*_2Zr(CO)_2$ with $Cp^*_2ZrH_2$ under an H_2 atmosphere,[1,3]

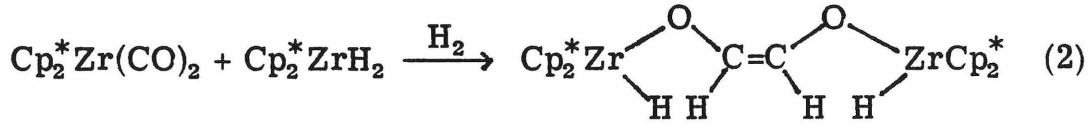

(2)

the proposed mechanism[1d] of which is shown in Scheme I. We have examined this mechanism in more detail by the syntheses of molecules similar to the unisolable intermediates invoked in Scheme I.

The initial step of Scheme I is the formation of a zirconium oxycarbene intermediate, similar to those isolated for Group V and VI

Scheme I

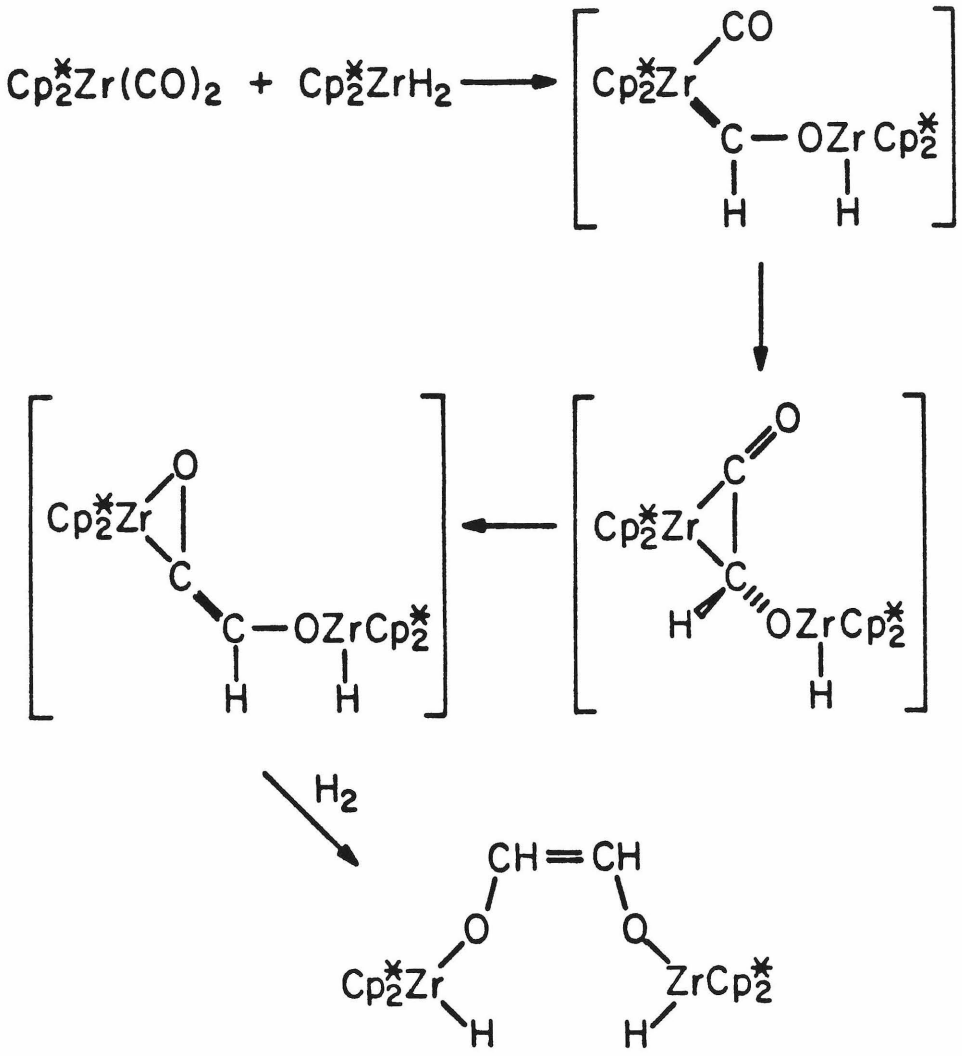
Cp*2Zr(CO)2 + Cp*2ZrH2
CO
Cp*2Zr
C — OZr Cp*2
H H
O
C
Cp*2Zr
C
H OZrCp*2
H
O
Cp*2Zr
C
C — OZrCp*2
H H
H2
CH = CH
O O
Cp*2Zr ZrCp*2
H H

transition metals. Without H_2, $Cp^*_2Zr(CO)_2$ and $Cp^*_2ZrH_2$ give a myriad of products, the first of which is a transient species exhibiting the down-field resonance in the ^1H NMR spectrum expected for the proton on an oxycarbene ligand.[5] The instability of the intermediate is presumably due to two factors; the unfavorable steric interaction of the two bulky decamethylzirconocene fragments in contact due to the two-atom zirconoxy carbene bridge, and the presence of a carbonyl ligand, which may lead to alternate pathways of rearrangement. In our effort to prepare stable zirconium oxycarbene complexes we have tried to minimize these factors.

The only previous reports of zirconium carbene complexes have been by Schwartz and co-workers. In 1980 the spectroscopic observation of $Cp_2Zr(CH_2)(PPh_2Me)$ was reported, though isolation of the

$$Cp_2Zr(PPh_2Me)_2 + CH_2{=}PPh_3 \rightarrow Cp_2Zr(CH_2)(PPh_2Me) + PPh_3 + PPh_2Me \quad (3)$$

product was prevented by its instability at room temperature under the reaction conditions.[6] Recently, this group has reported the isolation of $Cp_2(L)Zr{=}C(H)(CH_2R)$ (L = PPh_3, PMe_2Ph; R = t-Bu, C_6H_{11}, CH(Me)(Et)) as impure oils.[7]

The second step proposed in Scheme I, an intramolecular coupling of the carbene and carbonyl ligands to give a metal ketene intermediate, has very little precedence in the chemical literature and therefore also warranted further study. The use of transition metals to catalyze the formation of new C-C bonds is an important part of

industrial processes which use CO as a feedstock for products with more than one carbon atom. Commonly invoked mechanisms for metal catalyzed C-C bond making include carbonyl insertion[8] (hydroformylation) or olefin insertion into metal alkyl bonds[9] (Ziegler-Natta olefin polymerization - Cossee mechanism) and oligomerization of carbenes on metal surface to give linear hydrocarbons[10] (Fischer-Tropsch catalysis). However, the possibility of carbene-carbonyl coupling to give new C-C bonds has not received much attention.

In 1960 Schrauzer and Rüchardt reported that in the presence of $Ni(CO)_4$ diazomethanes give products, presumably arising from a nickel carbene intermediate that releases the substituted ketene (which was trapped with ethanol) upon decomposition.[11] Carbonylation of $(CO)_5Cr{=}C(OMe)Ph$[12] (150 atm. CO) or $Cp_2Mo_2(CO)_4(\mu\text{-}CR_2)$[13] ($R = C_6H_5$, 3 atm CO, 50° C) also yields the corresponding ketene. The preparation of tantalum[14] and osmium[15] ketene complexes by carbonylation of a metal carbene have been briefly reported. The most thoroughly examined system showing this type of reactivity to date has been reported by Herrmann and Plank in which the high pressure (650 atm) carbonylation of $CpMn(CO)_2(CPh_2)$ gives $CpMn(CO)_2(OCCPh_2)$.[16a] Further studies of the less stable manganese

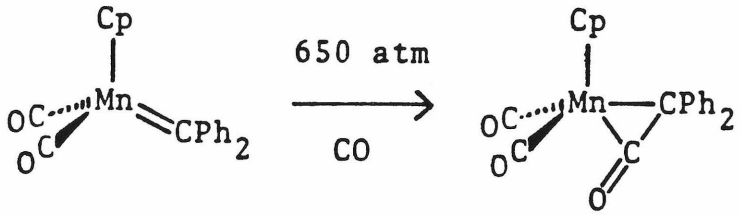

(4)

anthronyl carbene complex, in the presence of $CpMn(CO)_3$, have suggested that the ketene product is formed by the intermolecular transfer of the carbene to one of the manganese carbonyls of $CpMn(CO)_3$.[16b] Finally Beauchamp and Stevens have proposed that $CpFe(CO)(CH_2)^+$, observed by ion cyclotron resonance spectroscopy, is best formulated as the iron ketene adduct, $CpFe(OCCH_2)^+$.[17] However, none of these examples provides clear precedence for the intramolecular carbene-carbonyl coupling step proposed in Scheme I.

In this chapter we report the preparation of some stable zirconium oxycarbene complexes by the reaction of $Cp^*_2ZrH_2$ with a bis(cyclopentadienyl) zirconium monocarbonyl complex, a less sterically hindered zirconium carbonyl than $Cp^*_2Zr(CO)_2$. We have also investigated the reactivity of a oxycarbene-carbonyl complex of zirconocene, which undergoes facile carbene-carbonyl coupling to afford a metal-coordinated ketene intermediate, in particular with regard to the molecularity of the carbon-carbon bond forming step.

Results

The treatment of $Cp_2Zr(L)(CO)$ ($\underset{\sim}{1}$ L = CO, $\underset{\sim}{2}$ L = PMe_3) with $Cp^*_2ZrH_2$ (3) in toluene gives an immediate reaction at -78° C to afford the corresponding zirconoxy carbenes, $Cp_2(L)Zr{=}CHO{-}Zr(H)Cp^*_2$ ($\underset{\sim}{4}$ L = PMe_3, $\underset{\sim}{5}$ L = CO). In the case of L = PMe_3, $\underset{\sim}{4}$ is quite stable in

$$Cp_2Zr\begin{matrix}CO\\ \diagup\\ \diagdown\\ L\end{matrix} + Cp^*_2ZrH_2 \rightarrow Cp_2\underset{\underset{L}{|}}{Zr}{=}CHO{-}\underset{\underset{H}{|}}{ZrCp^*_2} \qquad (5)$$

$\underset{\sim}{1}$ L = CO $\underset{\sim}{3}$ $\underset{\sim}{4}$ L = PMe_3
$\underset{\sim}{2}$ L = PMe_3 $\underset{\sim}{5}$ L = CO

solution and can be isolated as red crystals in 84% yield, based on starting $\underset{\sim}{3}$, from a toluene/pet ether solution. The ^1H and ^{13}C NMR spectra of $\underset{\sim}{4}$ (Table I) are similar to those of previously reported zirconoxy carbenes, $Cp_2M{=}CHO{-}Zr(H)Cp^*_2$ (M = Cr, Mo, W)[3] and $Cp(R)Nb{=}CHO{-}Zr(H)Cp^*_2$ (R = H, CH_3, $CH_2C_6H_5$, $CH_2C_6H_4OCH_3$).[2] The carbene carbon and proton resonances appear at low field, 287.5 δ and 11.2 δ, with a $^1J_{CH}$ = 115 Hz. Two resonances are observed in the ^1H NMR spectrum for the C_5H_5 rings, presumably due to the absence of rotation around the zirconium-carbon bond. The π-interaction of the carbon p orbital and the zirconium $1a_1$ orbital in in the equatorial wedge of the Cp_2Zr metallocene fragment locks the carbene ligand with the proton directed toward one ring and the zirconoxy substituent toward the other. The lack of rotation of the carbene also makes the Cp* rings diastereotopic, as indicated by the inequivalent resonance signals in the ^1H and ^{13}C (methyl carbons only) NMR spectra. The zirconium hydride resonance at 5.7 δ is characteristic of compounds that have a zirconium-oxygen bond in the equatorial plane.

In contrast to 4, 5 is unstable in aromatic solvents at room temperature. However, $Cp_2(CO)Zr{=}CHO{-}Zr(H)Cp_2^*$ can be isolated as a tan powder in 53% yield by performing the reaction in pet ether, whereupon the slightly soluble carbene complex precipitates from solution as it is formed. The ^1H and ^{13}C NMR spectra of 5 (Table I) are similar to those of 4. The zirconium carbonyl exhibits a strong band at 1925 cm^{-1} in the IR spectrum and is assigned as the ν_{CO}. Treatment of 5 with ca. 3 equivalents of PMe_3 in a sealed NMR tube results in conversion to 4 over 2 hours at 25°C.

In toluene or benzene solution 5 converts to an extremely insoluble yellow crystalline compound (6) within 2 hours at room temperature. The IR spectrum of this product shows no bands corresponding to a metal carbonyl stretch, and the elemental analysis of 6 indicates that it has the same stoichiometry as 5, $(Cp_2Zr)(C_2H_2O_2)(Cp_2^*Zr)$.

The isolation and purification of $Cp_2(CO)Zr{=}CHO{-}Zr(H)Cp_2^*$ is hindered by the ability of a second molecule of $Cp_2^*ZrH_2$ to add to 5 to afford a new compound, $Cp_2Zr(C_2H_2O_2)(H)_2(ZrCp_2^*)_2$, (5a). This complex is observed as a contaminant in samples of 5 that are prepared under conditions that allow an excess of $Cp_2^*ZrH_2$ (relative to $Cp_2Zr(CO)_2$) in the reaction mixture. 5a can be prepared and purified in 50% yield by treatment of $Cp_2Zr(CO)_2$ with 2 equivalents of $Cp_2^*ZrH_2$. The ^1H and ^{13}C NMR spectra (Table I) of 5a show resonances for two inequivalent Cp rings, four inequivalent Cp^* rings, two different zirconium hydrides and a new ligand, coming from the carbonyls, containing a $\rangle CH{-}CH\langle$ fragment. The chemical shifts of the

resonances of $Cp_2Zr(C_2H_2O_2)(H)_2(ZrCp_2^*)_2$ are consistent with the structure shown, but further characterization has not been pursued.

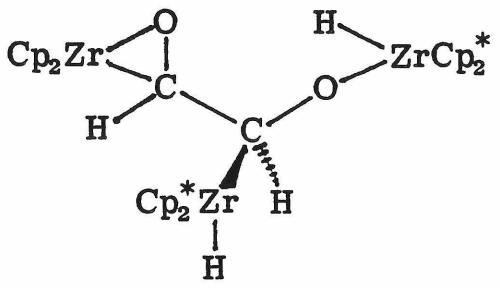

5a

Treatment of 5a with 2 equivalents of CH_3I in an NMR tube gives CH_4 and a new complex with a ^1H NMR spectrum similar to that of 5a, but without the resonance assigned to the zirconium hydrides.

With an excess of CO, in an NMR tube, 4 and 5 give very similar product distributions (after a clean conversion to 5 in the case of 4) consisting of $Cp_2Zr(CO)_2$ and $Cp_2^*Zr(CO)_2$ (identified by IR and NMR spectroscopy) as well as an unidentified Cp_2^*Zr product ($Cp_2^*Zr(CO)_2$/new Cp_2^*Zr about 3:1) with ^1H NMR resonances at 1.87 δ (30H) and 6.35 δ (2H), consistent with the formulation of $Cp_2^*\overline{ZrOCH=CHO}$. Attempts to isolate this new complex on a preparative scale were unsuccessful. Analysis of the gas remaining after the reaction of 4 with CO shows approximately equal equivalents of H_2 and $Cp_2^*Zr(CO)_2$ are produced (0.41 equivalents H_2/equivalent 4 vs. 35% of final Cp_2^*Zr as $Cp_2^*Zr(CO)_2$ by ^1H NMR integration of the remaining tar). Neither 4 nor 5 give clean products in the presence of H_2. Treatment of 5 with 1 equivalent of acetone in a sealed NMR tube cleanly produces $Cp_2Zr(CO)_2$

and $Cp^*_2Zr(H)(OCH(CH_3)_2)$ within 5 minutes at RT. These results

$$Cp_2Zr(CO)=CHO-ZrCp^*_2(H) + Me_2C=O \rightarrow Cp_2Zr(CO)_2 + Cp^*_2Zr(H)(OCHMe_2) \quad (6)$$

(5)

suggest that the addition of the zirconium hydride to the carbonyl might be reversible, and that the observed products could arise from trapping of liberated $Cp^*_2ZrH_2$ by CO or acetone. However, an NMR sample of 5 and 3 equivalents of $Cp_2Zr(^{13}CO)_2$ shows no ^{13}C incorporation into the carbene carbon prior to its conversion to 6.

Treatment of 4 with an excess of CH_3I liberates one equivalent of CH_4 and yields green, crystalline $Cp_2(PMe_3)Zr=CHO-Zr(I)Cp^*_2$ (7).

$$Cp_2Zr(PMe_3)=CHO-ZrCp^*_2(H) + CH_3I \rightarrow Cp_2Zr(PMe_3)=CHO-ZrCp^*_2(I) + CH_4 \quad (7)$$

(4) (7)

The ^1H and ^{13}C NMR spectra of 7 (Table I) are very similar to those of 4. In the presence of HCl 7 rapidly gives Cp_2ZrCl_2 and $Cp^*_2Zr(OCH_3)I$.[18]

$$Cp_2Zr(PMe_3)=CHO-ZrCp^*_2(I) + HCl\,(2\,eq) \rightarrow Cp_2ZrCl_2 + Cp^*_2Zr(OCH_3)I + PMe_3 \quad (8)$$

(7)

Crystals of 7 suitable for X-ray diffraction were grown by slow cooling of a saturated benzene solution. The unit cell parameters and data collection and refinement information are given in Table II. Atomic positions, Gaussian amplitudes, bond lengths, and bond angles are given in Tables III-V.

ORTEPs of 7, with important bond distances and angles are shown in Figure 1. Both zirconiums have the pseudo-tetrahedral

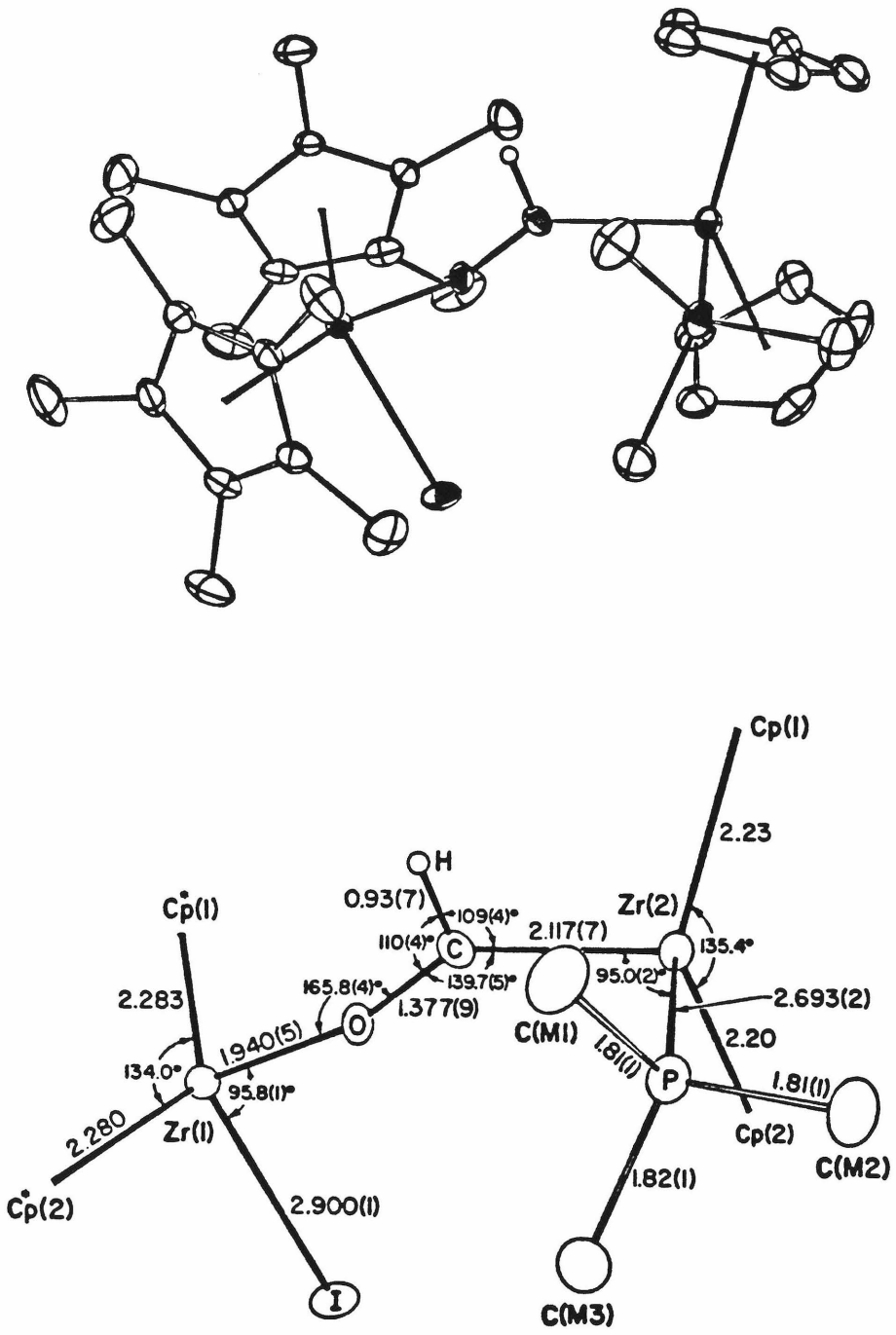

Figure 1. ORTEP drawings of $Cp_2(PMe_3)Zr{=}CHO{-}Zr(I)Cp^*_2$ including important bond distances (Å) and angles.

coordination geometries common for bent metallocene complexes. The Cp and Cp* ligands are coordinated in the conventional η^5 manner to the metals; Zr-C and C-C distances for any particular ring are identical within experimental error. The ring centroid-metal-ring centroid angles of 135.4° and 134.0° for the Cp_2Zr and Cp_2^* Zr fragments are typical for zirconium -bent metallocenes.[19] The Zr(2)-C(carbene) distance of 2.117(7) Å is the shortest reported zirconium-carbon bond, being ca. 0.15 Å shorter than that observed for carbon σ-bonded to a zirconium center (these values range from 2.25 Å for $(Indenyl)_2ZrMe_2$[20] to 2.33 Å for $Cp_2Zr(Ph)CH(SiMe_3)_2$).[21] The configuration of the carbene ligand is such that the proton and the zirconoxy substituents each eclipse a Cp ring in an arrangement that is required by the Zr-C π-bond between the carbon p orbital and the $1a_1$ orbital in the zirconium equatorial plane. The relatively short C-O (1.377(9) Å)[22] and Zr(1)-O (1.940(5) Å)[23,24] bond lengths suggest that all resonance structures shown in Figure 2 contribute to the bonding in this compound.

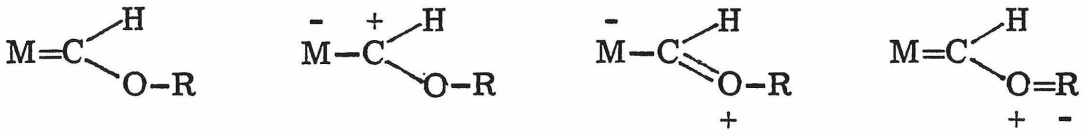

I II III IV

Figure 2. Oxycarbene Resonance Structures.

Treatment of $Cp_2(CO)Zr{=}CHO{-}Zr(H)Cp_2^*$ with CH_3I or, under carefully controlled conditions to avoid further reaction, $Cp_2(PMe_3)Zr{=}CHO{-}Zr(I)Cp_2^*$ with CO, yields a new intensely purple compound, $Cp_2^*\overline{ZrOCH{=}C(Zr(I)Cp_2)O}$ (8). The ^1H NMR spectrum (Table I) shows signals for the C_5H_5 and C_5Me_5 rings and a resonance, integrating to one proton, at 6.8 δ. The ^{13}C NMR spectrum of a sample prepared from $Cp_2(PMe_3)Zr{=}^{13}CHO{-}Zr(I)Cp_2^*$ (60% ^{13}C enriched) and ^{13}CO (99% ^{13}C enriched) shows two large resonances downfield at 234.97 δ (99% ^{13}C enriched) and 155.01 δ (60% ^{13}C enriched) with a $^1J_{CC}$ = 45 Hz, and indicates that the carbene and carbonyl carbons are coupled in the final product. The gated decoupled spectrum shows carbon-hydrogen coupling constants of $^1J_{CH}$ = 180 Hz and $^2J_{CH}$ = 24 Hz, values that are consistent with the formation of a new carbon-carbon bond. Treatment of unlabeled 7 with ^{13}CO gives incorporation of the labeled carbon only into the resonance at 235 δ with the small $^2J_{CH}$. The IR spectrum of a nujol mull of 8 shows no evidence of any metal carbonyls.

The extensive rearrangement that is necessary to transform either of the starting carbene complexes to 8 made the assignment of its structure impossible simply from the spectral data. Therefore suitable crystals for a single crystal X-ray diffraction structure determination were grown by slow cooling of a saturated benzene solution. The unit cell parameters as well as data collection and refinement information are given in Table VII. Atomic positions and Gaussian amplitudes, bond lengths and bond angles are listed in Tables VIII-X.

ORTEP drawings of 8 (Figure 3) confirm the structure of a

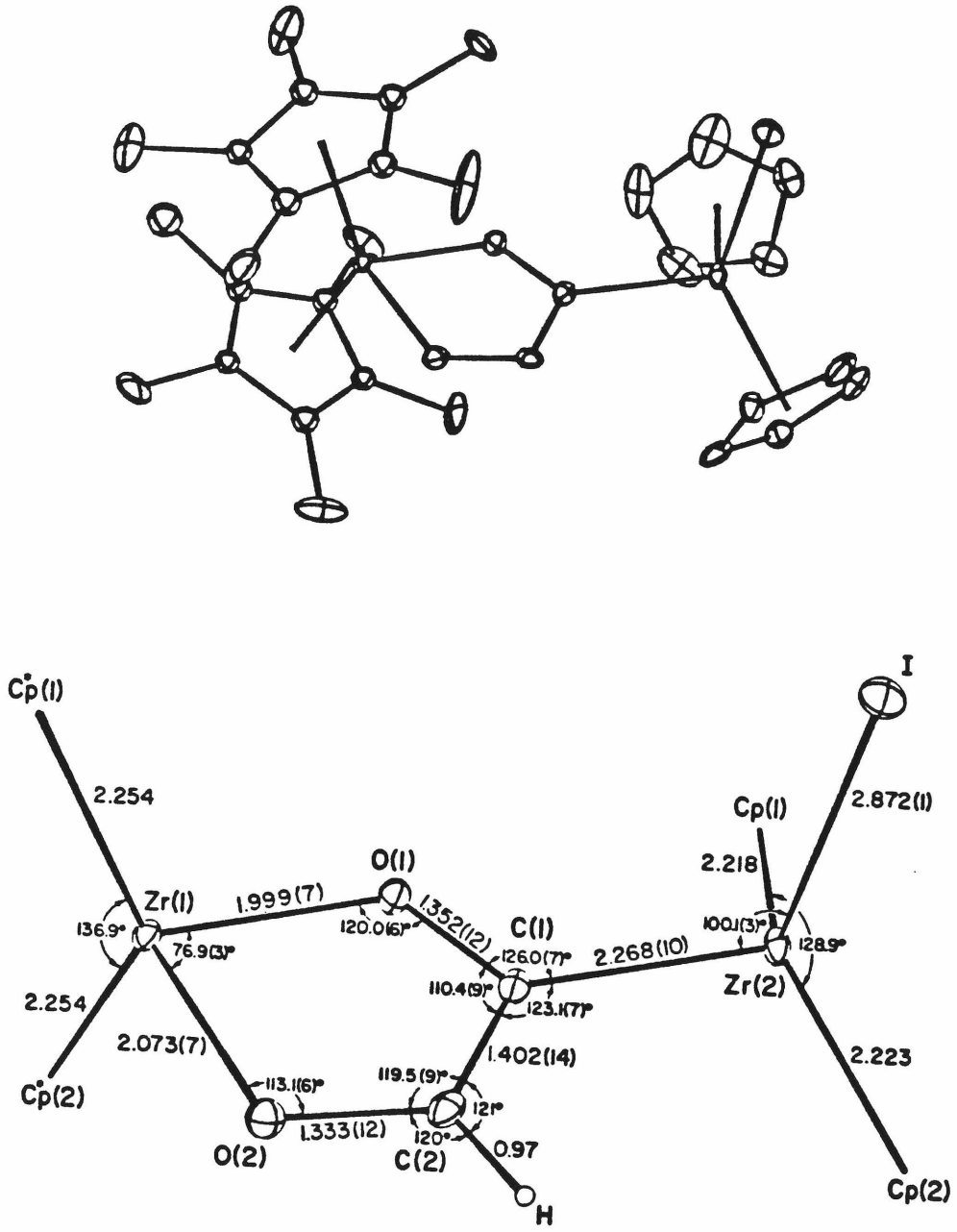

Figure 3. ORTEP drawings of $Cp_2^*\overline{ZrOCH=C(Zr(I)Cp_2^*)O}$ including important bond distances (Å) and angles.

zirconium substituted enediolate zirconocycle. Both zirconium atoms have pseudo-tetrahedral coordination geometries and the metal-to-ring bonding for the Cp and Cp* ligands is similar to that seen in the structure of 7. The five-membered metallocycle ring is planar within experimental error (Table XI lists deviations from the least-squares plane). The Zr(1)-O distances of 1.999(7) Å and 2.073(7) Å fall between those observed for zirconium acetylacetonate complexes[22] (2.10 - 2.25 Å; mixture of covalent and dative Zr-O interactions) and zirconium μ-oxo dimers[23] (1.95 Å; covalent Zr-O bond with significant π-bonding). The fact that the C-C bond, 1.402(14) Å, is slightly longer than that expected for a C-C double bond and the C-O bonds (1.352(12), 1.333(12) Å) are shorter than values for normal C-O single bonds[25] indicates that there is some π-delocalization throughout the metallocycle. Inclusion of a high-energy, empty zirconium orbital perpendicular to the bent metallocene equatorial plane and one lone pair on each oxygen with the C-C π-bond gives a 6-electron aromatic π framework consistent with the observed stability of molecules with a metallocycle enediolate structure. The orientation of the $Cp_2Zr(I)$ fragment, with the Zr and I atoms in the metallocycle plane, suggests that the metallocycle π-system delocalizes onto the Zr(2) center as shown by resonance structure II in Figure 4. The Zr(2)-C bond length,

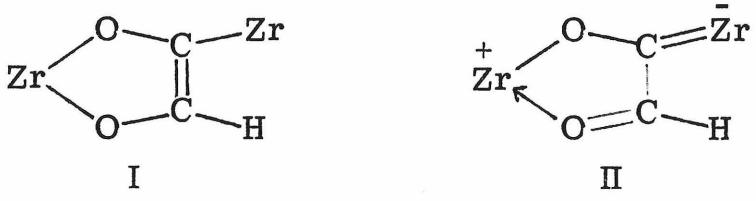

Figure 4. Enediolate Metallocycle Resonance Structures.

2.268(10) Å, is slightly shorter than the average observed for zirconium carbon σ bond lengths,[19,20] and is consistent with π-interaction between these two atoms. The extended π-delocalization increases the C(2)-O(2) bond order while weakening the Zr-O(2) bond, relative to the corresponding bonds involving O(1), thereby accounting for the different lengths of two Zr-O and two C-O bonds within the metallocycle.

The molecularity of the carbon-carbon bond forming step that leads to the generation of 8 was determined by an isotopic cross-over experiment. Treatment of a mixture of $Cp_2Zr(^{12}CO)_2$ and $Cp_2Zr(^{13}CO)_2$ (91% ^{13}C enriched) with $Cp^*_2ZrH_2$ followed by CH_3I yields 8 with only $5 \pm 5\%$ isotopic scrambling (Table XII); this value is indicative of an intramolecular carbonyl-carbene-coupling step.

These results suggest that the transformation of the carbene carbonyl complex to 6, which is not seen for the carbene-phosphine compounds, might be initiated by coupling of the two ligands to give a metal-bound ketene intermediate which oligomerizes or rearranges to give the isolated product. The reactivity of 5 with Lewis bases is of interest as these substrates are useful for stabilizing other Group IV metal ketene complexes by binding to the remaining coordination site on the metal,[26] thereby preventing oligomerization or further rearrangement.

Thus addition of ca. 4 equivalents of pyridine to an NMR sample of 5 in C_6D_6 affords a pyridine-trapped zirconium ketene complex, 9, rather than 6, after 2 hrs at room temperature. 9 can be isolated in

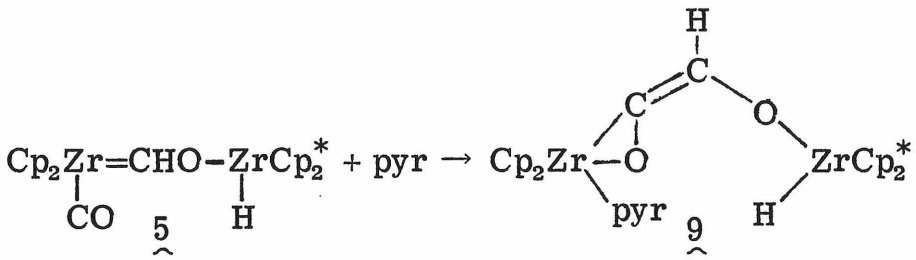

(9)

82% yield by either dissolving 4 in pyridine or treating $Cp_2Zr(CO)_2$ with $Cp^*_2ZrH_2$ in pyridine and precipitating the red product with pet ether. The ^1H NMR spectrum of 9 (Table 1) in C_5D_5N has single resonances for the Cp^* and Cp rings at 2.18 δ and 5.91 δ. No resonance can be assigned to the zirconium hydride in the 90 MHz spectrum; however, the 500 MHz spectrum has a small shoulder on the Cp peak at 5.92 δ in the region where the resonance for the hydride is expected to be. A peak integrating to one proton appears at 6.18 δ and is assigned as the resonance of the ketene hydrogen. This assignment is confirmed by the spectrum of 9 with the ketene carbons enriched in ^{13}C, prepared by treating $Cp_2Zr(^{13}CO)_2$ (70% ^{13}C enriched) with $Cp^*_2ZrH_2$ in C_5D_5N, which shows this resonance split by $^1J_{CH}$ and $^2J_{CH}$ of 183 and 22 Hz. The ^{13}C NMR spectrum (Table I) of the ^{13}C enriched sample of 9 shows the ketene carbon resonances at 165.7 δ ($^2J_{CH}$ = 22 Hz) and 123.4 δ ($^1J_{CN}$ = 183 Hz) with $^1J_{CC}$ = 78 Hz confirming that the product has a new carbon-carbon bond. The ketene complex is stable for over a month at room temperature in pyridine solution. In benzene or toluene, however, 9 gives 6 (identified by IR), releasing pyridine, until an approximately five-fold excess of free pyridine to 9 is reached; complete conversion to 6 can be achieved by removing the pyridine in vacuo.

Treatment of 9 in C_5D_5N with one equivalent of CH_3I in a sealed

NMR tube affords a new complex, 10, with ^{1}H and ^{13}C NMR spectra (Table I) similar to those of 9. A small peak due to CH_4 is also seen in the spectrum of the reaction solution. On a preparative scale this reaction yields 0.88 equivalents of CH_4, collected and measured with a Toepler pump; however, 10 can be isolated only as an impure red tar. These results are consistent with the formulation of 10 as $Cp_2(pyr)Zr(O{=}C{=}CHO{-}Zr(I)Cp^*_2)$.

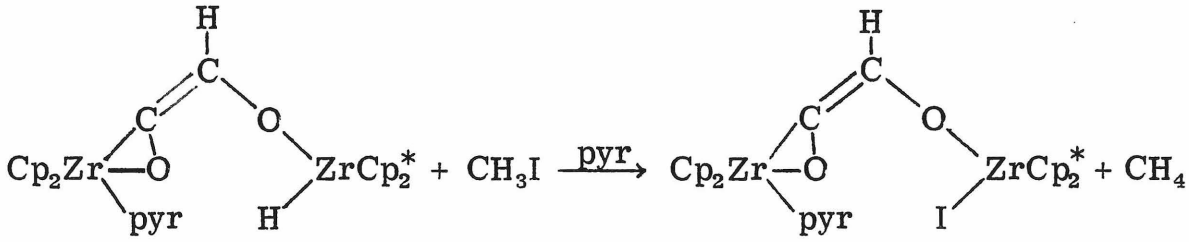

9 10 (10)

When the reaction of 9 and CH_3I is carried out in benzene or the isolated red tar is dissolved in C_6D_6, the ^{1}H spectrum obtained is identical to that of 8. Conversely, the ^{1}H NMR spectrum of a C_5D_5N solution of 8 is identical to that of 10. These results indicate that an equilibrium exists between 8 and 10, depending on pyridine concentration.

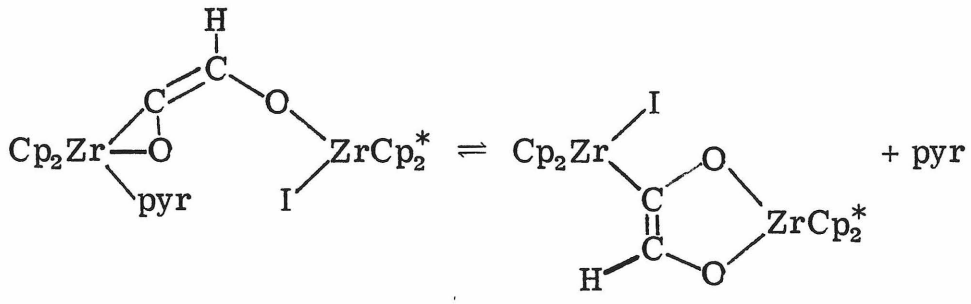

(11)

10 8

Other Lewis bases, such as phosphoranes, amines, or acetonitrile, are not useful for trapping of the zirconium ketene intermediate. Treatment of 5 with CH_2PMe_3 gives a complex mixture of unidentifiable products. NMe_3 is presumably too large to bind to the sterically hindered zirconium center and therefore does not affect the conversion of 5 to 6. In a manner similar to PMe_3, acetonitrile apparently displaces the remaining carbonyl of 5 to give a new carbene complex; however, this unstable intermediate has defied isolation.

Hydrogenation of 9 under a variety of conditions, in an attempt to obtain precedence for the final step of Scheme I, leads to a mixture of unidentifable products.

Discussion

The general reaction, shown in eq. 1, of the reduction of a transition metal carbonyl by bis(pentamethylcyclopentadienyl)-zirconium dihydride has been extended to afford some of the first isolable examples of Group IV transition metal-carbon multiple bonding. Zirconoxy carbene complexes of bis(cyclopentadienyl)-zirconium have been prepared by the treatment of the corresponding zirconium carbonyls with $Cp^*_2ZrH_2$. The ready formation of 4 and 5 lends support to the proposed initial step of the mechanism for the formation of cis-$(Cp^*_2ZrH)_2(\mu$-OCH=CHO-) from $Cp^*_2Zr(CO)_2$ and $Cp^*_2ZrH_2$ under H_2 (Scheme I).[1d] Comparison of the ^1H NMR spectra of 4 and 5 with that of the transient species observed during the course of this reaction in the absence of H_2 supports its formulation as a zirconium carbene intermediate. The large difference in the rate of attack of $Cp^*_2ZrH_2$ on the Cp_2Zr and Cp^*_2Zr carbonyls is probably due to the increased steric hindrance of the bulky Cp^* ligands. In addition, it may also be argued that the Cp^*_2Zr carbonyls are less susceptible to nucleophilic attack because of the greater electron-releasing character of the pentamethylcyclopentadienyl ligands relative to that of the cyclopentadienyl rings. However, replacement of one of the carbonyls of 1 with PMe_3, which increases the electron density on the remaining carbonyl, has no noticeable effect on the rate of carbene formation. A comparison of the carbonyl stretching frequencies of 2 (ν_{CO} = 1852 cm^{-1})[27] and $Cp^*_2Zr(CO)_2$ ($\nu_{CO(sym)}$ = 1945 cm^{-1}, $\nu_{CO(asym)}$ = 1852 cm^{-1})[18c] indicates that the carbonyl of 2 is more electron rich

than those of $Cp^*_2Zr(CO)_2$; that $Cp^*_2ZrH_2$ adds much more rapidly to 2 than to $Cp^*_2Zr(CO)_2$ discredits arguments that the difference in rates is due to electronic effects.

The bonding of a carbene ligand to a transition metal can be represented by the resonance structures I-III in Figure 2. Structure I describes the covalent bonding limit with the π electrons equally shared between the two atoms. If there is no π-back-bonding from the metal to the carbon the carbene is a σ-donating ligand only, illustrated by structure II. This structure may be stabilized, in the case of heteroatom substituted carbenes, by delocalization of a lone pair of the heteroatom onto the carbene carbon as represented by structure III. Fischer-type carbenes, in which the heteroatom substituent is usually an alkoxide or amide, are best described by III;[28] the electron donation by the O or N atom makes the carbene a good σ-donor but a poor π-acceptor. The electron deficiency of the carbene ligand is demonstrated by its reactivity as an electrophilic center. In contrast, early metal alkylidene complexes, such as $Cp_2Ta(CH_3)(CH_2)$ are better represented by I.[29] The presence of a strong π-interaction is shown by the high barrier to rotation around the metal-alkylidene bond. Calculations on the model molecule, $CpMn(CO)_2(CH_2)$,[30] have determined that the empty methylene π-orbital and occupied metal orbital with which it interacts are similar in energy, consistent with a significant π-interaction. The nucleophilic character of the alkylidene carbon also attests to it being a good π-acceptor ligand.[31]

The results of our research suggest that the electronic nature of the zirconoxy carbene ligand lies between these two extremes. The

ability of the $Cp^*_2(H)Zr(IV)$ center, as a Lewis acid, to remove electron density from the oxygen atom by interacting with one of the lone pairs in a π manner, illustrated by structure IV of Figure 2 where R is the electropositive Cp^*_2Zr moiety, reduces the oxygen donation in the reverse direction. This makes the zirconoxy carbene ligand a better π-acceptor than other Fischer-type, oxygen stabilized carbenes. The increased strength of the π-bonding interaction is apparent from the inequivalency of the two Cp resonances in the ^1H NMR spectra of 4, 5, and 7 indicative of restricted rotation around the zirconium-carbene bond. The carbonyl stretching frequencies of some zirconocene carbonyl complexes provide additional insights on the electronic nature of the carbene ligand. The CO stretching frequency of 5 (1925 cm^{-1}) is very similar to the mean CO stretching frequency of 1 (1930 cm^{-1} from $\nu_{CO(sym)}$ = 1975 cm^{-1} and $\nu_{CO(asym)}$ = 1886 cm^{-1})[32] suggesting that replacement of the carbonyl by the zirconoxy carbene does not significantly change the electron density in the bent metallocene equatorial plane. The ν_{CO} of 5 is much higher than that of 3 (ν_{CO} = 1852 cm^{-1}).[27] These results suggest that the zirconoxy carbene is a good π-accepting ligand, comparable to CO in its π back-bonding with the zirconocene fragment.

The carbon-hydrogen stretching frequency of the zirconoxy carbene C-H bond appears at relatively low energy in the IR spectra of 4, 5, and 7 (2755, 2755, 2755 cm^{-1}, respectively). It has been argued that distortion of the carbene ligand by lessening the metal-carbon-hydrogen angle parallels the lowering of ν_{CH},[33] perhaps because both are measures of the carbon p character of the C-H bond, which should

be increased in 4, 5 and 7 due to demand of the electropositive zirconium for more carbon s character in the metal carbene σ bond.

The oxycarbene-carbonyl complexes of zirconocene that we have prepared undergo a facile rearrangement to a zirconium ketene intermediate by coupling the two equatorial ligands. In the case of 4 the ketene adduct, 11, can be trapped by pyridine to afford the isolable zirconium ketene pyridine complex, 9, as outlined in Scheme II. In the absence of a trapping ligand 11 apparently isomerizes or oligomerizes to give 6.

The replacement of the remaining zirconium hydride of $Cp_2(CO)Zr{=}CHO{-}Zr(H)Cp_2^*$ with an iodide, either by treatment of 5 with MeI or 7 with CO, results in a carbene carbonyl iodide complex, 12, which can couple to a new ketene adduct, 13. However, neither of these intermediates has been detected. Instead, 13 rearranges to $Cp_2^*\overline{ZrO{-}CH{=}C(Zr(I)Cp_2)O}$ by exchange of the iodide and carbonyl oxygen atoms between the zirconiums (Scheme III). Presumably, the formation of the five-membered metallocycle is the driving force of this process. Several other Group IV transition metal complexes containing a cyclic enediolate substructure are known[24, 34] and have properties similar to 8. The formation of a ketene pyridine complex, 10, when reactions that give 8 in benzene are performed in pyridine, as well as the observed interchange of 8 and 10, depending on pyridine concentration, gives strong support for the presence of a ketene intermediate on the pathway to 8. Comparison of the ^{13}C NMR spectrum of 10 to those of 8 and 9 indicates that this compound is best formulated as a zirconium ketene complex with a structure similar to that of 9.

Scheme II

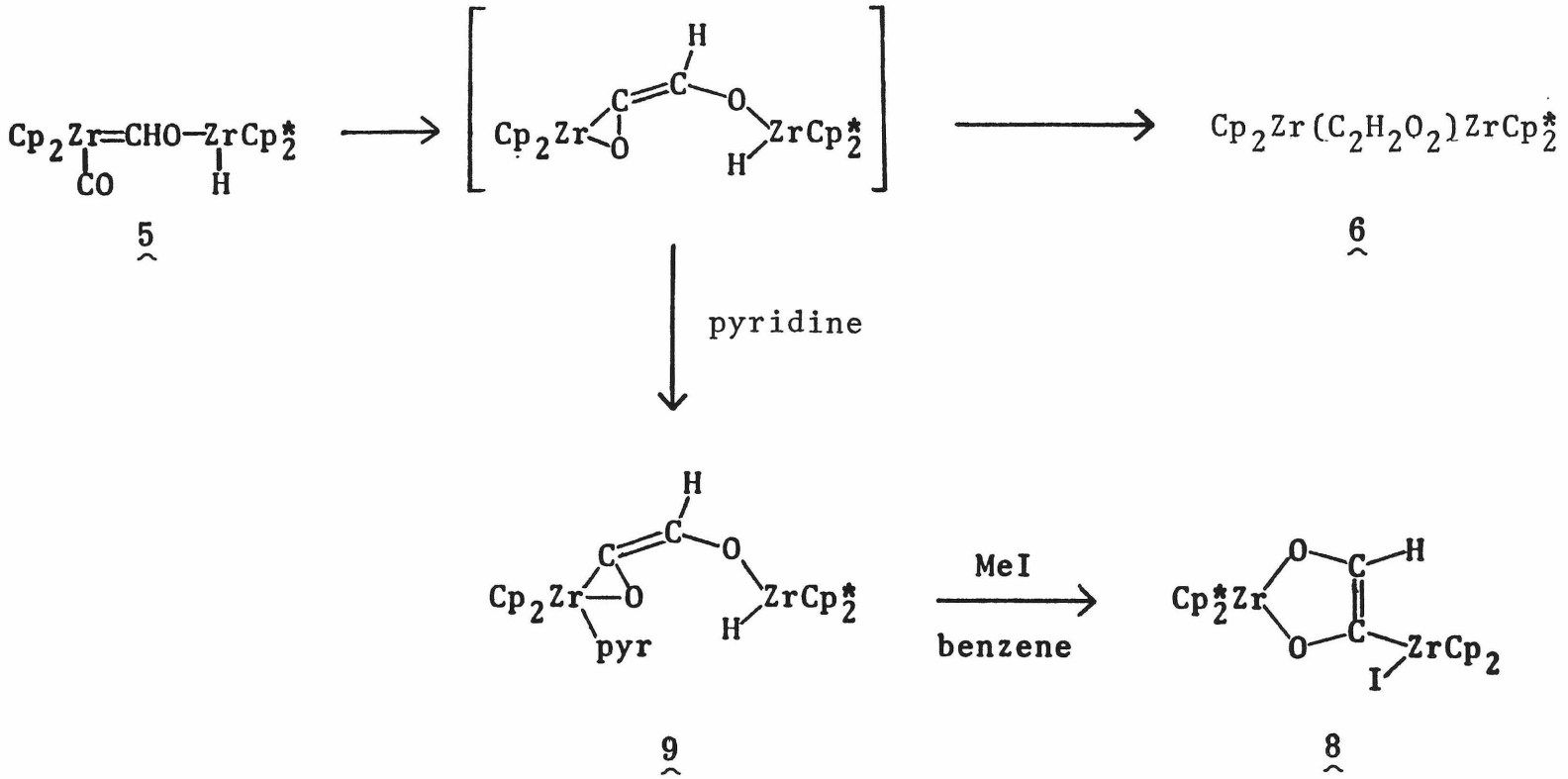

5 6 9 8

Scheme III

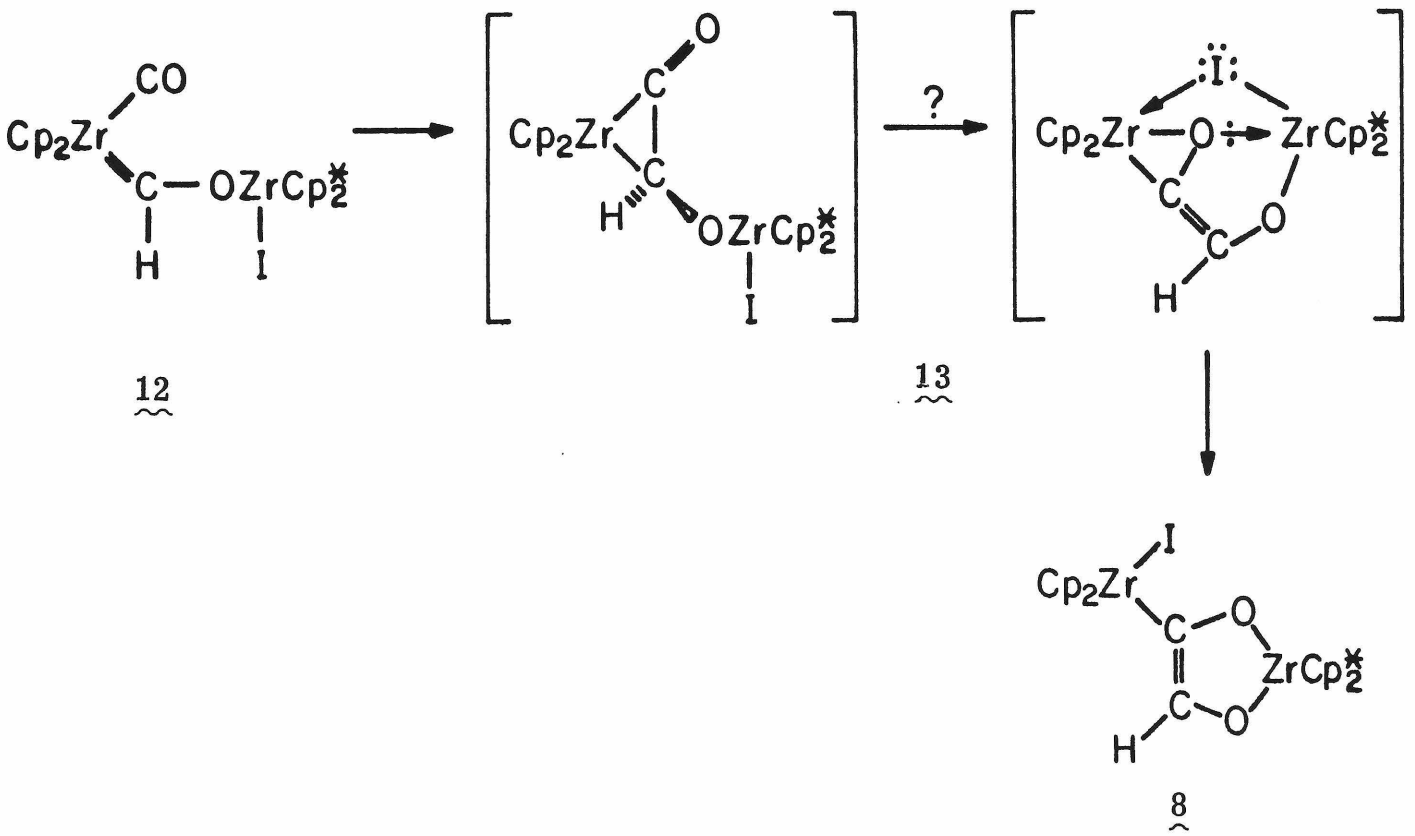
Cp2Zr
CO
C
OZrCp*2
H
I
12
Cp2Zr
C
O
C
H
OZrCp*2
I
13
?
Cp2Zr
:I:
O
ZrCp*2
C
O
C
H
8
I
Cp2Zr
C
O
ZrCp*2
C
O
H

The coupling of the carbene and carbonyl ligands described above can be rationalized by consideration of the metal-ligand bonding in the equatorial plane of the Cp_2Zr fragment.[35] The σ-bonding, derived from the ligand lone pairs and the empty metal b_2 and $2a_1$ orbitals, and π-bonding, involving the zirconium $1a_1$, carbene π and carbonyl π^* orbitals, are illustrated in Figure 5. Complete transfer

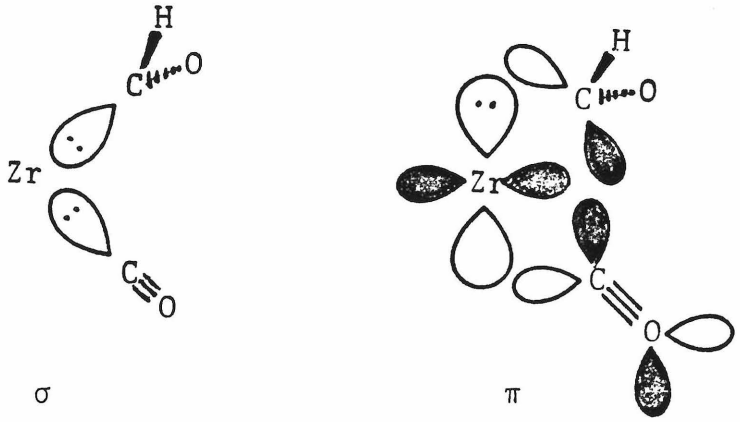

Figure 5. Bonding in the Zirconium Equatorial Plane in 5.

of the π electron pair from the metal to the ligand orbitals, to give a new C-C σ bond, with the simultaneous transformation of the ligand σ-donated electrons to covalent metal-ligand bonds gives the zirconium ketene complex in the Zr(IV) resonance structure (Figure 6a). This

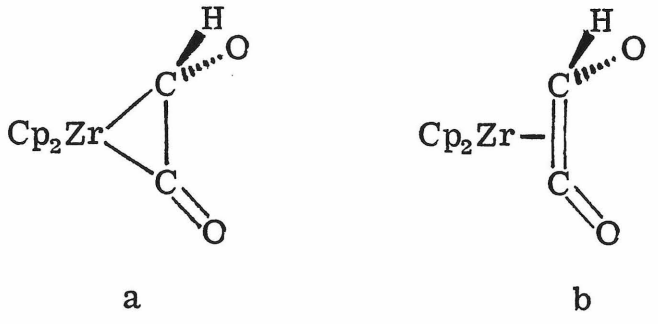

Figure 6. Zirconium-Ketene Resonance Structures.

intermediate can also be drawn as a zirconium(II) olefin adduct (Figure 6b). The proposed migration of the Cp_2Zr group to the carbonyl is similar to the fluctionality proposed for the iron allene bonding in $(CO)_4Fe(Me_2C{=}C{=}CMe_2)$[36] and is probably driven by the zirconium-oxygen interaction that is attained.

This interpretation of the carbene-carbonyl coupling mechanism suggests that the process should be favored by metal centers that can be easily oxidized, particularly if, as in the case of 5, the HOMO of the complex is a metal orbital π back-bonding to both the carbene and carbonyl ligands. The electrophilicity of the carbene ligand should also affect the coupling process. Therefore, heteroatom stabilized carbenes, in which the overlap of the carbene π orbital with the metal orbitals is diminished by the heteroatom donation, should be less susceptible to coupling than carbenes that have no such substituents.

A final point of consideration is that the carbonyl-carbene coupling may be assisted by Lewis bases, such as pyridine or iodide, which promote the electron transfer from the metal to the ligands by interacting to the zirconium $1a_1$ orbital of the carbene carbonyl complex. However, the fact that roughly similar rates are observed for the conversion of $Cp_2(CO)Zr{=}CHO\text{-}Zr(H)Cp_2^*$ to 9, in the presence of 4 equivalents of pyridine, or 6, in the absence of pyridine, as well as the formation of 8 from $Cp_2(CO)Zr{=}CHO\text{-}Zr(I)Cp_2^*$ suggests that any rate enhancement of the coupling step due to the presence of a Lewis base is minimal.

Attempts to prepare $(Cp_2ZrH)(\mu\text{-}OCH{=}CHO\text{-})(Cp_2^*ZrH)$ by hydrogenation of 10, similar to the last step proposed in Scheme I

have been unsuccessful. The presence of pyridine may slow the addition of H_2 to the Cp_2Zr center allowing other reaction pathways to become competitive. However, a very similar Lewis base stabilized zirconium ketene complex, $Cp^*_2(L)Zr(O{=}C{=}CHCMe_3)$ (L = pyr, CO, CH_2PMe_3) has been shown to hydrogenate cleanly to $Cp^*_2Zr(H)(OCH{=}CH(CH_2CMe_3))$, with a cis-arrangement of the bulky substituents on the C=C bond.[26b]

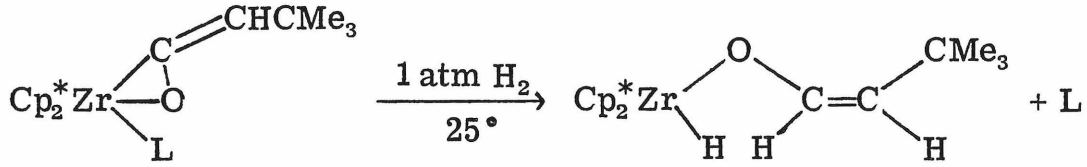

(L = pyr, CO, CH_2PMe_3) (12)

The results described above provide clear precedence for the carbon-carbon bond making step proposed in Scheme I for the formation of cis-$(Cp^*_2ZrH)_2(\mu$-OCH=CHO-). The carbene and carbonyl ligands of $Cp^*_2(CO)Zr{=}CHO{-}Zr(H)Cp^*_2$ should be more susceptible to coupling to those of $\underset{\sim}{5}$ since the more electron-releasing nature of the Cp^* rings, relative to Cp rings, should facilitate the transfer of the π electrons to the ligands by destabilizing the zirconium $1a_1$ orbital.

Table I. NMR[a] and IR[b] Data.

Compound	IR		NMR assignment	^{1}H		^{13}C{^{1}H}	
$Cp_2(PMe_3)Zr{=}CHO{-}Zr(H)Cp^*_2$ (4)	ν(C-H)	2755	Zr=<u>CH</u>O-Zr	11.29	$^3J_{PH}$=3	287.54	$^1J_{CH}$=115, $^2J_{CP}$=14
	ν(C-D)	2045	<u>C_5H_5</u>	5.35, 5.44	$^3J_{PH}$=2, 2	100.20, 101.58	
			$C_5(\underline{CH_3})_5$	2.00, 2.04		11.79, 12.22	
			<u>C_5</u>$(CH_3)_5$			116.67	
			$P(\underline{CH_3})_3$	0.93	$^2J_{PH}$=6	20.33	$^1J_{CP}$=18
			Zr<u>H</u>	5.70			
$Cp_2(CO)Zr{=}CHO{-}Zr(H)Cp^*_2$ (5)[c]	ν(C-H)	2755	Zr=<u>CH</u>O-Zr	11.58		295.02	$^1J_{CH}$=105
	ν(C-D)	2042	<u>C_5H_5</u>	5.44, 5.43		98.64, 100.28	$^1J_{CH}$=172, 176
	ν(CO)	1925	$C_5(\underline{CH_3})_5$	1.95, 1.93		11.61	$^1J_{CH}$=127
	ν(Zr-H)	1515	<u>C_5</u>$(CH_3)_5$			116.23	
			Zr<u>H</u>	5.47			
			Zr(<u>C</u>O)			262.11	
$Cp_2Zr(C_2H_4O_2)(ZrCp^*_2)_2$ (5a)[c]			<u>C_a</u>H-C_bH	7.62	$^3J_{HH}$=10	155.82	$^1J_{CH}$=169 $^1J_{CC}$=69
			C_aH-<u>C_b</u>H	5.45	$^3J_{HH}$=10	144.82	$^1J_{CH}$=111
			<u>C_5H_5</u>	6.26, 6.21			
			$C_5(\underline{CH_3})_5$	2.00, 2.02	2.03, 2.08		
			Zr<u>H</u>	5.71, 6.34			
$Cp_2(PMe_3)Zr{=}CHO{-}Zr(I)Cp^*_2$ (7)	ν(C-H)	2725	Zr=<u>CH</u>O-Zr	10.69	$^3J_{PH}$=4	286.32	$^1J_{CH}$=117 $^2J_{CP}$=14
	ν(C-D)	2020	<u>C_5H_5</u>	5.48, 5.55	$^3J_{PH}$=2, 2		
			$C_5(\underline{CH_3})_5$	2.07, 2.13			
			$P(\underline{CH_3})_3$	0.93	$^2J_{PH}$=6		

Table I (continued)

Compound	IR	assignment	^{1}H	^{13}C
$Cp_2^*\overline{ZrOCH=C(Zr(I)Cp_2)O}$ (8)		$\overline{ZrO\underline{C}H=C(Zr)O}$	6.77	155.01 $^1J_{CH}$=180, $^1J_{CC}$=45
		$\overline{ZrOCH=\underline{C}(Zr)O}$		234.97 $^2J_{CH}$=24
		$\underline{C}_5\underline{H}_5$	6.07	111.03
		$C_5(\underline{C}H_3)_5$	1.87	11.18
		$\underline{C}_5(CH_3)_5$		not assigned
$Cp_2(pyr)Zr(O=C=CHO-Zr(H)Cp_2^*$ (9)[d]		O=$\underline{C}$=CHO-Zr		165.65 $^2J_{CH}$=22, $^1J_{CC}$=77
		O=C=$\underline{C}$HO-Zr	6.20	123.40 $^1J_{CH}$=183
		$\underline{C}_5\underline{H}_5$	5.91	107.50 $^1J_{CH}$=170
		$C_5(\underline{C}H_3)_5$	2.20	11.67 $^1J_{CH}$=126
		$\underline{C}_5(CH_3)_5$		116.90
		Zr$\underline{H}$	5.92	
$Cp_2(pyr)Zr(O=C=CHO-Zr(I)Cp_2^*)$ (10)[d]		O=$\underline{C}$=CHO-Zr		170.81 $^1J_{CC}$=73
		O=C=$\underline{C}$HO-Zr	6.28	124.44
		$\underline{C}_5\underline{H}_6$	5.96	108.19
		$C_5(\underline{C}H_3)_5$	1.77	11.05
		$\underline{C}_5(CH_3)_5$		114.58

a) NMR spectra in benzene-$\underline{d}_6$ at 34° C at 90 MHz (^{1}H) or 22.5 MHz (^{13}C) unless otherwise noted. Chemical shifts in δ measured from internal TMS, coupling constants in Hz. All ^{13}C NMR samples were enriched with ^{13}C at the non-ring and non-phosphine carbons.

b) IR spectra recorded as nujol mulls. Values given in cm^{-1}. Detailed spectra are listed in the experimental section.

c) ^{1}H NMR spectrum recorded at 500 MHz.

d) Spectra recorded in pyridine-$\underline{d}_5$.

Table II. Crystal and Intensity Collection Data for $Cp_2(PMe_3)Zr{=}CHO{-}Zr(I)Cp^*_2 \cdot C_6H_6$

Formula	$C_{34}H_{50}OPZr_2I.C_6H_6$				
Formula weight	893.03 g/mol				
Space group	C2/c *				
a	27.318(4) Å				
b	19.895(3) Å				
c	19.932(5) Å				
β	132.188(10)°				
V	8027(3) Å^3				
Z	8				
ρ_{calc}	1.48 g/cm^3				
Crystal size	0.60 x 0.21 x 1.00 mm				
λ	0.71069 Å (MoKα, graphite monochromator)				
μ	1.338 mm^{-1}				
Scan range	1.0° in 2θ below $K\alpha_1$ 1.0° in 2θ above $K\alpha_2$				
2θ limits, scan rate,	3-35°	4.88 deg/min	1.0	2599	(+h,+k,±l)
bkgrd time/scan time,	3-35	8.37	1.0	2128	(+h,+k,±l)
number of reflns	35-46	3.91	1.0	1960	(+h,+k,±l)
	45-54	2.02	0.5	5302	(+h,+k,±l)
	3-30	9.77	1.0	3501	(+h,±k,±l)
Total number of averaged data	8169 (7961†) reflections				
Refinement on	F_o^2				
Weights w defined as	$[\sigma^2_{F^2} + 0.02 \times (\text{scan counts})^2]^{-2}$				
Final number of parameters	138(coords) + 241 (U's) + 1(scale) = 160				
Final agreement R_F ($F_o^2 > 0$)	0.082 ‡				
R_F ($F_o^2 > 3\sigma_{F^2}$)	0.050 (4604 reflections in sums)				
R_{wF}($F_o^2 > 0$)	0.104				
S	1.74				

*Data collected in I2/a: a=19.932(5), b=19.895(3), c=20.303(2) Å, β=94.482(9)°; all subsequent calculations carried out in C2/c.

†208 reflections deleted before final cycle of refinement; see text.

‡$R_F = \Sigma||F_o|-|F_c||/\Sigma|F_o|$, sums only include the 7179 reflections with $F_o^2 > 0$;

$R_{wF} = \{\Sigma w(F_o^2-F_c^2)^2/\Sigma wF_o^4\}^{\frac{1}{2}}$, sums include all 7961 reflections;

$S = \{\Sigma w(F_o^2-F_c^2)^2/(n-p)\}^{\frac{1}{2}}$.

Table III. Part A. Atomic Coordinates ($\times 10^4$) for $Cp_2(PMe_3)_2Zr{=}CHO{-}Zr(I)Cp_2^* \cdot C_6H_6$

	x	y	z
I	3004.8(2)	2451.9(3)	3765.7(3)
Zr(1)	3152.4(3)	997.4(3)	1334.7(4)
Zr(2)	4246.9(3)	2469.3(3)	4187.4(4)
P	3544.8(8)	−231.5(9)	2097.2(12)
C(1)	4389(4)	−464(4)	2681(5)
C(2)	3512(4)	−394(4)	2964(5)
C(3)	3104(4)	−957(4)	1360(5)
O	3968(2)	1870(2)	3217(2)
C(4)	3895(3)	1516(3)	2564(4)
C(11)	3525(4)	421(4)	597(5)
C(12)	2963(4)	785(4)	−83(5)
C(13)	3070(4)	1464(4)	93(4)
C(14)	3730(4)	1538(4)	899(5)
C(15)	4012(3)	902(4)	1221(5)
C(21)	2196(3)	611(4)	1161(6)
C(22)	2511(3)	1117(4)	1793(5)
C(23)	2432(3)	1722(4)	1399(5)
C(24)	2073(3)	1603(4)	479(5)
C(25)	1926(3)	905(4)	320(5)
C(31)	5167(4)	2341(3)	5962(4)
C(32)	5402(3)	2039(4)	5579(4)
C(33)	5007(3)	1477(3)	5079(4)
C(34)	4525(3)	1442(3)	5136(4)
C(35)	4615(4)	1965(3)	5673(4)
C(41)	5541(5)	2852(4)	6725(5)
C(42)	6053(4)	2179(5)	5829(5)
C(43)	5118(4)	978(4)	4637(5)
C(44)	4013(4)	878(4)	4730(5)
C(45)	4291(4)	2028(5)	6051(5)
C(51)	4706(3)	3299(3)	3761(4)
C(52)	4007(3)	3323(3)	3011(4)
C(53)	3719(3)	3598(3)	3323(4)
C(54)	4225(3)	3756(3)	4244(5)
C(55)	4843(3)	3599(3)	4518(4)
C(61)	5201(4)	3090(4)	3694(5)
C(62)	3660(4)	3143(4)	2048(5)
C(63)	2996(4)	3806(4)	2696(6)
C(64)	4134(5)	4128(4)	4819(6)
C(65)	5506(4)	3854(4)	5339(5)
C(71)	1454(5)	959(5)	3819(7)
C(72)	987(6)	479(6)	3382(8)
C(73)	855(5)	97(6)	2731(7)
C(74)	1199(5)	179(5)	2470(7)
C(75)	1708(6)	643(6)	2939(8)
C(76)	1838(5)	1047(5)	3610(7)
H(4)	4251(27)	1547(26)	2638(35)

Table III. Part B. Gaussian Amplitudes ($Å^2$, $\times 10^4$) for 7.

	U_{11}	U_{22}	U_{33}	U_{12}	U_{13}	U_{23}
I	496(3)	666(3)	776(4)	72(3)	500(3)	124(3)
Zr(1)	300(3)	454(3)	332(3)	12(3)	177(2)	14(3)
Zr(2)	368(3)	393(3)	367(3)	22(3)	254(3)	28(3)
P	427(9)	451(10)	476(10)	1(8)	252(9)	25(8)
C(1)	538(45)	673(51)	995(63)	135(39)	444(47)	135(46)
C(2)	846(56)	662(50)	591(47)	−47(42)	457(46)	115(39)
C(3)	925(60)	568(46)	788(53)	−194(47)	476(49)	−126(46)
O	299(21)	493(26)	290(21)	−16(18)	150(18)	−43(19)
C(4)	351(32)	496(38)	342(32)	37(27)	225(28)	6(28)
C(11)	956(62)	693(54)	742(54)	14(45)	691(53)	−49(43)
C(12)	1038(68)	765(58)	555(47)	−128(48)	597(51)	−85(42)
C(13)	677(49)	875(57)	368(38)	−171(45)	290(38)	−82(40)
C(14)	769(53)	740(53)	653(48)	−170(42)	570(46)	−83(41)
C(15)	596(45)	1072(66)	599(45)	225(46)	473(41)	239(46)
C(21)	395(39)	634(50)	1138(69)	−51(35)	494(47)	−56(48)
C(22)	456(39)	1058(65)	671(48)	70(42)	429(39)	68(47)
C(23)	467(40)	632(48)	875(57)	110(36)	448(43)	40(43)
C(24)	404(38)	893(58)	541(45)	182(39)	208(36)	25(43)
C(25)	278(33)	987(63)	671(49)	−32(39)	178(35)	−293(47)
C(31)	667(46)	626(48)	341(35)	−72(36)	274(35)	−39(32)
C(32)	484(40)	695(48)	428(39)	9(35)	266(34)	135(36)
C(33)	527(38)	559(42)	376(35)	79(34)	284(33)	82(33)
C(34)	594(42)	498(40)	452(38)	10(33)	340(36)	85(32)
C(35)	720(47)	576(44)	486(40)	27(37)	460(40)	56(35)
C(41)	1505(91)	871(63)	476(48)	−347(62)	541(59)	−244(46)
C(42)	498(46)	1061(66)	804(58)	70(45)	269(44)	400(51)
C(43)	916(59)	874(56)	567(45)	414(51)	487(45)	134(45)
C(44)	824(58)	517(48)	928(60)	−119(41)	500(52)	84(44)
C(45)	1122(75)	1397(82)	787(60)	313(62)	815(62)	269(57)
C(51)	393(32)	500(38)	453(36)	57(28)	323(31)	82(30)
C(52)	459(37)	475(38)	402(36)	50(30)	260(32)	120(30)
C(53)	485(39)	452(39)	675(47)	173(30)	400(38)	266(34)
C(54)	714(46)	493(39)	659(45)	−23(35)	577(42)	−6(35)
C(55)	560(42)	439(38)	520(41)	−99(31)	375(38)	−8(31)
C(61)	632(49)	880(58)	841(55)	−9(42)	592(47)	95(46)
C(62)	722(51)	749(54)	431(41)	59(42)	294(41)	141(39)
C(63)	660(53)	765(59)	1512(83)	346(44)	681(60)	638(57)
C(64)	1487(89)	724(60)	1353(80)	18(58)	1222(78)	−84(56)
C(65)	889(61)	723(55)	722(53)	−414(47)	441(49)	−161(44)
C(71)	113(3)*			*C*(72)	134(4)*	
C(73)	117(3)*			*C*(74)	113(3)*	
C(75)	121(4)*			*C*(76)	114(4)*	
H(4)	48(17)*					

*Isotropic Gaussian amplitude ($Å^2$, $\times 10^3$).

Table III. Part C. Hydrogen Coordinates ($\times 10^4$) and U's ($Å^2$), $\times 10^3$) for 7.

	x	y	z	U
$H(11)$	4731	−77	3123	89
$H(12)$	4454	−554	2229	89
$H(13)$	4538	−890	3060	89
$H(21)$	3700	24	3419	89
$H(22)$	3007	−430	2659	89
$H(23)$	3734	−806	3312	89
$H(31)$	2625	−948	1125	89
$H(32)$	3115	−984	889	89
$H(33)$	3323	−1388	1792	89
$H(11)$	3671	−156	708	85
$H(12)$	2616	254	−530	85
$H(13)$	2711	2017	−290	85
$H(14)$	3965	2017	1216	85
$H(15)$	4481	672	1740	85
$H(21)$	2096	177	1037	85
$H(22)$	2712	961	2422	85
$H(23)$	2544	2247	1498	85
$H(24)$	1833	1752	−247	85
$H(25)$	1661	573	−286	85
$H(411)$	5751	3214	6630	94
$H(412)$	5255	3083	6811	94
$H(413)$	5938	2620	7360	94
$H(421)$	5981	2464	5373	94
$H(422)$	6375	2407	6461	94
$H(423)$	6252	1712	5873	94
$H(431)$	5467	1151	4597	94
$H(432)$	4698	838	4017	94
$H(433)$	5330	531	5030	94
$H(441)$	3739	896	4889	94
$H(442)$	3730	844	4050	94
$H(443)$	4285	402	5008	94
$H(451)$	4267	2576	6129	94
$H(452)$	4608	1843	6689	94

Table III. Part C. (continued)

	x	y	z	U
H(453)	3861	1843	5651	94
H(611)	5603	3309	4125	99
H(612)	4992	3154	3038	99
H(613)	5247	2543	3789	99
H(621)	3258	3433	1674	99
H(622)	3992	3270	2004	99
H(623)	3585	2659	2012	99
H(631)	2958	4298	2547	99
H(632)	2922	3793	3193	99
H(633)	2700	3500	2230	99
H(641)	3881	4595	4442	99
H(642)	4513	4177	5379	99
H(643)	3752	3863	4723	99
H(651)	5490	4325	5434	99
H(652)	5856	3740	5278	99
H(653)	5645	3569	5887	99
H(71)	1520	1307	4330	139
H(72)	703	393	3604	139
H(73)	458	−293	2405	139
H(74)	1074	−136	1897	139
H(75)	2000	716	2732	139
H(76)	2252	1422	3980	139

Table IV. Bond Distances (Å) in 7.

Zr(2)-P	2.693(2)	Zr(1)-C(35)	2.605(8)
P-C(1)	1.81(1)	C(31)-C(32)	1.419(11)
P-C(2)	1.81(1)	C(32)-C(33)	1.402(11)
P-C(3)	1.82(1)	C(33)-C(34)	1.395(11)
Zr(2)-C(4)	2.117(7)	C(34)-C(35)	1.391(11)
C(4)-H(4)	0.93(7)	C(35)-C(31)	1.413(11)
C(4)-O	1.377(9)	C(31)-C(41)	1.518(13)
Zr(1)-O	1.940(5)	C(32)-C(42)	1.517(13)
Zr(1)-I	2.900(1)	C(33)-C(43)	1.489(12)
Zr(2)-C(11)	2.554(10)	C(34)-C(44)	1.533(12)
Zr(2)-C(12)	2.543(10)	C(35)-C(45)	1.506(14)
Zr(2)-C(13)	2.507(9)	Zr(1)-Cp*1[a]	2.283
Zr(2)-C(14)	2.498(9)	Zr(1)-C(51)	2.540(7)
Zr(2)-C(15)	2.514(9)	Zr(1)-C(52)	2.597(7)
C(11)-C(12)	1.385(13)	Zr(1)-C(53)	2.599(8)
C(12)-C(13)	1.376(13)	Zr(1)-C(54)	2.564(8)
C(13)-C(14)	1.401(13)	Zr(1)-C(55)	2.588(8)
C(14)-C(15)	1.395(13)	C(51)-C(52)	1.432(10)
C(15)-C(11)	1.418(13)	C(52)-C(53)	1.399(11)
Zr(2)-Cp1[a]	2.23	C(53)-C(54)	1.405(11)
Zr(2)-C(21)	2.515(9)	C(54)-C(55)	1.418(11)
Zr(2)-C(22)	2.473(9)	C(55)-C(51)	1.419(10)
Zr(2)-C(23)	2.512(9)	C(51)-C(61)	1.503(11)
Zr(2)-C(24)	2.509(9)	C(52)-C(62)	1.506(11)
Zr(2)-C(25)	2.500(9)	C(53)-C(63)	1.523(13)
Zr(2)-Cp2[a]	2.20	C(54)-C(64)	1.519(14)
C(21)-C(22)	1.373(13)	C(55)-C(65)	1.495(12)
C(22)-C(23)	1.373(13)	Zr(1)-Cp*2[a]	2.280
C(23)-C(24)	1.402(12)	C(71)-C(72)	1.344(20)
C(24)-C(25)	1.421(12)	C(72)-C(73)	1.328(20)
C(25)-C(21)	1.427(13)	C(73)-C(74)	1.355(18)
Zr(1)-C(31)	2.636(8)	C(74)-C(75)	1.382(19)
Zr(1)-C(32)	2.574(8)	C(75)-C(76)	1.386(19)
Zr(1)-C(33)	2.532(8)	C(76)-C(71)	1.378(18)
Zr(1)-C(34)	2.530(8)		

[a]Cp1 = C(11)-C(15) ring centroid, Cp2 = C(21)-C(25) ring centroid, Cp*1 = C(31)-C(35) ring centroid, Cp*2 = C(51)-C(55) ring centroid.

Table V. Bond Angles (deg) in 7.

I-Zr(1)-O	95.8(1)	C(35)-C(31)-C(41)	125.4(8)
Zr(1)-O-C(4)	165.8(4)	C(32)-C(31)-C(41)	125.4(8)
O-C(4)-H(4)	110(4)	C(31)-C(32)-C(42)	126.9(7)
O-C(4)-Zr(2)	139.7(5)	C(33)-C(32)-C(42)	123.6(7)
H(4)-C(4)-Zr(2)	109(4)	C(32)-C(33)-C(43)	125.9(7)
C(4)-Zr(2)-P	95.0(2)	C(34)-C(33)-C(43)	126.4(7)
Cp*1-Zr(1)-Cp*2[a]	134.0	C(33)-C(34)-C(44)	124.7(7)
Cp1-Zr(2)-Cp2[a]	135.4	C(35)-C(34)-C(44)	125.5(7)
Zr(2)-P-C(M1)	116.5(3)	C(34)-C(35)-C(45)	125.2(7)
Zr(2)-P-C(M2)	116.3(3)	C(31)-C(35)-C(45)	126.0(7)
Zr(2)-P-C(M3)	117.9(3)	C(51)-C(52)-C(53)	107.5(6)
C(11)-C(12)-C(13)	110.9(8)	C(52)-C(53)-C(54)	108.5(7)
C(12)-C(13)-C(14)	106.5(8)	C(53)-C(54)-C(55)	108.9(7)
C(13)-C(14)-C(15)	108.7(8)	C(54)-C(55)-C(51)	106.7(7)
C(14)-C(15)-C(11)	107.7(8)	C(55)-C(51)-C(52)	108.2(6)
C(15)-C(11)-C(12)	106.1(8)	C(55)-C(51)-C(61)	126.8(7)
C(21)-C(22)-C(23)	110.9(8)	C(52)-C(51)-C(61)	124.4(7)
C(22)-C(23)-C(24)	107.7(8)	C(51)-C(52)-C(62)	125.4(7)
C(23)-C(24)-C(25)	107.6(8)	C(53)-C(52)-C(62)	126.8(7)
C(24)-C(25)-C(21)	107.1(8)	C(52)-C(53)-C(63)	123.2(7)
C(25)-C(21)-C(22)	106.7(8)	C(54)-C(53)-C(63)	127.3(7)
C(31)-C(32)-C(33)	108.0(7)	C(53)-C(54)-C(64)	125.5(8)
C(32)-C(33)-C(34)	107.5(7)	C(55)-C(54)-C(64)	125.0(8)
C(33)-C(34)-C(35)	109.6(7)	C(54)-C(55)-C(65)	124.6(7)
C(34)-C(35)-C(31)	107.4(7)	C(51)-C(55)-C(65)	126.9(7)
C(35)-C(31)-C(32)	107.5(7)		

[a]Cp1 = C(11)-C(15) ring centroid, Cp2 = C(21)-C(25) ring centroid, Cp*1 = C(31)-C(35) ring centroid, Cp*2 = C(51)-C(55) ring centroid.

Table VI. Least-Squares Planes of Cp, Cp* and Benzene Rings of 7.

Atom	Deviation, Å	Atom	Deviation, Å
Cp1 Ring		Cp2 Ring	
C(11)	-0.003	C(21)	-0.014
C(12)	0.009	C(22)	0.015
C(13)	-0.011	C(23)	-0.009
C(14)	0.009	C(24)	0.000
C(15)	-0.004	C(25)	0.008
Cp*1 Ring		Cp*2 Ring	
C(31)	0.006	C(51)	-0.023
C(32)	-0.008	C(52)	0.013
C(33)	0.007	C(53)	0.002
C(34)	-0.003	C(54)	-0.016
C(35)	-0.002	C(55)	0.024
Benzene Ring			
C(71)	-0.018	C(74)	-0.025
C(72)	0.012	C(75)	0.019
C(73)	0.009	C(76)	0.002

Table VII. Crystal and Intensity Data for $Cp_2^* \overline{ZrOCH=C(Zr(I)Cp_2)O} \cdot \frac{1}{2}C_6H_6$.

Formula	$C_{32}H_{41}IO_2Zr_2 \cdot \frac{1}{2}C_6H_6$		
Formula weight	767.02 g/mol		
Space group	$P2_1/c$		
a	15.866(4) Å		
b	10.673(3) Å		
c	20.561(4) Å		
β	105.5(2)°		
V	3361(1) Å^3		
Z	4		
D_{calc}	1.52 g/cm^3		
Crystal size	0.07 x 0.32 x 0.70 mm		
λ	0.71069 Å		
μ	1.25 mm^{-1}		
Scan range	1.0° above $K\alpha_1$, 1.0° below $K\alpha_2$		
Refln settings	+h, +k, ±l		
2θ range, scan rate,	3<2θ<30°	3.91°/min	1250
and no. of reflns	30<2θ<45°	2.02°/min	3450
Backgrd time/scan time	1.00		
Total number of averaged data	4100		
Refinement on	F_o^2		
Final number of parameters	361		
Final cycle:†	uncorrected*	corrected*	limited*
R	.096(3891)	.074(3922)	.067(2513)
R'	.084(3162)	.059(3069)	.054(1992)
S	4.44(4100)	3.12(4100)	2.93(2691)

*Full data set, uncorrected for twinning used in refinement; full data set, corrected iteratively for twinning; limited data set, reflections affected by twinning deleted.

†Typical R-value, number of reflection used in sums given in parentheses. R' refers to R-value calculated for reflections with $F_o^2 > 3\sigma_{F^2}$. S is the goodness-of-fit; summations include all reflections.

Table VIII. Part A. Atomic Coordinations ($\times 10^4$) for $Cp_2^*\overline{ZrOCH{=}C(Zr(I)Cp_2)O}\cdot\frac{1}{2}C_6H_6$.

	x	y	z
I	8334.0(6)	4071.2(8)	5237.7(4)
$Zr(1)$	7311.8(7)	5951.6(8)	2294.2(4)
$Zr(2)$	8038.7(8)	2480.1(9)	4073.6(4)
$O(1)$	7928(5)	4642(6)	2941(3)
$O(2)$	6311(5)	5147(6)	2628(3)
$C(1)$	7468(7)	3891(9)	3252(4)
$C(2)$	6583(7)	4210(9)	3061(5)
$C(11)$	9588(14)	2870(15)	4255(10)
$C(12)$	9326(11)	2928(20)	3601(10)
$C(13)$	9034(13)	1731(24)	3375(7)
$C(14)$	9216(11)	1009(13)	3947(10)
$C(15)$	9586(10)	1739(16)	4493(7)
$C(21)$	7026(12)	1419(13)	4682(7)
$C(22)$	6522(10)	2015(11)	4138(6)
$C(23)$	6586(10)	1417(10)	3545(6)
$C(24)$	7210(12)	492(11)	3749(7)
$C(25)$	7494(12)	496(12)	4466(7)
$C(31)$	6765(8)	8036(9)	2625(6)
$C(32)$	7419(9)	8361(8)	2317(5)
$C(33)$	8238(8)	7913(9)	2678(6)
$C(34)$	8079(9)	7344(9)	3269(5)
$C(35)$	7197(10)	7450(10)	3220(6)
$C(31M)$	5873(12)	8335(14)	2433(10)
$C(32M)$	7292(16)	9273(11)	1722(6)
$C(33M)$	9069(11)	8092(19)	2579(11)
$C(34M)$	8763(13)	6811(13)	3831(8)
$C(35M)$	6752(17)	7032(14)	3756(9)
$C(41)$	6670(9)	6052(9)	1017(5)
$C(42)$	7560(9)	6085(10)	1111(5)
$C(43)$	7908(8)	4936(11)	1396(5)
$C(44)$	7200(9)	4204(9)	1451(5)
$C(45)$	6425(9)	4879(11)	1224(5)
$C(41M)$	6011(12)	7026(13)	623(7)
$C(42M)$	8077(13)	7080(14)	833(6)
$C(43M)$	8813(10)	4565(19)	1556(7)
$C(44M)$	7296(14)	2852(10)	1686(6)
$C(45M)$	5537(10)	4440(17)	1162(8)
$C(3)$	4305(9)	−13(12)	319(6)
$C(4)$	5074(10)	654(11)	586(6)
$C(5)$	5732(9)	692(11)	288(6)

Table VIII. Part B. Gaussian Amplitudes ($Å^2$, $\times 10^4$) for 8.

	U_{11}	U_{22}	U_{33}	U_{12}	U_{13}	U_{23}
I	814(7)	577(5)	447(4)	−54(5)	153(4)	−158(4)
Zr(1)	417(6)	199(4)	281(5)	−13(5)	78(4)	−2(4)
Zr(2)	614(7)	256(4)	318(5)	75(5)	118(5)	27(4)
O(1)	536(53)	343(38)	447(40)	−13(36)	100(37)	44(32)
O(2)	438(48)	362(39)	478(42)	37(35)	56(35)	10(33)
C(1)	585(77)	299(52)	290(49)	−46(52)	125(50)	−33(42)
C(2)	533(74)	299(55)	375(53)	−101(52)	147(49)	−59(46)
C(11)	1554(207)	665(102)	1575(173)	355(113)	1004(158)	−32(108)
C(12)	987(148)	1663(182)	1505(173)	992(139)	900(141)	1154(150)
C(13)	1074(156)	2286(236)	509(86)	814(171)	140(92)	−413(124)
C(14)	830(123)	604(91)	1530(158)	304(89)	268(116)	−193(102)
C(15)	732(111)	1203(132)	638(85)	434(101)	71(76)	104(89)
C(21)	1628(188)	623(87)	688(92)	−407(104)	604(107)	47(74)
C(22)	1038(117)	435(65)	488(72)	−57(70)	218(71)	−29(57)
C(23)	992(121)	345(63)	677(83)	−191(71)	132(78)	18(60)
C(24)	1429(161)	241(60)	792(92)	−208(79)	108(94)	−70(60)
C(25)	1486(173)	455(76)	816(102)	−247(93)	32(103)	349(73)
C(31)	630(87)	191(50)	722(80)	50(54)	266(67)	−77(51)
C(32)	909(105)	80(45)	410(60)	−125(56)	11(63)	−14(42)
C(33)	548(87)	287(57)	761(83)	−211(56)	72(67)	−298(56)
C(34)	875(108)	259(57)	464(66)	15(64)	−116(67)	−202(51)
C(35)	1241(134)	262(55)	541(70)	−81(74)	536(80)	−191(55)
C(31*M*)	856(137)	618(95)	1871(186)	96(93)	328(128)	−433(108)
C(32*M*)	3726(330)	212(67)	535(82)	−210(117)	462(133)	179(58)
C(33*M*)	623(121)	1317(155)	2380(228)	−450(112)	551(137)	−1090(159)
C(34*M*)	1886(213)	572(90)	1070(123)	207(110)	−1072(134)	−145(85)
C(35*M*)	3367(320)	657(97)	1400(145)	−836(144)	1888(187)	−465(98)
C(41)	911(108)	322(59)	244(51)	78(65)	−68(57)	−99(46)
C(42)	693(93)	470(66)	356(57)	−113(66)	197(57)	−46(51)
C(43)	587(85)	601(73)	308(56)	121(66)	139(54)	−130(51)
C(44)	934(107)	278(55)	270(51)	−48(62)	213(57)	−69(44)
C(45)	643(92)	618(77)	280(56)	−146(68)	−39(55)	−221(53)
C(41*M*)	1430(159)	754(97)	647(91)	449(101)	−389(94)	−82(76)
C(42*M*)	2583(235)	824(103)	485(78)	−730(124)	874(110)	−185(71)
C(43*M*)	520(98)	1800(172)	750(94)	350(109)	111(76)	−355(107)
C(44*M*)	2724(247)	167(59)	490(75)	173(92)	261(108)	87(52)
C(45*M*)	585(103)	1310(135)	992(109)	−353(98)	214(85)	−469(103)
C(3)	595(93)	575(74)	800(89)	1(70)	262(73)	114(68)
C(4)	932(122)	477(72)	628(80)	−24(77)	93(81)	19(62)
C(5)	660(92)	544(76)	592(74)	−62(68)	44(65)	37(62)

Table VIII. Part C. Hydrogen Coordinates ($\times 10^4$) for 8.

	x	y	z
H	6158	3759	3242
$H(11)$	9737	3620	4514
$H(12)$	9290	3564	3247
$H(13)$	8782	1329	2953
$H(14)$	9044	101	3984
$H(15)$	9818	1472	4942
$H(21)$	7065	1625	5140
$H(22)$	6177	2781	4151
$H(23)$	6227	1604	3092
$H(24)$	7415	−73	3442
$H(25)$	7881	−55	4738
$H(311)$	5544	8812	1948
$H(312)$	5503	8958	2692
$H(313)$	5313	7643	2337
$H(321)$	7842	9905	1652
$H(322)$	7171	8974	1187
$H(323)$	6830	10030	1589
$H(331)$	9600	7410	2644
$H(332)$	9568	8826	2813
$H(333)$	9190	8401	2072
$H(341)$	9499	7056	3947
$H(342)$	8962	5809	3882
$H(343)$	8801	6867	4369
$H(351)$	7071	6186	4123
$H(352)$	6733	7563	4204
$H(353)$	6140	6593	3693
$H(411)$	6311	7566	367
$H(412)$	5800	7520	932
$H(413)$	5527	6602	329
$H(421)$	8539	7430	1219
$H(422)$	8356	6700	526
$H(423)$	7693	7773	659
$H(431)$	9327	4863	2002
$H(432)$	9265	4711	1232
$H(433)$	9049	3566	1650
$H(441)$	7891	2490	2058
$H(442)$	7309	2034	1370
$H(443)$	6873	2358	1952
$H(451)$	5324	3955	1574
$H(452)$	5190	3703	814
$H(453)$	4937	5002	1048

Table IX. Bond Distances (Å) in 8.

Zr(1)-O(1)	1.999(7)	Zr(1)-C(34)	2.53(1)
Zr(1)-O(2)	2.073(7)	Zr(1)-C(35)	2.53(1)
O(1)-C(1)	1.352(12)	Zr(1)-Cp*(1)[a]	2.254
O(2)-C(2)	1.333(12)	C(31)-C(32)	1.39(2)
C(1)-C(2)	1.402(14)	C(32)-C(33)	1.40(2)
C(1)-Zr(2)	2.268(10)	C(33)-C(34)	1.44(2)
Zr(2)-I	2.872(1)	C(34)-C(35)	1.38(2)
Zr(2)-C(11)	2.42(2)	C(35)-C(31)	1.39(2)
Zr(2)-C(12)	2.52(2)	C(31)-C(31M)	1.40(2)
Zr(2)-C(13)	2.53(2)	C(32)-C(32M)	1.54(2)
Zr(2)-C(14)	2.51(2)	C(33)-C(33M)	1.40(2)
Zr(2)-C(15)	2.51(2)	C(34)-C(34M)	1.47(2)
Zr(2)-Cp(1)[a]	2.218	C(35)-C(35M)	1.52(2)
C(11)-C(12)	1.31(3)	Zr(1)-C(41)	2.56(1)
C(12)-C(13)	1.38(3)	Zr(1)-C(42)	2.57(1)
C(13)-C(14)	1.38(3)	Zr(1)-C(43)	2.53(1)
C(14)-C(15)	1.37(2)	Zr(1)-C(44)	2.52(1)
C(15)-C(11)	1.30(2)	Zr(1)-C(45)	2.55(1)
Zr(2)-C(21)	2.55(2)	Zr(1)-Cp*(2)[a]	2.254
Zr(2)-C(22)	2.49(1)	C(41)-C(42)	1.39(2)
Zr(2)-C(23)	2.55(1)	C(42)-C(43)	1.41(2)
Zr(2)-C(24)	2.50(1)	C(43)-C(44)	1.40(2)
Zr(2)-C(25)	2.50(2)	C(44)-C(45)	1.39(2)
Zr(2)-Cp(2)[a]	2.223	C(45)-C(41)	1.41(2)
C(21)-C(22)	1.35(2)	C(41)-C(41M)	1.56(2)
C(22)-C(23)	1.40(2)	C(42)-C(42M)	1.55(2)
C(23)-C(24)	1.39(2)	C(43)-C(43M)	1.44(2)
C(24)-C(25)	1.43(2)	C(44)-C(44M)	1.52(2)
C(25)-C(21)	1.38(2)	C(45)-C(45M)	1.46(2)
Zr(1)-C(31)	2.54(1)	C(3)-C(4)	1.40(2)
Zr(1)-C(32)	2.58(1)	C(4)-C(5)	1.34(2)
Zr(1)-C(33)	2.56(1)	C(5)-C(3)'	1.43(2)

[a]Cp(1) = C(11)-C(15) ring centroid, Cp(2) = C(21)-C(25) ring centroid, Cp*(1) = C(31)-C(35) ring centroid, Cp*(2) = C(41)-C(45) ring centroid.

Table X. Bond Angles (deg) in 8.

Zr(1)-O(1)-C(1)	120.0(6)	C(35)-C(31)-C(31M)	129(1)
O(1)-C(1)-O(2)	110.4(9)	C(32)-C(31)-C(31M)	125(1)
C(1)-C(2)-O(2)	119.5(9)	C(31)-C(32)-C(32M)	124(1)
C(2)-O(2)-Zr(1)	113.1(6)	C(33)-C(32)-C(32M)	123(1)
O(2)-Zr(1)-O(1)	76.9(3)	C(32)-C(33)-C(33M)	131(1)
O(1)-C(1)-Zr(2)	126.0(7)	C(34)-C(33)-C(33M)	124(1)
C(2)-C(1)-Zr(2)	123.1(7)	C(33)-C(34)-C(34M)	124(1)
C(1)-Zr(2)-I	100.1(3)	C(35)-C(34)-C(34M)	128(1)
Cp*1-Zr(1)-Cp*2[a]	136.9	C(34)-C(35)-C(35M)	125(1)
Cp1-Zr(2)-Cp2[a]	128.9	C(31)-C(35)-C(35M)	124(1)
C(11)-C(12)-C(13)	107(2)	C(41)-C(42)-C(43)	108(1)
C(12)-C(13)-C(14)	105(2)	C(42)-C(43)-C(44)	106(1)
C(13)-C(14)-C(15)	109(2)	C(43)-C(44)-C(45)	110(1)
C(14)-C(15)-C(11)	105(2)	C(44)-C(45)-C(41)	106(1)
C(15)-C(11)-C(12)	113(2)	C(45)-C(41)-C(42)	110(1)
C(21)-C(22)-C(23)	110(1)	C(45)-C(41)-C(41M)	124(1)
C(22)-C(23)-C(24)	106(1)	C(42)-C(41)-C(41M)	126(1)
C(23)-C(24)-C(25)	109(1)	C(41)-C(42)-C(42M)	126(1)
C(24)-C(25)-C(21)	107(1)	C(43)-C(42)-C(42M)	124(1)
C(25)-C(21)-C(22)	109(1)	C(42)-C(43)-C(43M)	126(1)
C(31)-C(32)-C(33)	112(1)	C(44)-C(43)-C(43M)	127(1)
C(32)-C(33)-C(34)	104(1)	C(43)-C(44)-C(44M)	123(1)
C(33)-C(34)-C(35)	108(1)	C(45)-C(44)-C(44M)	127(1)
C(34)-C(35)-C(31)	111(1)	C(44)-C(45)-C(45M)	128(1)
C(35)-C(31)-C(32)	105(1)	C(41)-C(45)-C(45M)	127(1)

[a]Cp1 = C(11)-C(15) ring centroid, Cp2 = C(21)-C(25) ring centroid, Cp*1 = C(31)-C(35) ring centroid, Cp*2 = C(41)-C(45) ring centroid.

Table XI. Least-Squares Planes of Enediolate Metallocycle, Cp and Cp* Rings of 8.[a]

Atom	Deviation, Å	Atom	Deviation, Å
	Enediolate Metallocycle		
Zr(1)	0.035	O(2)	0.038
Zr(2)	0.058	C(1)	-0.071
O(1)	-0.026	C(2)	-0.034
	Cp1 Ring		Cp2 Ring
C(11)	-0.034	C(21)	-0.027
C(12)	0.029	C(22)	0.032
C(13)	-0.014	C(23)	-0.023
C(14)	-0.004	C(24)	0.007
C(15)	0.023	C(25)	0.012
	Cp*1 Ring		Cp*2 Ring
C(31)	0.022	C(41)	0.005
C(32)	-0.024	C(42)	-0.009
C(33)	0.016	C(43)	0.009
C(34)	-0.002	C(44)	-0.006
C(35)	-0.012	C(45)	0.001
C(31M)	-0.035	C(41M)	-0.217
C(32M)	-0.308	C(42M)	-0.264
C(33M)	-0.099	C(43M)	-0.036
C(34M)	-0.066	C(44M)	-0.102
C(35M)	-0.101	C(45M)	-0.085

[a]A positive deviation is a deviation toward the metal atom.

Table XII. Cross-Over Experiment.

$Cp_2Zr(^{12}CO)_2$ + $Cp_2Zr(^{13}CO)_2$ + $Cp^*_2ZrH_2$ + MeI

0.263 mmol (99% ^{12}C) | 0.176 mmol (91% ^{13}C) | 0.422 mmol

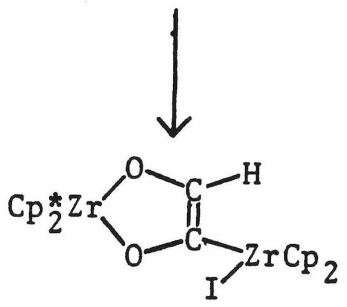

	$^{12}C^{12}C$	$^{12}C^{13}C$	$^{13}C^{13}C$
calculated	.59	.08	.33
observed	.58	.10	.32

5 ± 5 % Cross-over

Experimental

General Considerations: All manipulations were performed under an inert atmosphere by employing a nitrogen-filled glove box and vacuum-line techniques. Hydrogen, nitrogen and argon were purified by passing through MnO on vermiculite[37] and activated 4 Å molecular sieves. Benzene, toluene and pet ether (30°-60°), including NMR solvents, were vacuum transferred from $LiAlH_4$ or molecular sieves, then from "titanocene"[38] prior to use. Pyridine and methyl iodide were vacuum transferred from CaH_2; d_5-pyridine and acetone were transferred from 4 Å molecular sieves. Carbon monoxide (MCB), ^{13}C-carbon monoxide (Monsanto-Mound) and PMe_3 (Strem) were used as received.

$Cp_2Zr(CO)_2$,[32] $Cp_2Zr(CO)(PMe_3)$[27] and $Cp^*_2ZrH_2$[1b] were prepared by literature methods. $Cp_2Zr(^{13}CO)_2$ was made by photolysis of $Cp_2Zr(CO)_2$ under a ^{13}CO atmosphere. $Cp^*_2ZrD_2$ was prepared by treatment of $[Cp^*_2ZrN_2]_2N_2$ with D_2 at low temperature and used promptly.

^1H NMR spectra were recorded using C_6D_6, C_7D_8 or C_5D_5N as solvent with TMS as an internal reference using Varian EM-390, JOEL FX90Q and Bruker WM-500 spectrometers. ^{13}C NMR spectra were obtained using the JOEL instrument. IR spectra were recorded as nujol mulls on a Beckmann IR 4240 spectrophotomer. Elemental analyses were performed by Alfred Bernhardt Analytical Laboratory and Dornis and Kolbe Microanalytical Laboratory.

Procedures. $Cp_2(PMe_3)Zr{=}CHO{-}Zr(H)Cp^*_2$ (4). At -196° C 20 ml toluene was added to a mixture of $CpZr(CO)(PMe_3)$ (1.30 g,

4.00 mmol) and $Cp_2^*ZrH_2$ (1.45 g, 4.00 mmol). The solution was stirred at -78° C for 30 minutes to react, then warmed to room temperature. After filtration the solution was concentrated to 10 ml and 15 ml pet ether added to precipitate the red crystalline product. $Cp_2(PMe_3)Zr{=}CHO{-}Zr(H)Cp_2^*$ (2.30 g, 84%) was isolated by filtration and washed with cold pet ether. Anal. Calcd for $C_{34}H_{51}OPZr_2$: C, 59.25; H, 7.46; O, 2.32; P, 4.49; Zr, 26.47. Found: C, 58.69; H, 7.36; Zr, 26.79. IR (nujol mull): 2755 w, 1560 w, 1280 w, 1100 s, 950 m, 775 m.

$Cp_2(PMe_3)Zr{=}CDO{-}Zr(D)Cp_2^*$ was prepared in a similar manner using $Cp_2Zr(CO)(PMe_3)$ and $Cp_2^*ZrD_2$. IR (nujol mull): 2045 vw, 1580 w, 1280 w, 1100 s, 950 m, 775 m.

$Cp_2(CO)Zr{=}CHO{-}Zr(H)Cp_2^*$ (5). A pet ether solution of $Cp_2^*ZrH_2$ (250 mg, 0.69 mmol) was slowly added to a pet ether solution of $Cp_2Zr(CO)_2$ (210 mg, 0.76 mmol) at ca. -10° C, resulting in an immediate color change from dark green to red. The solution was concentrated and cooled to -78° C to precipitate the product as a tan solid. $Cp_2(CO)Zr{=}CHO{-}Zr(H)Cp_2^*$ (230 mg, 53%) was isolated by filtration at -78° C, washed with cold pet ether, and dried in vacuo. Due to the instability of 4 in solution recrystallization proved impossible. IR (nujol mull): 2755 w, 1925 vs, 1620 w, 1515 w, 1170 s, 1155 s, 1005 w, 780 m.

$Cp_2(CO)Zr{=}CDO{-}Zr(D)Cp_2^*$ was prepared by using $Cp_2Zr(CO)_2$ and $Cp_2^*ZrD_2$. IR (Nujol mull): 2042 w, 1925 vs, 1570 w, 1170 s, 1155s, 1005 w, 780 m.

$[Cp_2Zr(C_2H_2O_2)ZrCp_2^*]_x$ (6). A mixture of $Cp_2Zr(CO)_2$ (190 mg, 0.69 mmol) and $Cp_2^*ZrH_2$ (250 mg, 0.69 mmol) was dissolved in 15 ml

benzene and stirred a room temperature for 10 hr. The insoluble, yellow product precipitated from the reaction solution. 6 (115 mg, 25%) was isolated by filtration and washed with copious amounts of pet ether. Anal. Calcd. for $C_{32}H_{42}O_2Zr_2$: C, 59.95; H, 6.60; O, 4.99; Zr, 28.46. Found: C, 59.82; H, 6.68. IR (nujol mull): 1552 w, 1527 s, 1318 w, 1120 s, 1012 m, 967 w, 858 m, 794 s, 782 sh.

$Cp_2Zr(C_2H_4O_2)(ZrCp^*_2)_2$ (5a). Toluene was condensed onto $Cp_2Zr(CO)_2$ (81 mg, 0.29 mmol) and $Cp^*_2ZrH_2$ (202 mg, 0.56 mmol) at -196° C and warmed to room temperature. The solution lightened from the dark red color of 5 to light orange after ca. 10 minutes. The light yellow product (145 mg, 50%) was isolated by concentration, addition of pet ether and filtration at -78° C. IR (nujol mull): 1570 w, br, 1519 s, 1225 m, 1052 m, 1020 w, 790 m, 728 w, 696 s, 680 s.

$Cp_2(PMe_3)Zr{=}CHO{-}Zr(I)Cp^*_2$ (7). $Cp_2(PMe_3)Zr{=}CHO{-}Zr(H)Cp^*_2$ (1.50 g, 2.18 mmol) was dissolved in 30 ml toluene. Methyl iodide (2.18 mmol), premeasured in a calibrated volume, was condensed into the reaction flask at -78° C. The solution was stirred at room temperature for 30 minutes to effect reaction, indicated by a color change from red to green. The toluene was removed to yield the green crystalline product. $Cp_2(PMe_3)Zr{=}CHO{-}Zr(I)Cp^*_2$ (1.48 g, 83%) was washed with ca. 40 ml pet ether at -78° C and isolated by filtration. Anal. Calcd for $C_{34}H_{50}IOPZr_2$: C, 50.10; H, 6.18; I, 15.57; O, 1.96; P, 3.80; Zr, 22.38. Found: C, 49.84; H, 5.97; I, 15.86; P, 3.63. IR (nujol mull): 2725 vw, 1280 w, 1075 s, 950 m, 780 m.

$Cp_2(PMe_3)Zr{=}CDO{-}Zr(I)Cp^*_2$ was prepared in a similar manner from $Cp_2(PMe_3)Zr{=}CDO{-}Zr(D)Cp^*_2$ and MeI. IR (nujol mull): 2020 vw,

1280 w, 1075 s, 950 m, 780 m.

$Cp^*_2\overline{ZrO-CH=C(Zr(I)Cp^*_2)O}$ (8). Toluene (25 ml) was condensed onto a mixture of $Cp_2Zr(CO)_2$ (0.83 g, 3.00 mmol) and $Cp^*_2ZrH_2$ (1.07 g, 3.00 mmol) at -196° C and then warmed to 0° for ca. 5 minutes to effect formation of 5. The reaction mixture was re-cooled to -196° C and MeI (13 mmol) was added. On stirring for $3\frac{1}{2}$ hr at room temperature the solution turned purple. On concentration of the toluene and addition of pet ether a dark purple solid was obtained. $Cp^*_2\overline{ZrO-CH=C(Zr(I)Cp_2)O}$ (1.38 g, 60%) was recrystallized from benzene.

The above procedure was carried out employing a mixture of $Cp_2Zr(CO)_2$ (73 mg, 0.263 mmol) and $Cp_2Zr(^{13}CO)_2$ (49 mg, 0.176 mmol) 91 ± 3% ^{13}C enriched). The ^{13}C NMR spectrum of the resulting product showed a ratio 8(^{13}C, ^{13}C)/8(^{12}C, ^{13}C) of 3.2 ± 0.4. Using this ratio and the initial amounts of $Cp_2Zr(CO)_2$ and $Cp_2Zr(^{13}CO)_2$ the calculated (no isotopic cross-over) and actual 8(^{12}C, ^{12}C):8(^{12}C, ^{13}C):8(^{13}C, ^{13}C) ratios were determined and are tabulated in Table XII. The difference corresponds 5 ± 5% isotopic cross-over on the formation of 8.

In an alternative synthesis of 8, a benzene solution of $Cp_2(PMe_3)Zr=CHO-Zr(I)Cp^*_2$ (710 mg, 0.87 mmol) was stirred under 200 Torr CO for $3\frac{1}{2}$ hr at room temperature. Longer reaction times or higher CO pressures led to a diminished yield of 8 due to further reaction. Removal of solvent and liberated PMe_3 in vacuo, washing with cold pet ether and recrystallization from benzene to remove unreacted 7 gave $Cp^*_2\overline{ZrO-CH=C(Zr(I)Cp_2)O}$ in ca. 30% yield. Anal.

Calcd for $C_{32}H_{41}IO_2Zr_2$: C, 50.11; H, 5.39; I, 16.55; O, 4.17; Zr, 23.79. Found: C, 50.34; H, 5.38; I, 16.38. IR (C_6D_6): 1433 m, 1380 w, 1250 m, 1120 w, 1020 w, 800 m.

$Cp_2(pyr)Zr(O=C=CHO-Zr(H)Cp_2^*)$ (9). At -196° C 15 ml pyridine was condensed onto a mixture of $Cp_2Zr(CO)_2$ (425 mg, 1.53 mmol) and $Cp_2^*ZrH_2$ (550 mg, 1.52 mmol). The solution was stirred at room temperature for 1 hr. Concentration of the solution to ca. 1 ml and addition of pet ether gave orange crystals. $Cp_2(pyr)Zr(O=C=CHO-Zr(H)Cp_2^*)$ (890 mg, 82%) was isolated by filtration, washed with cold pet ether and dried in vacuo. Anal. Calcd for $C_{37}H_{47}NO_2Zr_2$: C, 61.68; H, 6.58; N, 1.95; O, 4.45; Zr, 25.34. Found: C, 61.73; H, 6.91; N, 1.96. IR (nujol mull): 1600 m, 1518 w, 1216 w, 1110 s, 1008 m, 831 w, 788 s.

$Cp_2(pyr)Zr(O=^{13}C=^{13}CHO-Zr(H)Cp_2^*)$ was prepared by using $Cp_2Zr(^{13}CO)_2$ (70% ^{13}C enriched) in place of $Cp_2Zr(CO)_2$ in the above procedure.

$Cp_2(pyr)Zr(O=C=CHO-Zr(I)Cp_2^*$ (10). CH_3I (0.061 mmol) was added to a NMR sample tube of 9 (40 mg, 0.056 mmol) in C_5D_5N at -196° C, which was sealed. On warming to room temperature the ^1H NMR spectrum showed 10. In a separate experiment CH_3I (0.134 mmol) was added to 9 (92 mg, 0.128 mmol) in pyridine at -196° C and warmed to room temperature for 30 minutes; upon completion of the reaction 0.113 mmol CH_4 (0.88 equivalents CH_4/equivalent 9) were recovered by Toepler pump. An NMR sample of 9 (20 mg, 0.028 mmol) and CH_3I (0.14 mmol) is C_6D_6 gives an ^1H NMR spectra identical to that obtained for 8 in C_6D_6 with one equivalent of pyridine. Likewise, a

sample of 8, dissolved in C_5D_5N, has the same spectrum as 10 prepared from 9.

Structure Determination for $Cp_2(PMe_3)Zr{=}CHO{-}Zr(I)Cp^*_2$.

A large single crystal was mounted approximately along the c-axis in a glass capillary under N_2. A series of oscillation and Weissenberg photographs indicated monoclinic symmetry and a centered lattice, and our initial choice of axes conformed to I2/a (hkl absent for h+k+l odd, h01 absent for h odd); data were collected on a locally-modified Syntex $P2_1$ diffractometer with this cell. To be consistent with space group C2/c, all reflection indices were transformed for the subsequent calculations ($h' = h+1$, $l' = -h$). The lattice constants reported in Table 1 were obtained by least-squares refinement of thirty 2θ values ($25 < 2\theta < 44°$), where each 2θ value was an average of two measurements at $\pm 2\theta$. The three check reflections indicated no decomposition and the data were reduced to F_0^2; the form factors for all atoms were taken from reference 39, and those for Zr and I were corrected for anomalous dispersion. The details on unit cell parameters and data collection are given in Table II.

The positions of the Zr and I atoms were derived from the Patterson map, and the Fourier map phased on these three atoms revealed the remaining non-hydrogen atoms of the Zr complex. Least-squares refinement of atomic coordinates and U's, minimizing $\Sigma w[F_0^2 - (F_c/k)^2]^2$ gave $R_F = 0.131$. A molecule of benzene and all hydrogen atoms were located from difference maps. The benzene molecule is apparently ordered and the coordinates of the carbon atoms were refined; all hydrogen atoms except H(4) were introduced into the

model with fixed coordinates and isotropic B's. The refinement of all non-hydrogen atoms in the Zr-complex with anisotropic U's, carbon atoms in the benzene molecule with isotropic B's, and the carbene hydrogen atom H(4) using all the data (8169 reflections) led to $R_F = 0.082$; the scale factor and Gaussian amplitudes in one block and the coordinates in the other. A number of reflections had large weighted residuals, and examination of the diffractometer data indicated that most of these reflections had unusual backgrounds or scans; these 208 reflections were deleted before the final cycle of refinement. All calculations were carried out on a VAX 11/780 using the CRYM system of programs.

Structure Determination for $Cp^*_2\overline{Zr\text{-}OCH{=}C(Zr(I)Cp_2)O}$. Single crystals were mounted in glass capillaries under N_2. Oscillation, Weissenberg, and precession photographs indicated a monoclinic lattice, space group $P2_1/c$ (0k0 absent for k odd, h01 absent for l odd), and twinning by reticular pseudo-merohedry across the ab-plane with a twin index of 3: the $h, \bar{k}, -l-2h/3$ reflections of the twin lattice were superimposed onto the h, k, l reflections of the parent lattice. (The metric relation between a, c, and β is $3c\cos\beta = -a$.) The twin fraction varied with each crystal, indicating macroscopic twin domains. One of these crystals was selected for data collection on a locally modified Syntex $P2_1$ diffractometer; details on unit cell parameters and the data collection are given in Table VIII. The three check reflections indicated no decomposition and the data were reduced to F_0^2.

The positions of the Zr and I atoms were derived from a Patterson map, and an electron density Fourier map phased on these

three atoms revealed the remaining non-hydrogen atoms of the Zr-complex and a benzene molecule of crystallization. Least-squares refinement of atomic coordinates and U's minimizing $\Sigma w[F_o^2-(F_c/k)^2]^2$ gave $R_F = 0.144$;[40] the form factors for all atoms were taken from reference 39. The hydrogen atoms were then located from difference maps and introduces into the model with fixed coordinates and isotropic B's. The refinement of non-hydrogen atoms with anisotropic U's using all the data (4100 reflections) led to $R_F = 0.096$, $R'_F = 0.084$, and $S = 4.44$.

At this stage, the F_o^2 were corrected for twinning in an iterative manner by subtracting off an estimate of the twin contribution to the intensity.[41] This led to an improved data set, as evident from the lower goodness-of-fit: $S = 3.04$ ($R_F = 0.074$, $R'_F = 0.059$). After another cycle of least-squares refinement, the F_o^2 data were corrected again, but the correction differed marginally from the first pass: the volume ratio of the twins was 0.19:1; the final results are indicated in Table 1. The remaining errors in the data appear to be normally distributed. To check this, we carried out a parallel refinement in which all affected reflections were deleted. Refinement with this data set led to coordinates and U's that were insignificantly different (within 2σ) from the starting set; the goodness-of-fit (2.93, 2691 reflections total) is essentially the same as from the full data set refinement, and indicates that the twin correction is adequate ($R_F = 0.067$, $R'_F = 0.054$). All results quoted hereafter refer to refinement with the full data set.

References

1. (a) Manriquez, J. M.; McAlister, D. R.; Sanner, R. D.; Bercaw, J. E. J. Amer. Chem. Soc. 98, 6733 (1976); (b) Manriquez, J. M.; McAlister, D. R.; Sanner, R. D.; Bercaw, J. E. J. Amer. Chem. Soc. 100, 2716 (1978); (c) Bercaw, J. E. Adv. Chem. Ser. No. 167, 136 (1978); (d) Wolczanski, P. T.; Bercaw, J. E. Acc. Chem. Res. 13, 121 (1980).
2. Threlkel, R. S.; Bercaw, J. E. J. Amer. Chem. Soc. 103, 2850 (1981).
3. Wolczanski, P. T.; Threlkel, R. S.; Bercaw, J. E. J. Amer. Chem. Soc. 101, 218 (1979).
4. Chapter I of this thesis.
5. Fryzuk, M. D.; Bercaw, J. E.; unpublished results.
6. Schwartz, J.; Gell, K. I. J. Organomet. Chem. 184, C1 (1980).
7. Hartner, F. W.; Schwartz, J.; Clift, S. M. J. Amer. Chem. Soc. 105, 641 (1983).
8. (a) Heck, R. F.; Breslow, D. S. J. Amer. Chem. Soc. 83, 4023 (1961); (b) Calderazzo, F. Angew. Chem. Int. Ed. Engl. 16, 299 (1977).
9. (a) Cossee, P. J. Catalysis 3, 80 (1964); (b) Cossee, P. Rec. Trav. Chim., Pays-Bas 85, 1151 (1966); (c) Henrici-Olivé, G.; Olivé, S. Fortschr. Chem. Forsch. 67, 107 (1976).
10. (a) Fischer, F.; Tropsch, H. Brennst.-Chem. 7, 97 (1926); Chem. Ber. 59, 830 (1926);

(b) Brady, R. C., III; Pettit, R. J. J. Amer. Chem. Soc. 102, 6181 (1980); ibid. 103, 1287 (1981).

11. Rüchardt, C.; Schrauzer, G. N. Chem. Ber. 93, 1840 (1960).

12. Dorrer, B.; Fischer, E. O. Chem. Ber. 107, 2683 (1974).

13. Messerle, L.; Curtis, M. D. J. Amer. Chem. Soc. 102, 7791 (1980).

14. Messerle, L.; Ph.D. Thesis, Massachusetts Institute of Technology, 1979.

15. Roper, W. R.; Abst. of Amer. Chem. Soc. Nat. Meet., Kansas City, Mo., September 5-10, 1982.

16. (a) Herrmann, W. A.; Plank, J. Angew. Chem. Int. Ed. Engl. 17, 525 (1978);

(b) Herrmann, W. A.; Plank, J.; Ziegler, M. L.; Weidenhammer, K. J. Amer. Chem. Soc. 101, 3133 (1979).

17. Stevens, A. E.; Beauchamp, J. L. J. Amer. Chem. Soc. 100, 2584 (1978).

18. The ^{1}H NMR spectrum of $Cp^*_2Zr(OCH_3)I$ has not been reported; it is (C_6D_6, 34° C) 1.86 δ (s, Cp^*), 3.67 δ (s, OCH_3).

19. (a) Sanner, R. D.; Manriquez, J. M.; Marsh, R. E.; Bercaw, J. E. J. Amer. Chem. Soc. 98, 8351 (1976);

(b) McKenzie, T. C.; Sanner, R. D.; Bercaw, J. E. J. Organomet. Chem. 102, 457 (1975);

(c) Lappert, M. F.; Martin, T. R.; Atwood, J. L.; Hunter, W. E. J. Chem. Soc., Chem. Commum., 522 (1976).

(d) Jeffery, J.; Lappert, M. F.; Luong-Thi, N. T.; Webb, M.; Atwood, J. L.; Hunter, W. E. J. Chem. Soc., Dalton Trans., 1593 (1981).

(e) Fachinetti, G.; Fochi, G.; Floriani, C. ibid., 1946 (1977);

(f) Hunter, W. E.; Atwood, J. L.; Fachinetti, G.; Floriani, C. J. Organomet. Chem. 204, 67 (1981).

20. Atwood, J. L.; Hunter, W. E.; Hrncir, D. C.; Samiel, E.; Alt, H.; Rausch, M. D. Inorg. Chem. 14, 1757 (1975).

21. Jeffrey, J.; Lappert, M. F.; Luong-Thi, N. T.; Atwood, J. L.; Hunter, W. E. J. Chem. Soc., Chem. Commum. 1081 (1978).

22. (a) Cardin, D. J.; Cetinkaya, B.; Lappert, M. F. Chem. Rev. 72, 575 (1972);

(b) Cotton, F. A.; Lukehart, C. M.; Prog. Inorg. Chem. 16, 243 (1972).

23. (a) Silverton, J. V.; Hoard, J. L. Inorg. Chem. 2, 243 (1963);

(b) Stezowski, J. J.; Eick, H. A. J. Amer. Chem. Soc. 91, 2890 (1969);

(c) Von Dreele, R. B.; Stezowski, J. J.; Fay, R. C. J. Amer. Chem. Soc. 93, 2887 (1971);

(d) Elder, M. Inorg. Chem. 8, 2103 (1969);

(e) Chun, H. K.; Steffan, W. L.; Fay, R. C. Inorg. Chem. 18, 2458 (1979).

24. (a) Clarke, J. F.; Drew, M. G. B. Acta Cryst. B30, 2267 (1974);

(b) Petersen, J. L. J. Organomet. Chem. 166, 179 (1979).

25. (a) Dunitz, J. D. "X-Ray Analysis and the Structure of Organic Molecules"; Cornell University Press: Ithaca, NY, 1979; p. 338;

(b) "Interatomic Distances, Supplement", Sutton, L. E., Ed.; Special Publication No. 18, The Chemical Society: London, 1965.

26. (a) Straus, D. A.; Ph.D. Thesis, California Institute of Technology, 1983;
(b) Moore, E. J.; Straus, D. A.; Armantrout, J.; Santarsiero, B. D.; Grubbs, R. H.; Bercaw, J. E. J. Amer. Chem. Soc., manuscript accepted for publication.

27. Demerseman, B.; Bouquet, G.; Bigorgne, M. J. Organomet. Chem. 132, 223 (1977).

28. Brown, F. J. Prog. Inorg. Chem. 27, 1 (1980).

29. (a) Schrock, R. R.; Sharp, P. R. J. Amer. Chem. Soc. 100, 2389 (1978);
(b) Schrock, R. R. Acc. Chem. Res. 12, 98 (1979).

30. Calabro, D. C.; Lichtenberger, D. L.; Herrmann, W. A. J. Amer. Chem. Soc. 103, 6852 (1981).

31. Schrock has argued that early metal alkylidene ligands, such as methylene in $Cp_2Ta(CH_2)(CH_3)$, should be considered as π-donors to the metal center since the carbene π-orbital is probably lower in energy that the metal orbitals, similar to the energy ordering of the metal and oxygen π-orbitals in metal oxo complexes.[29b]

32. Demerseman, B.; Bouquet, G.; Bigorgne, M. J. Organomet. Chem. 107, C19 (1976).

33. Wood, C. D.; McLain, S. J.; Schrock, R. R. J. Amer. Chem. Soc. 101, 3210 (1979).

34. (a) Manriquez, J. M.; McAlister, D. R.; Sanner, R. D.; Bercaw, J. E. J. Amer. Chem. Soc. 100, 2716 (1978); (b) Straus, D. A.; Buchwald, S.; Grubbs, R. H.; manuscript in preparation.

35. Lauher, J. W.; Hoffmann, R. J. Amer. Chem. Soc. 98, 1729 (1976).

36. (a) Ben-Shoshan, R.; Pettit, R. J. Amer. Chem. Soc. 89, 2231 (1967); (b) Foxman, B.; Marten, D.; Rosan, A.; Raghu, S.; Rosenblum, M. ibid. 99, 2160 (1977).

37. Brown, T. L.; Dickerhof, D. W.; Bafus, D. A.; Morgan, G. L. Rev. Sci. Instrum. 33, 491 (1962).

38. Marvich, R. H.; Brintzinger, H. H. J. Amer. Chem. Soc. 93, 2046 (1971).

39. International Tables for X-ray Crystallography, Vol. IV, pp. 72-98 (1974).

40. $R_F = \Sigma||F_o|-|F_c||/\Sigma|F_o|$, sums include only those reflections with $F_o^2 > 0$. $R'_F = R_F$, but the sums include only those reflections with $F_o^2 > 3\sigma_{F^2}$. $S = [\Sigma w(F_o^2 - F_c^2)^2/(n-p)]^{\frac{1}{2}}$, where n = total number of reflections and p = total number of parameters in the least-squares refinement.

41. The twin fraction δ is defined by the relation $(kF_o)^2 = F_{cP}^2 + \delta F_{cT}^2$, where k is the scale factor (estimated from the reflections unaffected by the twinning), F_o is the observed structure factor amplitude of the parent reflection, F_{cP} is the F_c of the parent reflection, and F_{cT} is the F_c of the twin reflection. The least-

squares solution for δ gives $\delta = [k^2 \Sigma w F_o^2 F_{cT}^2 - \Sigma w F_{cP}^2 F_{cT}^2] / \Sigma w F_{cT}^4$; the weight w is the least-squares weight for the twin reflection. The corrected F'_o is then calculated: $(kF'_o)^2 = (kF_o)^2 - \delta F_{cT}^2$, and used in the next cycle of least-squares refinement of coordinates and U's.